DEVELOPING MODEL FOR PRESSURE DROP FOR DENSE-PHASE PNEUMATIC CONVEYING OF FLY ASH.

A

THESIS

Submitted in partial fulfillment of the requirement for the award of degree of

Master of Engineering

In

Thermal Engineering

Submitted by

MOHIT ARORA

(ROLL NO. 801083016)

UNDER THE GUIDANCE OF

Dr. S.S. MALLICK

(ASSISTANT PROFESSOR)

Department Of Mechanical Engineering

Thapar University, Patiala

July 2012

CERTIFICATION

I, Mohit Arora, declare that this thesis submitted toward fulfillment of the requirements for the award of Master's degree in Thermal engineering, in the Mechanical Department, Thapar University, Patiala, is wholly my own work. This document has not been submitted for any degree in any other institution.

Date: 10-7-2012

Place: PATIALA.

Mohit Arora

801083016

Thapar University, Patiala

This is to certify that the above statement made by the candidate is correct and true to the best of my knowledge

10/7/12

Supervisor:
Dr. S.S. Mallick
Assistant Professor
Mechanical Engineering Department
Thapar University, Patiala

Countersigned by

Prof. Dr. Ajay Batish
Head
Mechanical Engineering Department
Thapar University, Patiala

Prof. Dr. S. K. Mahapatra
Dean
Academic Affairs
Thapar University, Patiala

AKNOWLEDGEMENT

I wish to express my deep sense of gratitude and indebtedness to Dr. S.S. Mallick , Department of Mechanical Engineering, Thapar University, Patiala, for introducing the present topic and for their inspiring guidance, constructive criticism and valuable suggestion during this work.

Mohit Arora

801083016

Thapar University, Patiala.

Table of contents

CHAPTER 1: INTRODUCTION AND OBJECTIVES

1.1 Introduction

The term pneumatic conveying is defined as the transportation of various materials either in powdered form (e.g. fly ash, cement, limestone) or in granular form (e.g. crushed coal, grain) through a flow channel (e.g. pipeline) using gas as transport medium either with vacuum or with positive pressure (Mallick, 2010). The pneumatic conveying systems are broadly two types: dilute phase (can also be called as lean phase or fully suspended flow) conveying and dense phase conveying. In dilute phase conveying the gas volume and velocity is sufficiently high to keep the particles in suspension (Wypych, 2003). This means the material is not accumulating or rolling at the bottom of the conveying line at any point of time or space. To have dilute phase conveying, the gas velocity must be sufficiently high and above the saltation velocity (i.e. the gas velocity is insufficient to maintain the solids in suspension and the solids begin to settle out in the bottom of the pipe) (Mallick, 2010).

The dense phase pneumatic conveying system are pressure dependent, uses low volume and relies on a continuously expanding volume of air pushing slugs and dunes of material along the pipe. Dense phase technology reduces the air consumption by allowing the system to convey at maximum density. This maximum density conveying technique has following advantages:

1. When the conveying pipe is at high density, only a small percentage of the particles are in contact with the conveying pipe at any given time. The majority of the particles are in the interior of the pipe, therefore no pipe wear was occurred due to low conveying velocity.
2. Increasing the particle density, conveying velocity can be decreased for a given transfer rate and pipe diameter (Klinzing, 1990).

Fluidized Dense Phase:

This mode of transfer takes advantage of the fluidization and air retention properties of the bulk material. Fluidization describes the state which some bulk materials achieve when a gas has been entrained into the void spaces between the particles of the material. Material when in highly fluidized state tends to behave like a fluid (as the term implies) than solid bulk material (Mallick, 2010).

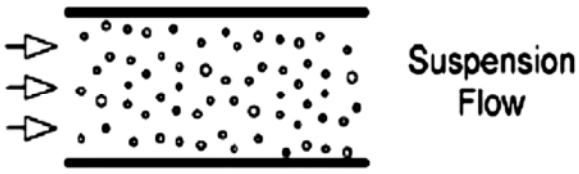

Figure 1.1: Fluidized dense phase (Rabinovich and Kalman, 2010)

The system is characterized by high velocities, although not as high as for dilute phase systems. Product degradation and pipe wear may be lower in dense phase. Some materials that are being conveyed successfully in fluidized dense-phase include cement, fly ash, pulverized coal, soap powder, zircon sand, crushed bauxite, electrolytic manganese dioxide, lead dust, limestone and flour.

Apart from merits there are some demerits for dense phase conveying system as well. Dense phase conveying system is widely used in industries, but there is a challenging job for accurately understanding and modelling the flow phenomena of gas-particle transport (Wypych, 2003). Some fundamental methods which are based on the powder mechanics have been developed for various products and modes of flows, such as low velocity slug-flow, low velocity plug-flow. Various empirical power function based models (dimensionless) for solid friction have been developed and employed over the years by various researchers to avoid the need to develop the fundamental relationships between friction factor and the relevant particle and bulk properties (Mallick, 2010). These dimensionless models were developed with the help of Buckingham π theorem.

The strand flow conveying is used where there is non-uniform particle size (wide size distribution): Indian fly ash. The particle of the Indian fly ash is non-linear means they are of various sizes ranges: 5 μm – 200 μm, which is the major problem for conveying in the pipe because of the heavy particles (particle density 2600 kg/m^3). Comparing the Indian fly ash with Australian fly ash, the Australian fly ash goes in the fluidized dense phase, whereas the Indian fly ash goes in a combination of strand and fluidized dense-phase flow. The prediction of the pressure drop for dense phase flow for a four layer in the pipe is a major task because several layers are present in this flow with various particle size, starts from bottom: strand flow (stationary bed) particle size > 200μm, then strand flow (moving bed) particle size 150 - 200μm, then fluidized dense phase particle size 70 - 150μm and dilute phase flow particle size 10 - 70μm at the top. Various researchers (Wypych, 1994, Jones and Williams, 2003, Mallick, 2010) had developed models for pressure drop prediction for two and three layers but no work has been done till now to model for four layers of dense phase flow.

Objectives

- Dimensionless modelling and validation for pressure drop in dense phase pneumatic conveying of fine powders.

- To develop and validate the four layer modelling for predicting the pressure drop in dense phase pneumatic conveying system in horizontal pipe.

CHAPTER 2: LITERATURE REVIEW

This Chapter is mainly to present a review on the various studies conducted over the years (by different researchers) in the subject of modelling pressure drop for dense-phase pneumatic conveying of fine powders. During the thesis the study was focused on the straight pipe (horizontal one), then in between the modelling it was noticed that we cannot neglect the bends as it played an important role for predicting the total pipe line pressure drop and due attention was provided in this area. Previous case studies of researchers and various modelling methods are illustrated in chronological order further in this chapter.

As Pneumatic conveying is a material transportation process, in which bulk particulate materials are moved over horizontal and vertical distances within a piping system with the help of a compressed air stream or vacuum. Using either positive or negative pressure of air or other gases, the material to be transported is forced through pipes and finally separated from the carrier gas and deposited at the desired destination. Pneumatic systems are completely enclosed. Product contamination, material loss and dust emission (thus, environment pollution) are reduced or eliminated in this case. In general, pneumatic conveying system falls into two main categories on the basis of flow mode: dilute phase, dense phase. Dilute phase conveying is characterized by low product to air mass flow ratio. Dense-phase system is characterized by low velocity and high product to air ratio. Pneumatic conveying of fine powders (which goes in fluidised dense-phase mode), especially for dense-phase conditions is becoming increasingly popular in various industries such as power, cement, chemical, pharmaceutical, alumina, limestone, refinery, due to the reasons of high efficiency, reduced gas flows and power consumption, improved product quality and increased workplace safety (Mallick, 2010).

2.1 Types of flow mode:

- Fluidised dense phase flow
- Slug flow
- Plug flow
- Strand flow

Fluidized Dense Phase:

This mode of transfer takes advantage of the fluidization and air retention properties of the bulk material. Fluidization describes the state which some bulk materials achieve when a gas has been entrained into the void spaces between the particles of the material. Material when in highly fluidized state tends to behave like a fluid (as the term implies) than solid bulk material (Mallick, 2010).

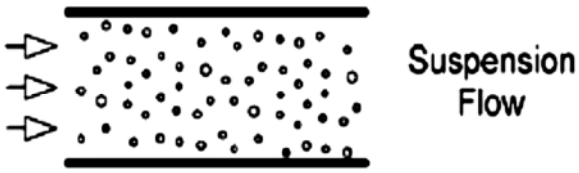

Figure 2.1: Fluidized dense phase (Rabinovich and Kalman, 2010)

The system is characterized by high velocities, although not as high as for dilute phase systems. Product degradation and pipe wear may be lower. Some materials that are being conveyed successfully in fluidized dense-phase include cement, fly ash, pulverized coal, soap powder, zircon sand, crushed bauxite, electrolytic manganese dioxide, lead dust, limestone and flour.

Slug flow: - This mode is suitable for granular products (e.g. sugar, wheat, skim milk powder, poly pellets, peanuts, milled grain, powdered and granulated coffee, sand grinding media).

There is very little inter-particle movement in the full-bore moving slugs.

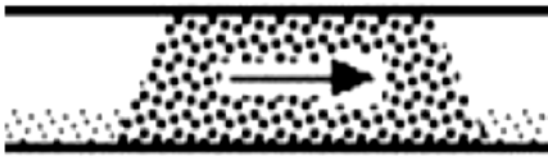

Figure 2.2: Slug Flow (Bhatia, Pneumatic Conveying System)

Plug flow: - The plug flow systems typically transport the product as a series of discrete plugs. This mode appears similar to slug-flow but actually this technology does not produce a stationary layer of material. It provides a solution to the problems of conveying delicate granular materials and products such as plastic granules in high velocity conveying systems.

Figure 2.3: Formation of Plug (Rabinovich and Kalman, 2010)

Strand flow: - In this conveying state, under conditions of constant solid mass flow rate, the pressure drop increases with decreasing air velocity. There is no sharp transition from fully suspended flow to strand type conveying.

At low air velocities and low solid mass flow rate, the strand is stationary and the pressure drop increases (Klinzing, 1990).

Figure 2.4: Strand flow (Mcglinchey et al., 2007)

Industries e.g. cement, chemical, alumina, limestone, pharmaceuticals, carbon fines, milk powders, food, refinery, glass etc. where high efficiency, less power consumption, product quality, workplace safety are the main factors, dense phase conveying plays a crucial role in transporting the materials to a suitable place through the pipeline. Beside this, there are some advantages of pneumatic conveying (dense phase) i.e. various products can be conveyed /transported in a clean manner, it doesn't harm the environment (Mallick, 2010). Various bends can be used to change the directions of the flow of a product.

2.2 Particle characterization:

The particle characterization was an important parameter for predicting the dense phase capabilities of materials (Sanchez et al., 2003). The characteristics of the particle are mentioned as below:

1) Particle size/Particle size distribution
2) Shape
3) Permeability
4) De-aeration
5) Elasticity

1) Particle size/Particle size distribution: The particle size/ particle size distribution are crucial parameters to assess whether materials will be conveyed in dense phase flow. Talking about the Geldart classification and Dixon slugging Diagram which was divided into four areas A, B, C, D. It was suggested that these four areas grouped together products with similar flow capability (Jones and Mills, 1990). According to the Geldart classification diagram group A products are considered to be powders which have good fluidising capability and are identified with the moving bed type flow regime, and group B products are coarser materials which are not likely to be conveyed in dense phase in a conventional system whereas group C products are cohesive, fine powders which can be fluidised although they often have very

good air retention characteristics once mixed with air. The group D products are larger granular products which are possibly candidates for plug or slug flow. This broad classification was an useful guide but it is not reliable (Jones and Mills, 1990).

2) Shape: this also an important factor assess whether the particle flow in plug flow or in wave – like motion flow of solids (Sanchez et al., 2003). These are of two type:

a) Interlocking: If the particles have an interlocking tendency, it will easy to maintain the plug's integrity, but any degradation of the plug would present problems on reformation of the plugs.

b) Spherical: Those particles which are having spherical shape will flow in dilute phase region.

3) Permeability: This parameter depends on particle size/ particle size distribution and shape and offers extremes, from a uniform-sized Geldart group D material with larger permeability factor to a cohesive group C material with low permeability factor. The permeability factor of material decreases, the formation of self-forming plugs decreases. The low-permeability factor of materials will have a greater tendency to convey in a dense phase wave-like motion of flow (Sanchez et al., 2003).

4) De-aeration: The finer the material, the more difficult the experiment and its reproducibility is. Air bubbles can be entrapped in the materials which will cause in the de-aeration process. Larger particles have short de-aeration times then the denser material which reduces them. Fine materials often have a tendency to retain the air longer than the coarser materials (Sanchez et al., 2003).

5) Elasticity: Large particles that are elastic in nature have unique properties. They have the tendency to stick with the pipe surface and to themselves. If this stickiness is dominant, conveying pneumatically is indeed a challenge. The stickiness can assist in the formation of a plug and increases the integrity of the plug. This stickiness also can increase friction at the wall of the pipe, requiring more force and thus more pressure to move the plug (Sanchez et al., 2003).

Modelling by other researchers:

2.3 Pressure drop and solid friction models:

Stegmaier (1978) had worked on an innovative idea of using the power function type formats to represent solids friction factor. His work was further considered by Weber (1981) and other researchers. Stegmaier investigated a number of fine and coarse particles, including fly ash, alumina, quartz powder, sand, catalyst for horizontal transport (with particle size and particle density ranging from 15 to 112 μm and 1500 to 4100 kg/m3, respectively) and established a correlation for solids friction factor, which can be expressed as:

$$\lambda_s = 2.1 m^{*-0.3} Fr^{-1} {Fr_s}^{0.25} (D/d)^{0.1} \quad (2.1)$$

From the range of values of Fr shown in the plot of $\lambda_s m^{*0.3} Fr {Fr_s}^{-0.25} (D/d)^{-0.1}$ versus Fr (Stegmaier, 1978), it seems that Stegmaier had conveyed the products from dilute to dense-phase. However, there appear to be some uncertainties in the definition of Fr_s.

Molerus (1981) defined the full suspended flow with combination of non-dimensional groups i.e. normalized pressure drop in combination with particle Froude number and a Froude number which contains particle fall velocity and pipe diameter. This combination of nondimensional groups defined fully suspended flow. In comparison with pressure drop for pneumatic conveying in horizontal pipes which included changes in particle size, particles density and pipe diameter, these parameters was used to predict the pressure drop and particles slip velocity. His considerations regarding the state diagram of conveying with particle strand in which non-dimensional pressure drop is given as:

$$\frac{\Delta P_z}{(\rho_s-\rho_f)(1-\varepsilon)g f_r \Delta L} \tag{2.2}$$

Vs. the friction number

$$F_{ri} \equiv \frac{\vartheta}{\sqrt{(f_r(\frac{\rho_s}{\rho_f}-1)(1-\varepsilon)Dg)}} \tag{2.3}$$

With the help of state diagram for pneumatic conveying one can differentiate the steady states of pneumatic conveying from instationary states and predicted the pressure drop, which is necessary for the design of transport of the solid material. It was concluded that further experimental work is needed for evaluation of open regime for fully suspended flow of fine particles.

Wirth and Molerus (1981) developed models for finding the pressure drop in strand type pneumatic conveying. Additional pressure drop for strand type pneumatic conveying is given as:

$$\frac{\Delta P_z}{\rho_{s(1-\frac{\rho_f}{\rho_s})(1-\varepsilon)gf_r\Delta L}} = f(F_{ri}, \frac{\rho_f}{\rho_{s(1-\varepsilon)}}\mu, \varepsilon) \tag{2.4}$$

Model for pressure drop with pneumatic conveying over settled layer

$$\frac{\Delta P_z}{\rho_{s(1-\frac{\rho_f}{\rho_s})(1-\varepsilon)gf_r\Delta L}} = \frac{1}{\lambda}\frac{4}{\pi}\frac{[4\phi(1-\phi)]^{1/3}}{\phi^3}F_{ri}^2 \tag{2.5}$$

They had derived some new dimensionless groups and also calculated the behavior of the pressure drop by varying the particle density by a factor up to 2.6, fluid density by a factor up to 1.7, pipe diameter by a factor up to 4 and particle diameter by the factors up to 36.

Rizk (1982) attempted to identify the factors that contributed to the overall solids friction factor (λ_s). He mentioned that λ_s can be separated into two terms:

$$\lambda_s = \lambda_s{}^* \frac{C}{V} + \frac{2\beta}{Fr^2 C/_V} \tag{2.6}$$

Where, λs^* is related to the impact and friction of the solid particles (particle to particle/wall). The term $[2\beta/\{(C/V)Fr^2\}]$ takes into account the influence of weight (i.e. energy loss due to keeping the particles in suspension). It is interesting to note that β refers to the particle fall velocity in a cloud. He considered the individual particles in suspension to be influenced by its surrounding particles.

Klinzing et al. (1989) developed a new correlation for solid friction factor in horizontal pneumatic conveying, based on the unified theory of Yang. They conveyed three types of glass particles (two spherical and one crushed; d as 67,450 and 900 μm; ρ_p as 2470, 2395 and 2464 kg/m^3) and iron ore (flake; d as 400 μm; ρ_p as 5004 kg/m^3) from two horizontal pipes with ID as 0.0266m and 0.0504m. Using Yang's unified theory and knowing the particle velocity as a function independent of □$_s$, they proposed following model:

$$\lambda_s = \frac{3C_{ds}\varepsilon^{-4.7}\rho(V-C)^2 D}{4(\rho_p-\rho)dC^2} \tag{2.7}$$

Here as per the Newton's regime drag coefficient (C_{ds}) is 0.44 and pressure drop is obtained as:

$$\frac{\Delta P_s}{L} = \frac{2\lambda_s \rho_p C^2(1-\varepsilon)}{D} \tag{2.8}$$

The results from above models were compared with the experimental data and the overall standard relative deviation (SRD) is obtained as 42.1%, which is better than the original Yang's model.

Chattopadyay (1989) planned pilot plant/test setup and the experiments was conducted on it with different types of materials and then compared with the conventional dilute phase system. His work was the development of a dense phase conveyance system utilizing secondary air supply line. Various materials were conveyed in the dense phase mode successfully. The Dixon graph (Dixon, 1979) was taken as a reference in which materials was grouped accordingly to their flow criteria without discussing about the particle size distribution, which is mentioned as: Group-A materials e.g. fly ash are easily fluidizable, they collapse only very slowly after the fluidizing air was shut off. Powdery solids belonging to Group-B e.g. fine sand are also easily fluidized but they cannot retain air when the fluidizing air supply was stopped. Group-C materials e.g. raw meal are very cohesive which are difficult to fluidize because the inter particle forces are too long. Group-D materials are very dense powders, often granules. They conclude, the dense phase pneumatic conveying technique was more economical, as far as power consumption was concerned.

Wypych et al. (1990, 1990a) conducted further investigations into long distance conveying of fine pulverised coal (d_{50} = of 21μm; ρ_s = 1495 kg/m3). Experimental PCC (for pipeline of length up to 947.5 m) showed important design criteria, such as the unstable duning boundary. A model for solids friction was presented as:

$$\lambda_s = (m^*)^{-0.4555} (Fr_m)^{-1.13419} (\rho_m)^{-0.2931} (D)^{-0.1088} \quad (2.9)$$

Weber (1991) investigated several formats of solid friction factor for fine granular solids. Where the pressure drop due to air-only and that due to solids-only were considered separately, he suggested that the pressure drop of the solids air mixture was an integral magnitude (i.e. the pressure drop due to air-only and that due to the solids-only were difficult to separate individually). There was a very

strong interaction between the solid and the air during transportation and because the solid, due to contact with the wall, was always transported more slowly that the air.

He developed a new format for representing the pressure drop :

$$\Delta P = \lambda_T \rho \frac{v^2 l}{2} \tag{2.10}$$

Wypych and Pan (1991) modified the incompressible flow formulae to allow for the compressibility effect. The air-only data obtained on straight pipes and bends was used. The experimental facility was set up with a 52 mm I.D. mild steel pipeline and a 2.m manometer with coloured water were used to measure the pressure in the two long pipe which were directly connected to test bends. The least square method was used and the exponents in the modified formulae were determined by minimised the sum of squared errors of the measured pressure along the two straight pipe section.

Formulae used for conveying air:

For bends:

$$\lambda_{fb} = \frac{X_1 \alpha}{R_e^{X_2}} \left(\frac{R}{r_o}\right)^{X_3} \qquad R_e\left(\frac{r}{R}\right)^2 > 91 \tag{2.11}$$

$$\lambda_{fb} = \frac{X_4 \alpha}{R_e^{X_5}} \left(\frac{R}{r_o}\right)^{X_6} \qquad R_e\left(\frac{r}{R}\right)^2 < 91 \tag{2.12}$$

Where:

$$\alpha = 0.95+1.72 \left(\frac{R}{r_o}\right)^{-1.96} \qquad \left(\frac{R}{r_o}\right) < 19.7 \tag{2.13}$$

$$\alpha = 1 \qquad \left(\frac{R}{r_o}\right) > 19.7 \tag{2.14}$$

For straight pipe:

$$\lambda_{fb} = \frac{X_7}{R_e^{X_8}} \qquad \text{or} \qquad \lambda_{fb} = \frac{X_9}{\left[\ln\left(\frac{\varepsilon}{3.7D} + \frac{X_{10}}{R_e^{X_{11}}}\right)\right]^2} \tag{2.15}$$

Where: X_1 to X_{11} are the constants.

It was found that these constants did not vary significantly (i.e. with respect to original incompressible formulae), as long as mean condition (based on average air density) for each straight section of pipe and condition at the outlet of bend were used in the analysis. They showed that modified formulae are able to predict accurately not only the air-only pressure drop due to bends and straight sections of pipes but also the total air-only pressure drop for different configuration of pneumatic conveying pipe line subjected to different operating conditions.

Hong et. al. (1993) developed physical model for gas-solid stratified flow with high solids/gas mass flow rate ratio in horizontal pneumatic conveying. Then the predicted data coincides with ± 30% with experimental data for transporting medium size sand and fine lime in an 8 m long pipe with diameter of 20 mm I.D. The prediction of phase diagram, flow configuration and velocity of sliding bed was also done with their predicted model. Their predicted model is given below:

$$\frac{\Delta P}{L} = \frac{\lambda_{1g}\,\epsilon_1 U_{1ga}^2}{2D_1}\,\frac{P_1}{P_1+P_s} + \frac{\lambda_{2g}\,\epsilon_2 U_{2ga}^2}{2D_2}\,\frac{P_2}{P_2+P_s} + \frac{f_{1s}\,1-\epsilon_1 \rho_s U_{1s}^2}{2D_1}\,\frac{P_1}{P_1+P_s} + f_w D_t\left[2C_2 K_2^2 U_{1s}^2 \theta \rho_s (1-\epsilon_1) + \frac{C_1 g \theta A_1 (1-\epsilon_1)(\rho_s-\rho_g)}{\rho_s(1-\epsilon_1)}\right] + 0.5 g D_1 (1-\epsilon_1)(\rho_s-\rho_g)(\sin\theta - \theta\cos\theta) \tag{2.16}$$

They concluded the stratified flow configuration and velocity of the sliding bed seem to be better predicted by their present model than other models.

Molerus and Burschka (1995) their work was concerned with a simple modification of the Wirth's diagram (Wirth, 1980). The state diagram which represented the stable strand flow was suggested by the Wirth. However, in their state diagram all the non-dimensionless groups contains parameters which have to be determined experimentally. The measured result compared and indicated the applicability of the new diagram even for flow regimes which exceeds strand flow. Various pressure drop predictions have been done in their work. The results were presented in the form of graphs between Friction number (which is $\text{fri} \equiv \frac{v}{\sqrt{\text{fr}\left(\frac{\rho_s}{\rho_f}-1\right)(1-\varepsilon)\text{Dg}}}$) versus Euler number (which is $Eu_p \equiv \frac{(\Delta P_p/\Delta L)2D}{\rho_f v^2}$).

Pan and Wypych (1998) derived a model based on the experimental data from four different fly ash samples with median particle size ranging from 3.5 to 58 μm, particle density and loose poured bulk density ranging from 2180 to 2540 kg/m3 and 634 to 955 kg/m3, respectively. Although this model is a semi-empirical one, it was derived for fly ash of different size range, which covers the median size of the given fly ash samples (30 and 16 μm). Hence, this model was considered relevant for evaluation in this study (for fly ash cases).

$$\lambda_s = 3.2343\ (m^*)^{-0.4673}\ (Fr_m)^{-1.5560}\ (\rho_m)^{-0.4312} \qquad (2.17)$$

Pan (1999) developed a new flow mode diagram based on experimental results and theoretical analysis for the purpose of selecting suitable flow mode for a particular material. The particle/air interaction characteristics are a function of basic particle properties, such as particle size, size distribution, density and shape. From the developed flow mode model, they classified the bulk solid materials into three groups PC1, PC2, PC3 as stated below:

Materials in group PC1 can be transported smoothly and gently from dilute to fluidised dense phase. Materials in group PC2 can be transported in dilute-phase, unstable zone or slug-flow and materials in group PC3 are conveyed in dilute phase only. He concluded that, good accuracy was achieved when many test results with the observed flow modes are superimposed on the developed flow mode diagram, but some exceptions can occur for bulk solids that displayed unusual particle and bulk properties, these bulk solid materials are transported in dilute-phase only.

Laouar and Molodtsof (1997) worked on the characterizing the pressure drop in dense phase pneumatic conveying at very low velocity of 0.2 m/s. In their experimental setup, sand particles of diameter 0.2 mm were transported in horizontal pipes of diameter: 20, 30, 50 and 56 mm and length of approximately 7 m. They investigated two different flow regimes: slug flow and plug flow. They obtained a general pressure drop expression which was shown to be independent for flow regime and pipe diameter. They concluded that the pressure drop law which was derived, accounts for the separate effects of gas volumetric flow rate and solid mass flow rate, which appeared to be the only variables governing the local pressure gradient. The constants involved in the equations are believed to be characteristic for the studied gas-solid system within the considered range of operation.

$$Q(x)|p(x) + P_a| = P_a Q_L \tag{2.18}$$

Where:

$p(x)$ = local relative pressure (kPa)

Q(x) = local gas volumetric flow rate (m^3/s)

Q_L = gas volumetric flow rate evaluated at pipe outlet (m^3/s)

P_a = atmospheric pressure (kPa)

Unit pressure drop was expressed as

$$-\frac{d_p}{d_x} = \frac{a(Q_m - Q)}{cQ + f} \tag{2.19}$$

Where a, Q_m, c, f are functions of the solid flow rate.

Levy and Mason (2000) studied the two-layer model for non-suspension gas-solid flow in pipes. This concept, which was first developed by Wilson (1976) for liquid-solids flow has been adapted to model dense phase conveying of powders in pneumatic conveying system. The flow in a horizontal pipe was modelled as consisting of two layers: a dilute gas solids- mixture, gas and solid phases. Additionally, mass and momentum transfer between two-layers was also calculated. In their work a parametric study was conducted to assess the influence of the boundary conditions on the overall behaviour of the model. They concluded further experimental work was required to obtain sufficient data for model validation.

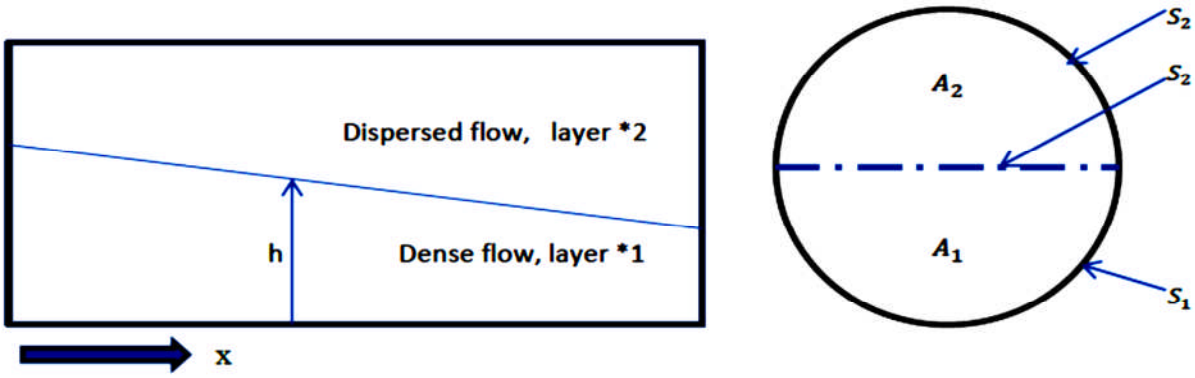

Figure 2.5 The figure shows the two-layer flow (Levy and Mason, 2000)

For two-layer model, Levy and Mason (2000) proposed:

Mass balance equation for the gas and solid phases (dense flow):

$$\frac{d}{dx}\left(r_{g1}\rho_{g1}U_{g1}A_1\right) = S_{mg} \tag{2.20}$$

$$\frac{d}{dx}(r_{s1}\rho_s U_{s1}A_1) = S_{ms} \quad (2.21)$$

Momentum balance equations for the gas and solids phases (dense flow):

$$\frac{\mathrm{d}}{\mathrm{dx}}\left(\rho_{g1}\mathrm{r}_{g1}\mathrm{A}_1\mathrm{U}_{g1}^2\right) = \mathrm{S}_{mg}\mathrm{U}_{g1} - \tau_{g1}\mathrm{r}_{g1}\mathrm{S}_1 - \mathrm{r}_1\mathrm{A}_1\frac{\mathrm{dP}_1}{\mathrm{dx}} - \rho_{g1}\mathrm{r}_{g1}\mathrm{A}_1\mathrm{gsin}(\beta) + \mathrm{F}_{d1} \quad (2.22)$$

$$\frac{\mathrm{d}}{\mathrm{dx}}(\rho_{s1}\mathrm{r}_{s1}\mathrm{A}_1\mathrm{U}_{s1}^2) = \mathrm{S}_{ms}\mathrm{U}_{s1} - \tau_{s1}\mathrm{r}_{s1}\mathrm{S}_1 + \left(\mathrm{r}_{g2}\tau_{gsi} + \mathrm{r}_{s2}\tau_{ssi}\right)\mathrm{r}_{s1}\mathrm{s}_i - \mathrm{r}_{s1}\mathrm{A}_1\frac{\mathrm{dP}_1}{\mathrm{dx}} - \rho_{s1}\mathrm{r}_{s1}\mathrm{A}_1\mathrm{gsin}(\beta) + \mathrm{F}_{d1} \quad (2.23)$$

Fluid-particles interaction for drag force per unit length was given as:

$$\mathrm{F}_{d1} = \frac{3\mathrm{r}_{s1}\mathrm{A}_1}{4\mathrm{D}_p}\mathrm{C}_{d1}\rho_{g1}\left(\mathrm{U}_{g1} - \mathrm{U}_{s1}\right)|\mathrm{U}_{g1} - \mathrm{U}_{s1}| \quad (2.24)$$

Hirota et al. (2002) studied the effect of mechanical properties and the angle of inclined pipe on the pressure drop for pneumatic conveying of fine powders. The experimental results were compared with their predicted values using model. The experimental programme was conducted to find the pressure drop of pneumatic conveying of fine powders with angles: 0, 20, 30, 45, 60 and 90° pipe inclination and pressure drop was estimated from dynamic friction factor coefficient. In their experimental program, three test powders: fly ash, silica and soft flour were used, whose data are given in the table below: -

Table 2.1: - Properties of sample powders

Sample powders	Medium particle diameter, (μm)	Particle density, (kg/m^3)	Coefficient of dynamic internal friction
Silica	3.2	2650	0.84
Fly ash	13.2	2320	0.60
Soft flour	26.0	1400	0.76

Silica was conveyed in the strand, fly ash in slug and the soft flour were conveyed in fully suspended flow. Based on the results obtained they concluded that pressure drop in the pneumatic conveying of fine powder can be estimated from dynamic friction coefficient and the inclined angle of the pipe.

Pressure drop of powder plug conveying in a horizontal pipe, proposed by Tsuji (1984):

$$\frac{\Delta p}{L} = 2\mu_{di}(1-\varepsilon)\rho_p g \tag{2.25}$$

Equation for the pressure drop proposed by Morikawa (1988):

$$\frac{\Delta p}{L} = \mu_w(1-\varepsilon)\rho_p g \tag{2.26}$$

Jones and Williams (2003a) worked on developing the model for solid friction factor for fluidized dense-phase conveying. The series of calculation was performed on experimental data in order to estimate solid friction factor (λ_s) for four types of material conveyed in the fluidized dense phase flow regime.

Table 2.2: Bulk materials conveyed in dense phase modes of flow

Material	Mean diameter, (μm)	Size range 2.5% -97.5%, (μm)	Particle density, (kg/m^3)	Mode of flow
PFA	42	5-120	2446	Fluidized
Iron powder	64	20-100	5710	Fluidized
Copper	55	11-600	3950	Fluidized
Flour	90	40-120	1470	Fluidized
Poly pellets	4000	4000-4000	912	Slug/plug

Two phase fluid pressure drop model:

$$\Delta P = (\lambda_f + m^* \lambda_s) \frac{\rho_{f,ave} v_{ave}^2}{2} \frac{L}{D} \quad (2.27)$$

Model for solid friction factor for dense phase (λ_s) was derived as:

$$\lambda_s = \frac{83}{m^{*0.9} Fr_i^2} \quad (2.28)$$

Where, Froude number is at inlet of pipe:

$$Fr_i = \frac{v}{(gD)^{0.5}} \quad (2.29)$$

Wypych and Yi (2003) suggested that optimum pneumatic conveying of the bulk materials could be achieved by controlling the air mass flow rate within certain range, and appropriate selection of pipe diameters. They presented a new theoretical model based on the observed unstable flow mechanism and stability criteria for the purpose of predicting transport boundaries. The pneumatic conveying of granular material through a horizontal pipe can exhibit three main flow modes: low-velocity slug flow, dilute-phase flow with suspended particles/strands and strand flow over a stationary layer (for low solid mass flow rates) or moving layer (for high solid mass flow rate). They concluded,

modelling relies on the particle and bulk properties of the material being conveyed and pipe wall properties.

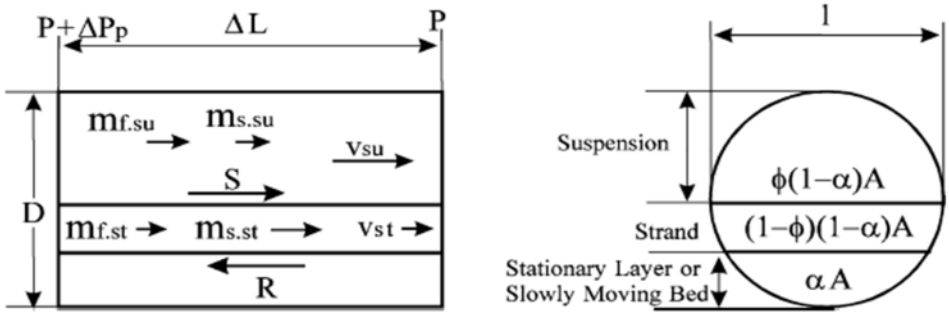

Figure 2.6 Flow elements in horizontal pipe for strand flow (Wypych and Yi, 2003)

For three layer flow, model for transition zone was provided as;

Non-dimensional pressure in horizontal pipe was expressed by:

$$\frac{\Delta P_P}{f_P \rho_P (1-\rho_f/\rho_P)(1-\varepsilon) g \Delta L} = (1 - \emptyset) \tag{2.30}$$

Non-dimensional friction number was given as :

$$F_{ri}^2 = \frac{v^2}{f_P (\rho_f/\rho_P)(1-\rho_f/\rho_P)(1-\varepsilon_{st}) gD} \tag{2.31}$$

Jones and William (2003b) reviewed classification diagrams used to predict the basic modes of flow of bulk materials in dense phase pneumatic conveying. An extensive conveying trial was done with wide range of materials. Results show that while these classifications are helpful for selecting the flow modes for various materials, they do not provide a totally reliable prediction. In this paper the work showed the potential for the use of loose-poured bulk density instead of the particle density and permeability instead of mean particle size. These parameters provided an improved method of classification of material for pneumatic conveying capability. In results they concluded that the initial

investigation of these parameters have the potential to provide an improved method of predicting pneumatic conveying capability, however considerable work is required to develop and refine the technique.

Sanchez et al. (2005) reviewed the models and correlations for dense phase conveying. Series of experiments with industrial scale tests showed agreement with Mi. (1994) model. They examined existing models of dense phase conveying with experimental data of: Muchelknautz and Krambrock (1969), Konrad (1981), Kano et al. (1984), Borzone (1985), Gu (1988), Aziz (1990), Mi. (1994) and Koldehoff (1999) were used to evaluate the accuracy in the models for pressure drop. All the models were tested with the available data and analysed. They concluded that from the various researcher models, Mi model gave good agreement with most of the data evaluated, falling ±25% of the model. This model was an improvement over Konrad model.

Table 2.3 Dense Phase Conveying Model:

Reference	Dense phase conveying mode
Muchelknautz and Krambrock (1969)	All modes
Konrad (1981)	Plug
Kano et al. (1984)	Plug
Borzone (1985)	Plug
Gu (1988)	Plug
Aziz (1990)	Plug/High Loading
Mi. (1994)	Plug
Koldehoff (1999)	Plug

Table 2.4 Comparison of Mi (1994) data with Muchelknautz and Krambrock (1969) model (as per Sanzhez, 2005) :

Range	Mi (1994)	Data Muchelknautz and Krambrock (1969)
<25%	88%	100%
>25%–<50%	11%	0%
>50%–<75%	0%	0%
>50%–<75%	1%	0%
>100%	0%	0%

Table 2.5 Evaluation of data with Mi (1994) model (as per Sanchez, 2005) :

Range error	Mi	Brozone	Aziz	Gu	Kano
<25%	90.8%	98.1%	85.5%	97.9%	72.7%
>25%–<50%	8.3%	1.9%	14.5%	2.1%	13.6%
>50%–<75%	0.0%	0.0%	0.0%	0.0%	9.1%
>50%–<75%	0.8%	0.0%	0.0%	0.0%	4.5%
>100%	0.0%	0.0%	0.0%	0.0%	0.0%

Rizk (2006) used various dimensionless numbers for the scale-up models which were regarded as applicable and for safe design. For the design of a pneumatic conveying system, flow modes and the flow properties of the designated product must be known. The scale-up functions in turned constituted of dimensionless numbers that described the gas-solid flow in pipes. Also these can be used for describing the boundaries i.e. avoidance of erosion.

Pressure loss due to presence of solid particle in the air stream:

$$\frac{\Delta P_s}{\Delta L} = 0.5\ \mu\ \lambda_s\ Fr^2\ \rho_{fg} \tag{2.32}$$

Where Dimensionless additional pressure drop:

$$\lambda_s = \lambda^*_{ifr}\frac{c}{v} + \frac{2\beta}{Fr^2\frac{c}{v}} \tag{2.33}$$

From the above equation three boundaries can be derived:

Case 1: Gas velocity very high (dilute phase and low mass loadings):

$$\lambda_s = \lambda^*_{ifr}\frac{c}{v} \tag{2.34}$$

Case 2: Gas velocity lower (medium gas velocities, above saltation velocity):

$$\lambda_s = \lambda^*_{ifr}\frac{c}{v} + \frac{2\beta}{Fr^2\frac{c}{v}} \tag{2.35}$$

Case 3: Gas velocity below saltation (dunes and plugs):

$$\lambda_j = \lambda^*_{fr}\frac{c}{v} \tag{2.36}$$

Satisfactory results obtained when the material Polypropylene was used in their test set-up with distances ΔL = 300,700 and 1100 meter with pressure of approximate ΔP = 3 - 3.3 bar with mass load ratios μ = 2. . They concluded the use of a data base with dimensionless number will help access to interpolate and gained time for estimation of pressure loss of a new system to be designed.

Wypych and Hastie (2006) investigated the power- function modelling of solids friction factor for the dilute-phase and fluidised dense-phase conveying of powders.The three different diameters/ lengths

(69 mm-168 m, 105 mm-168 m, 69 mm-554 m) of the pipe line were used to generate the wide range of steady state data and also explored important scale-up issues. Straight pipe frictional data was taken into consideration for scaling-up and general power function format was used throughout for their work.

General power function (e.g. Stegmaier,1978):

$$\lambda_s = \mathrm{K}\,(\mathrm{m}*)^{\mathrm{a}}\,(\mathrm{Fr_m})^{\mathrm{b}} \tag{2.37}$$

$$\lambda_s = \mathrm{K}\,(\mathrm{m}*)^{\mathrm{a}}\,(\mathrm{Fr_m})^{\mathrm{b}}\left(\frac{\rho_{fm}}{\rho_s}\right)^{c}\left(\frac{d}{D}\right)^{d} \tag{2.38}$$

The two methods for solving λ_s was suggested by them (i) either calculating manually using Excel or (ii) commercial software package called Sigma plot.

For investigating the scale-up issues in their experimental test programme fly ash was used for two straight pipe sections for analysis and comparisons. They concluded that power function with tapping's P11-P12 for 69 mm – 168 m with K=1 and R^2 = 0.976:

$$\lambda_s = (\mathrm{m}*)^{-0.2683}\,(\mathrm{Fr_m})^{-1.5454}\ \text{(Manually calculated method)} \tag{2.39}$$

$$\lambda_s = (\mathrm{m}*)^{-0.2746}\,(\mathrm{Fr_m})^{-1.5329}\ \text{(By Sigma Plot software)} \tag{2.40}$$

gave good results in predicting the pressure drop with plotted PCC and also for scale-up conditions.

Jones and Williams (2008) discussed about the techniques available, which are commonly used for predicting mode of flow. Two types of predicted charts were defined: basic particle parameter based (e.g. particle size and density) and air-particle parameter based (e.g. permeability and de-aeration). The basic particle techniques generally given an accurate prediction of fluidised dense phase capabilities and to a lesser extent, the plug flow capable materials when loose poured bulk density is applied. However, it must be noted that the air particle parameter based technique had a smaller set of bulk material data to compare predictive performance. They showed in the results that the

potential for the use of loose-poured bulk density as an alternative to the density and the permeability. These two parameters provided an improved method of classification of materials for pneumatic conveying capability and overcome the problems with determining de-aeration values.

Rinoshika and Suzuki (2010) focused on the effect of the mounted dune model in the horizontal pneumatic conveying system in terms of pressure drop, power consumption and conveying velocity. Their experimental setup consisted of a horizontal smooth acrylic tube with an inside diameter of 80 mm and length of about 5 m. Polyethylene spherical particles with particle density of 952 kg/m^{3}and diameters of 2.3 and 3.3 mm were used as conveying materials. The mean air velocity was varied from 9 to 16 m/s and the solid mass flow rate was varied from 0.25 to 0.45 kg/s.

They found at the lower air velocity range the pressure drop of the pneumatic conveying with dune model (see following equation) is lower than that of a conventional pneumatic conveying dune model for total pressure drop and power consumption was given by :

$$E = \frac{\Delta p Q_a}{g G_s L} \tag{2.41}$$

Mallick (2010) developed the two layer model based on the actual flow condition in dense-phase (i.e. considering the presence of a non-suspension layer), as shown in the figure below:

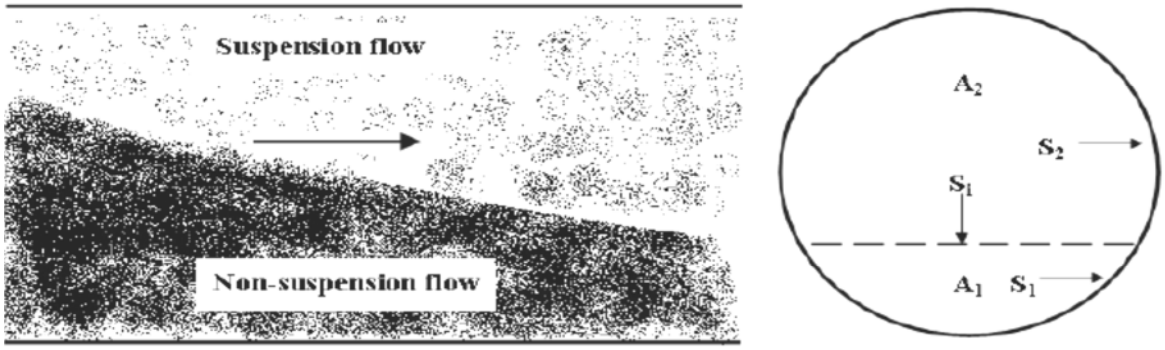

Figure 2.7 Shows Two-Layer Flow of Fine Powders in Dense-phase region (Mallick, 2010)

He considered in his thesis that, as the interface between the non-suspension and suspension layers are not very distinct under real flow conditions and also the height of the non-suspension layer keeps on fluctuating due to the highly turbulent nature of flow.

For two layer model, (Mallick,2010) proposed:

$$\Delta P = (L/A)\ (\tau_1 S_1 + \tau_2 S_2) \tag{2.42}$$

$$\tau_1 = 0.5\ (\lambda_{non\text{-}sus})\ (\rho_{non\ sus})\ V^2 \tag{2.43}$$

For the suspension layer (Barth,1958):

$$\tau_2 = 0.5\ (\lambda_f + m^*\lambda_{sus})\ \rho\ V_1^2 \tag{2.44}$$

Whereas λ_{sus} can be found out from "modified Weber A4 model":

$$K_1 = [\{(V-C)/w_{f0}\}^2\ 2\ (C/V)/(\lambda_s\ Fr\ *^2)]^{0.5} \tag{2.45}$$

Recently, Rinoshika and Yan (2011) analyzed the particle velocity and concentration characteristics in the horizontal pneumatic conveying with dune mode, so as to reveal the mechanism of low-conveying velocity and energy saving conveying. Their test setup consisted of horizontal smooth acrylic tube with an inside diameter of 80 mm and length of about 5 m. The polyethylene particles with density 978 kg/m^3 and 952 kg/m^3 with diameter of 2.3 and 3.3 mm was used as conveying materials. In their test set up they used high speed PIV (particle image velocimetry) to measure the time averaged particle velocity. The particle velocity and concentration distribution were measured at mean air velocities of 12 m/s and 13 m/s and the solid mass flow rates of 0.45 kg/s and 0.43 kg/s. They compared the particle velocity and concentration profiles between dune model and non-dune model. They concluded that the effect of dune model (it was a new method for saving potential energy in pneumatic conveying system by low pressure and low velocity and using minimum kinetic energy to convey particles) on the velocity profile of relatively small particles is larger than that of larger particles.

Cai et al. (2011) studied the influence of moisture content on conveying characteristics with conveying pressure up to 4 MPa in their test set up. Soft coal and lignite with similar density and particle size was included in the test setup. With an increase in moisture content, conveying mass flow rate decreased for lignite (3.24 %< M < 8.18 %) and for soft coal it first increased and then decreased (0.4 % < M < 6.18 %) at same operating parameters. They investigated the particle charge and surface moisture content to indicate the influence mechanism of moisture content on mass flow rate in pneumatic conveying at high pressure. Pressure drop of soft coal was greater than that of lignite for the same test setup. The electrostatic forces decreased with increasing moisture content because of the conductive properties of water and liquid bridge of coal particles decrease flow ability. They concluded that when the moisture content exceeded 8.18 %, the conveying pipe was often blocked and the pulverized coal could not be conveyed properly.

2.4 Bend models:

Although in recent years some efforts have been made to model the solids friction factor for fine powder and hence the pressure drop for straight horizontal pipe lengths, but the issue of investigating the impact of selection of a bend model on the prediction of total pipeline pressure loss has not been given similar attention. As a result, the number of bend models available in literature for evaluation/use for the cases of fine powder systems is somewhat limited. The literatures studied regarding the bend models are listed below:

Chambers and Marcus (1968) presented the total pressure loss in bends due to the solids and flow of air, which was given as below:

$$\Delta p\, b = N\, B\, (1+ m^*)\, \rho\, V^2/2 \qquad (2.46)$$

Other researchers (Jones and Williams, 2003; Williams and Jones, 2006) used this bend model in their "back calculation" method of deriving an expression for the solids friction factor. The model was selected for evaluation in the present study due to its apparent popularity.

Marcus et al. (1985) studied the pressure loss due to initial acceleration and flow through bends. For bend pressure loss and proposed model for acceleration pressure loss formulas are given below:

$$\Delta P_{accel} = m^* \rho V C \quad (2.47)$$

$$\Delta P_b = B \rho V^2/2 \quad (2.48)$$

Where ρ and V are the density and velocity of the gas at the solid intake zone respectively as per Marcus et al.(1990) and the value of B can be taken from the following table which indicates that the sharper the bend, the higher the calculated pressure drop:

Table 2.6: values of bend pressure loss factor, Marcus et al. (1985)

Bend radius/ Pipe diameter (R_B/D)	B
2	1.5
4	0.75
6	0.5

Pan and Wypych (1998) conducted test on a scaled-up design procedure by conveyed four different samples of fly ash (ρ_s 2197 to 2540 kg/m^3; ρ_{bl} 634 to 955 kg/m^3; d_{50} 4 to 58 μm) in various test rig combination (D = 52.5 to 105 mm; L = 70 to 564 m). It was found that different fly ash samples produced different conveying characteristics. The corresponding models for bends were found to be different. Combining the data of all four fly ash samples, the following correlations were derived:

$$\Delta p\, bs = 0.5\, m^*\, \lambda bs\, \rho bo\, V_{bo}^2 \quad (2.49)$$

$$\Delta \lambda bs = 0.0097\, (m^*)^{0.57} (Frbo)^{0.97}\, (\rho bo)^{-0.62} \quad (2.50)$$

CHAPTER 3: Dimensionless Modelling For Pressure Drop For Dense Phase Pneumatic Conveying.

3.1 Developing Model Approach:

From the review of the literature (chapter 2), it appears that for representing the pressure drop for a solid-gas mixture the most popular form was through a straight horizontal section of pipe by using the Stegmaier (1978) equation. As the main challenge was to determine the solid friction factor accurately because the modelling of the dense phase conveying of powders (e.g. fly ash and ESP dust) have been a difficult problem to solve. Previous investigations (Chapter 2) to examine the scale-up accuracy and stability of the different "existing" models for solids friction (Stegmaier, 1978; Weber, 1981; Pan and Wypych, 1998; Jones and Williams, 2003), compared the predicted and experimental pneumatic conveying characteristics (PCC) for fly ash and ESP dust. It shows that the models generally can provide inaccuracy under significant scale-up conditions of diameter and length. The findings demonstrated that the limitation of the existing models (derived by various researchers), the investigation would have been more fair and comprehensive if new models have been derived using the conveying data of the same powders (i.e. fly ash and ESP dust) and then evaluated under different diameter and length scale-up conditions. The pressure drop characteristics of pneumatic conveying systems depends on the product properties to a great extent, such as particle size, size distribution, particle and bulk densities, shape and surface roughness (Pan, 1992). A change in any (or in combinations) of the above can cause significant variations in solids friction, even for the same pipe (Wypych, 1989). Therefore, an effort has been made to develop a model which will predict the pressure drop with significant accuracy under scale up conditions. The design parameters are chosen in such a way that the effect of every parameter came into play directly or indirectly.

Keeping above points in mind, the pressure drop per unit length of solid $\left(\frac{\Delta P_s}{L}\right)$ is assumed to be a function of diameter of the particle (d), difference between velocity of air and that of particle $(V_a - V_p)$, density of air (ρ_a) and mass flow rate of solid (m_s) . The expression obtained is as follows:

$$\frac{\Delta P_s}{L} = f\,(m_s, (V_a - V_p), \rho_a, D)$$

In particular, certain assumption may be necessary in the development of mathematical models, such as perfectly spherical particles, perfectly smooth particles.

The development of the model is done on the basis of "BUCKINGHAM π THEOREM" which states that "If there are n variables in a problem and these variables contain m primary dimensions (for example M, L, T) the equation relating all the variables will have (n-m) dimensionless groups" (Cengel, 2003). In this theorem the repeating variables have been selected, are those which we think will appear in all or most of the π groups, and are an influence in the problem.

The primary variables are:

$$\frac{\Delta P_s}{L}, m_s, (V_a - V_p), \rho_a, D$$

The repeating variables were selected in a way that one variable contains geometric property, other variable contain flow property and third variable contain fluid property:

Repeating variables are as follows:

$$m_s, (V_a - V_p), \rho_a$$

Where:

m_s = geometric property

$(V_a - V_p)$ = flow property

ρ_a = fluid property

Where:

$\frac{\Delta P_s}{L}$ $[M\ L^{-2}T^{-2}]$

m_s $[M\ T^{-1}]$

$(V_a - V_p)$ $[LT^{-1}]$

ρ_a $[ML^{-3}]$

D [L]

Note: [M, L, T] are the fundamental dimensions.

Now the number of π terms can be finding as (n – m) where 'n' is the primary variable and 'm' is the repeating variable.

So, n – m = 5 - 3 = 2 π terms.

Now

First π term:

$\pi_1 = m_s^{a1} (V_a - V_p)^{b1} \rho_a^{c1} \frac{\Delta P_s}{L}$

$[M^0L^0T^0] = [M\ T^{-1}]^{a_1}\ [LT^{-1}]^{b_1}\ [M\ L^{-3}]^{c_1}\ [M\ L^{-2}T^{-2}]$

$M = a_1+c_1+1 = 0$

$L = b_1- 3c_1-2 = 0$

$T = -a_1-b_1-2 = 0$

Solving for the above equations for the values of $a_1,\ b_1,\ c_1$ you will get:-

$$a_1 = 0.5$$

$$b_1 = -2.5$$

$$c_1 = -1.5$$

Now, $\pi_1 = m_s^{0.5} (V_a - V_p)^{-2.5} \rho_a^{-1.5} \frac{\Delta P_s}{L}$

$$\frac{m_s^{2.5} \frac{\Delta P_s}{L}}{(V_a - V_p)^{2.5} \rho_a^{1.5}} = \pi_1 \qquad (3.1)$$

Similarly for the second π term same procedure will be followed i.e.

$\pi_2 = m_s^{a2} (V_a - V_p)^{b2} \rho_a^{c2} D$

$[M^0L^0T^0] = [M\ T^{-1}]^{a_2}\ [LT^{-1}]^{b_2}\ [M\ L^{-3}]^{c_2}\ [L]$

$M = a_2 + c_2 = 0$

$L = b_2 - 3c_2 + 1 = 0$

$T = -a_2 - b_2 = 0$

Solving the above equations for the values of a_2, b_2, c_2 you will get:-

$$a_2 = -0.5$$

$$b_2 = 0.5$$

$$c_2 = 0.5$$

Now, $\pi_2 = m_s{}^{-0.5} (V_a - V_p)^{0.5} \rho_a{}^{0.5} D$

$$\pi_2 = \frac{D (V_a - V_p)^{0.5} \rho_a{}^{0.5}}{m_s{}^{0.5}} \quad (3.2)$$

But:

$$f(\pi_1, \pi_2) = 0$$

It can be written as:

$$\pi_1 = f(\pi_2)$$

Now:

$$\frac{m_s{}^{2.5} \frac{\Delta P_s}{L}}{(V_a - V_p)^{2.5} \rho_a{}^{1.5}} = k \left(\frac{D (V_a - V_p)^{0.5} \rho_a{}^{0.5}}{m_s{}^{0.5}} \right) \quad (3.3)$$

After getting both the π terms, assuming $\pi_1 = X$ and $\pi_2 = Y$, now combining these in one equation which is as follows:-

$$\frac{\Delta P_s}{L} = K X^a Y$$

Where K = constant.

Now $\frac{\Delta P_s}{L}$ can be rewritten by putting the values of X & Y in the above given equation, we get:

$$\frac{\Delta P_s}{L} = K \left(\frac{D (V_a - V_p)^{0.5} \rho_a{}^{0.5}}{m_s{}^{0.5}} \right)^a \left(\frac{\rho_a{}^{1.5} (V_a - V_p)^{2.5}}{m_s{}^{0.5}} \right) \quad (3.4)$$

Where 'a' is the exponent.

Assuming that $V_p = 0.8\,V_a$ because in the dense phase region velocity of the particle decreases. When the percentage of the particle decreases it means they moved from dilute phase to dense phase region. The particle in this region (dense phase) was conveyed in either slug flow or in plug flow, so the above equation was written as:

$$\frac{\Delta P_s}{L} = K \left(\frac{D\,(0.2V_a)^{0.5}\,\rho_a{}^{0.5}}{m_s{}^{0.5}}\right)^a \left(\frac{\rho_a{}^{1.5}(0.2V_a)^{2.5}}{m_s{}^{0.5}}\right) \qquad (3.5)$$

The coefficient 'K' and exponent 'a' can be found out with the help of regression method. Once getting the values then comparing with the experimental values and check if the predicted values are correct or not.

For $P_9 - P_{10}$, these were the static pressure measurement tapping points which were installed to provide "straight pipe" pressure loss data for the modelling of solids friction**:**

When K ≠ 1, the values are:

$$\frac{\Delta P_s}{L} = K \left(\frac{D\,(0.2V_a)^{0.5}\,\rho_a{}^{0.5}}{m_s{}^{0.5}}\right)^a \left(\frac{\rho_a{}^{1.5}(0.2V_a)^{2.5}}{m_s{}^{0.5}}\right) \qquad (3.6)$$

Coefficient 'K' $= 10^{-6.30236}$

Exponent 'a' = -4.6436

Correlation coefficient R^2 = 0.914

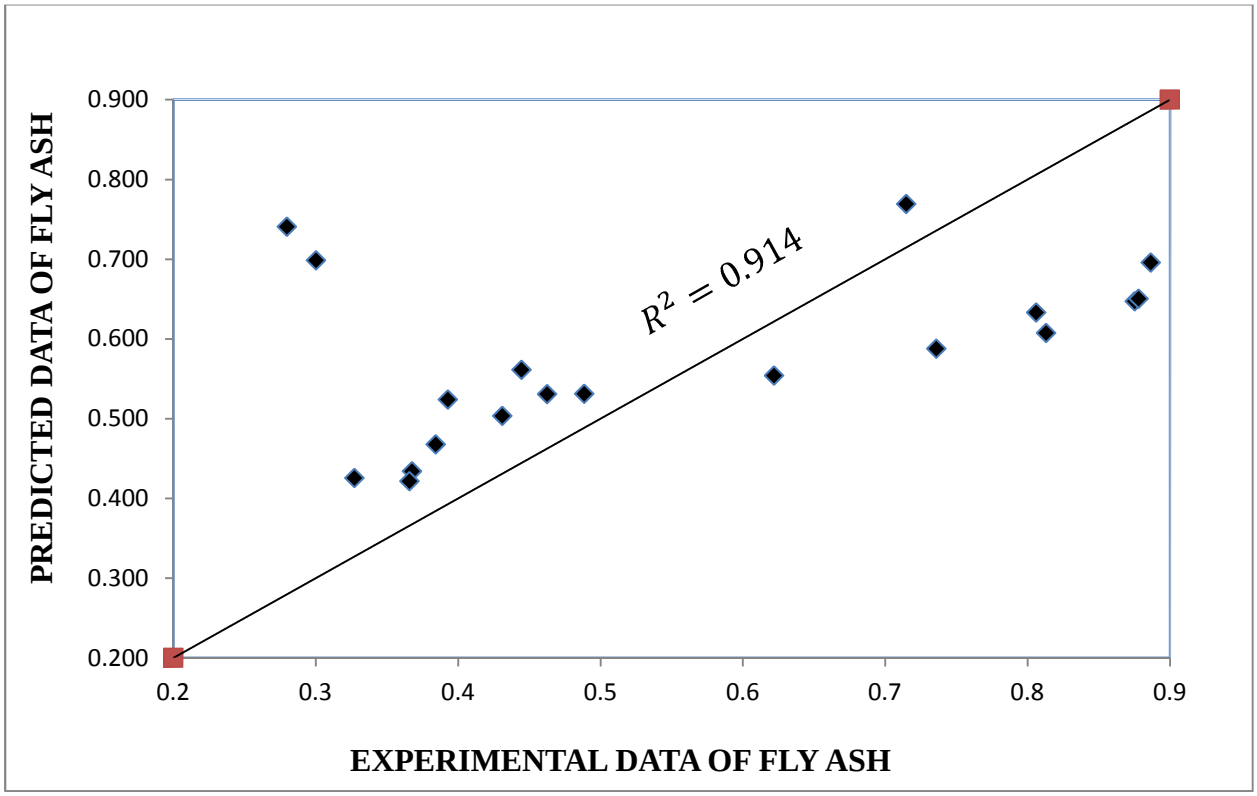

Figure 3.1: Experimental Versus Predicted data of P9-P10 for 69-168.

When K = 1, the values are:-

K = 10^0

a = 0.871288

R^2 = 0.69

The low value of R^2 for the model suggests that the agreement between the experiment and the predicted values was not good, so it should not be considered as the chances of getting errors were more.

For $P_{11} - P_{12}$, these were the static pressure measurement tapping points which were installed to provide "straight pipe" pressure loss data for the modelling of solids friction:

When K ≠ 1, values are:

K = $10^{-6.2298}$

a = -4.46366

R^2 = 0.939

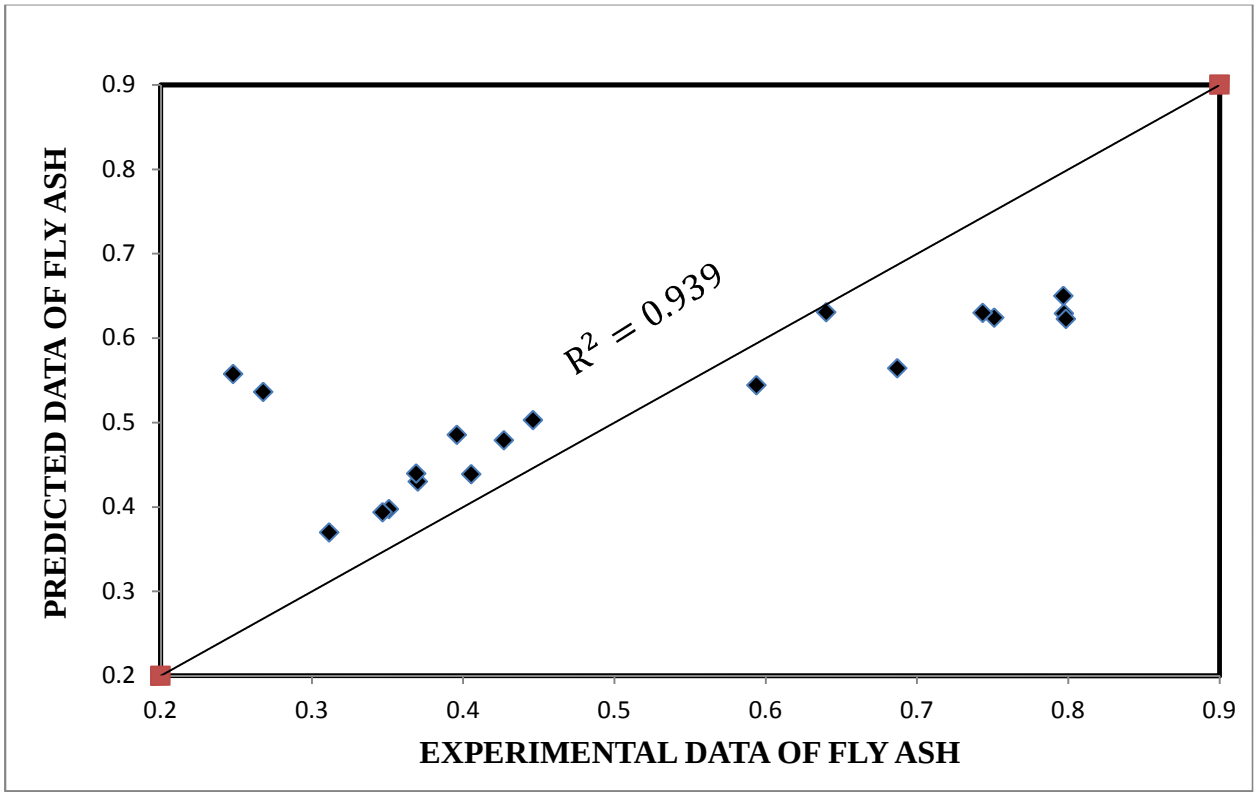

Figure3.2: Experimental Versus Predicted data of P11-P12 for 69-168.

When K = 1, values are:-

K = 10^0

a = 0.98779

R^2 = 0.749

The above value of R^2 is less so it should not be considered because it is not satisfying the experimental values against which we use that developed model. The low value of R^2 indicates that the chance of error were more.

The points plotted in the graph (i.e. figure 3.1 and 3.2) between the experimental values and predicted values gave satisfactory results, as the value of R^2 was high which indicates that the agreement between experimental and predicted values was good. As the model developed for "fly ash" with the static pressure measurement tappings P9-P10 and P11-P12 showed good results with high R^2 value. So this model was chosen for predicting the pressure drop under scaling-up conditions.

The calculation of the pressure drop was done with the help of "MACRO" it is the iterative programme used in Excel 2003. This software was used for predicted the pressure drop in the total pipeline. A macro is an action or a set of actions that you can use to automate tasks. Macros are recorded in the Visual Basic for Applications programming language. This programme made the calculation easier for very complex problems. This method was originally used by Mallick (2010) in their thesis. The programme works like this, the pipeline was firstly divided small parts then taking the end point as the entry point while assuming the pressure to an atmospheric pressure (i.e. 1 bar). Then for an each section of the pipe-line the pressure was calculated, through this at the entry of the pipe line the pressure drop in the straight-line was obtained, similarly in case of bends. At the end of the each segment of the pipe the pressure was assumed as atmospheric and then iteration was performed on them. Iterations was performed in the solver which was used in excel. The whole programme was edited or written in the Visual Basic Editor (VBE), which performed iterations to a significant accuracy. The programme was written and used by Mallick (2010) which was further

modified by changing the expression for calculating pressure drop, the sample of the modified programme for 69 mm ID and 168 m long pipe line is provided in Appendix A.

The model used for predicting the pressure drop and obtaining the PCC:

$$\frac{\Delta P_s}{L} = \left[K \left(\frac{D\,(0.2V_a)^{0.5}\,\rho_a{}^{0.5}}{m_s{}^{0.5}} \right)^{a} \left(\frac{\rho_a{}^{1.5}(0.2V_a)^{2.5}}{m_s{}^{0.5}} \right) + \frac{\lambda_f Va^2 \rho_a L}{2D} \right] \tag{3.7}$$

3.2 Pneumatic Conveying Characteristic (PCC):

3.2.1 FLY ASH:

The total pipeline Pneumatic Conveying Characteristics was obtained for fly ash with 69 mm ID-168 m Length, 105 mm ID-168 m Length, 69 mm ID-554 m Length are presented in figures while assuming the velocity of the particle (V_p) will be 80% of the velocity of the air (V_a). The total pipeline pressure drop (ΔP) includes all the losses across the entire pipeline, such as the losses occurring in the straight horizontal lengths, bends, and verticals and due to initial acceleration (at the entry/feed point of the pipe). These PCC was obtained while taking the experimental data and solved with the predicted model with the help of "MACRO" the iterative programme used for finding the pressure drop in total pipeline. As this starts at the exit of the pipeline and goes up to the inlet of the pipe where the pressure drop in all the segments of pipeline was individually calculated, while doing this we got the pressure drop in the total pipe line. However, the pressure drop in the bends was also calculated. Then while putting the different values of mass flow rate of air(m_f) we got the different pressure drop points in each section of the pipeline.

Below PCC are plotted for 69 mm ID-168 m Length, 105 mm ID-168 m Length and 69 mm ID-554 m Length for P9-P10 tapings with K≠1:

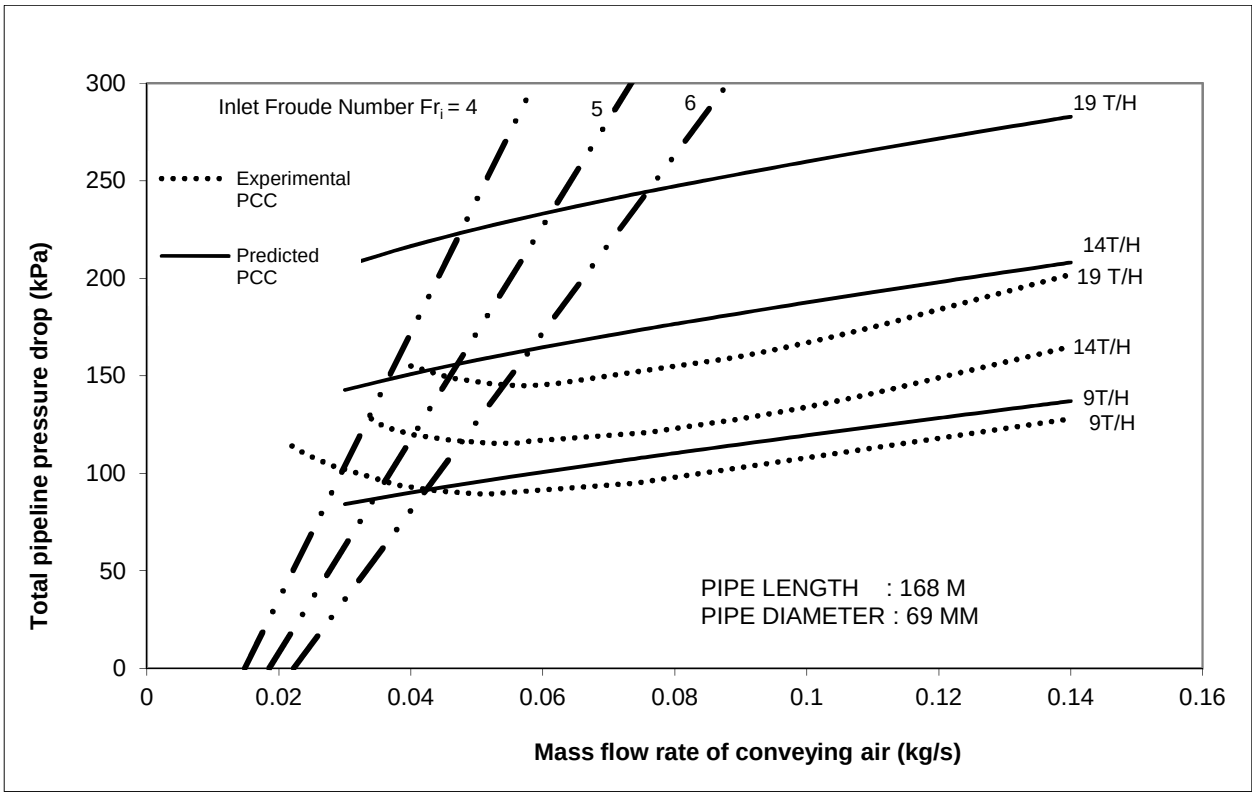

Figure 3.3: Comparison of Experimental and Predicted values of total pipeline pressure drop (fly ash: 69 mmI.D.-168 m length, for P9-P10 model-I, where K≠ 1)

The results showed in above figure for the 69 mm ID × 168 m L with K≠ 1 , the predicted PCC over-predict the experimental PCC quite considerably. For 9 t/h the predicted line somewhat closer to the experimental line, but as the mass flow rate of solid increases (19 t/h and 14 t/h) the predicted line over predicts the experimental line. However, no line results in "U"-shaped PCC.

Even within the dense-phase region, the predicted pressure drop values continue to decrease with decrease in air flow rate, i.e. trends of predictions are similar to a dilute-phase model.

The result showed in the above plotted PCC that as the mass flow rate of solid increases the predicted line over predicts the experimental line. Now for avoiding the over prediction of the predicted line

the percentage of velocity of particle (V_p) from 80% was changed to first 90%, 70% then 50% to see how the pressure drop values obtain. However, after getting the models of changed V_p (velocity of particle) it was solved with “MACRO” after that PCC were plotted accordingly. The PCC plotted over the Experimental data, results showed that the values came was different to the previous model values and for that reason different PCC were plotted to see for what percentage the model give results. While changing the percentage of velocity of air the values of the pressure drop in the pipeline was change linearly and the results are showed below.

The PCC plotted for the same 69 mm I.D.-168 m length between the pressure tapings P9-P10 but with the scale-up percentage of velocity of particle (V_p).

Model for $V_p = 0.9V_a$:

$$\frac{\Delta P_s}{L} = \left[K \left(\frac{D\,(0.2V_a)^{0.5}\,{\rho_a}^{0.5}}{{m_s}^{0.5}} \right)^{a} \left(\frac{{\rho_a}^{1.5}(0.2V_a)^{2.5}}{{m_s}^{0.5}} \right) + \frac{\lambda_f V a^2 \rho_a L}{2D} \right] \quad (3.8)$$

For 69 mm ID-168 m L, P9-P10 (when $V_p = 0.9V_a$):

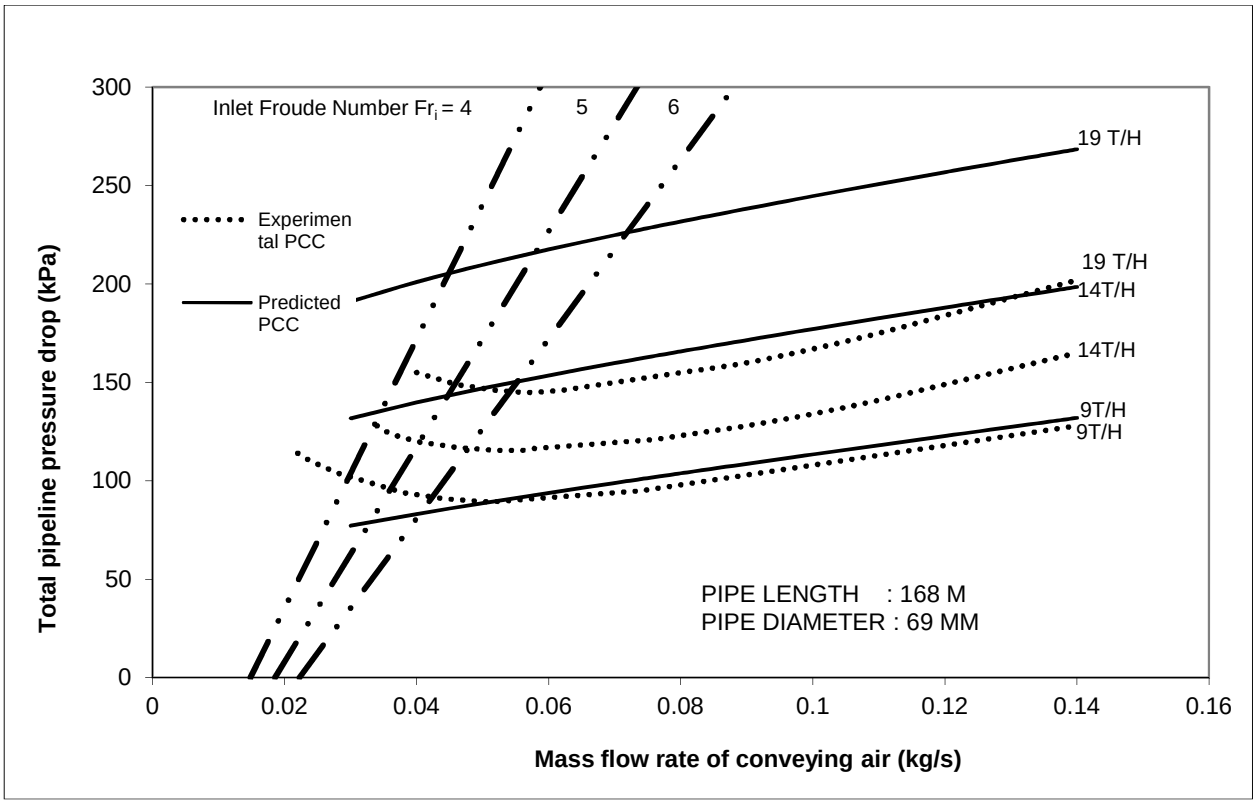

Figure 3.4: Comparison of Experimental and Predicted values of total pipeline pressure drop (fly ash: 69 mm I.D.- 168 m length, for P9-P10 model-I, where K≠ 1)

The figure 3.4 showed that the predicted line of 9 t/h of mass flow rate of solid was very close to the experimental line, but the same over prediction can be seen as the mass flow rate of solid increased (19 t/h and 14 t/h). Hence no U-shaped trend was obtained in the above figure.

Model for $V_p = 0.7V_a$:

$$\frac{\Delta P_s}{L} = \left[K \left(\frac{D\,(0.2V_a)^{0.5}\,\rho_a{}^{0.5}}{m_s{}^{0.5}} \right)^{a} \left(\frac{\rho_a{}^{1.5}(0.2V_a)^{2.5}}{m_s{}^{0.5}} \right) + \frac{\lambda_f V a^2 \rho_a L}{2D} \right] \tag{3.9}$$

For 69 mm ID-168 m L, P9-P10 (when $V_p = 0.7V_a$):

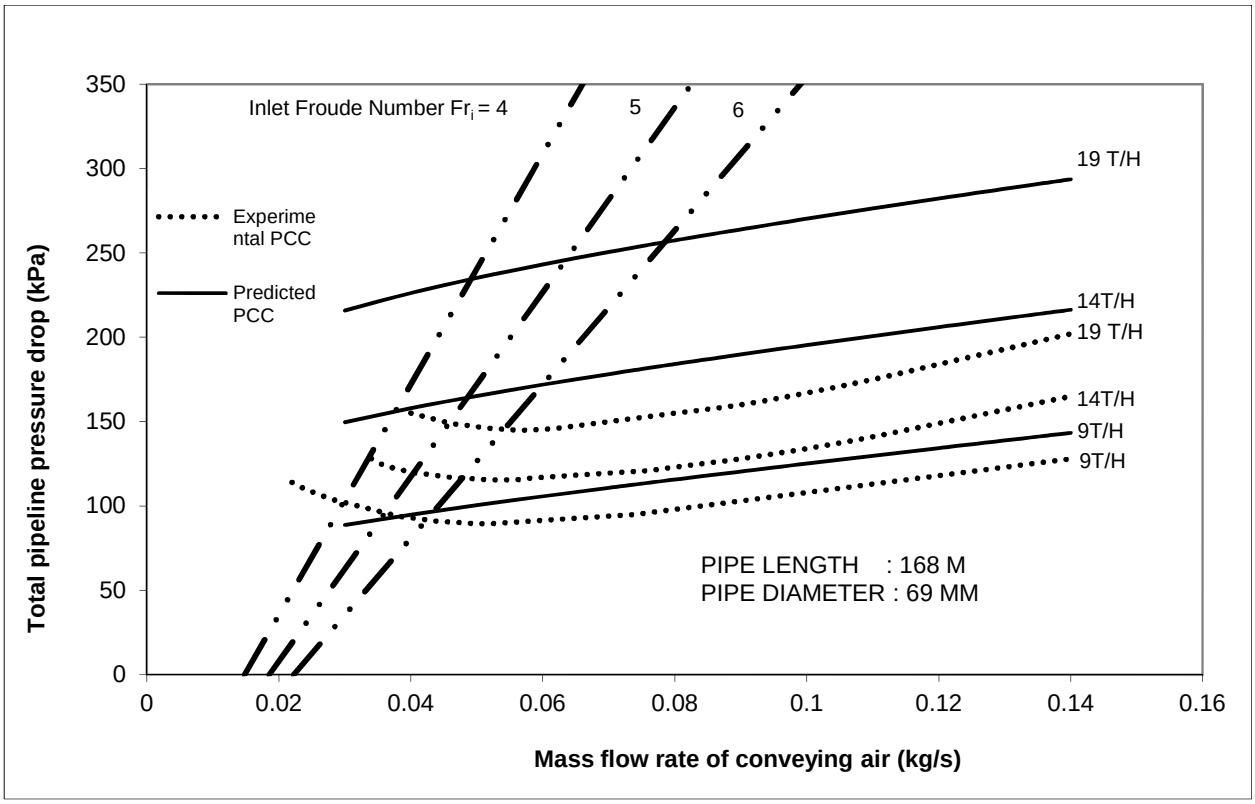

Figure 3.5: Comparison of Experimental and Predicted values of total pipeline pressure drop (fly ash: 69 mm I.D.-168 m length, for P9-P10 model-I, where K≠ 1)

Similar results were obtained as in figure 3.3. The predicted line for 9 t/h of mass flow rate of solid seems to be shifted upward as compared to the previous figure 3.4. But the predicted lines of 19 t/h and 14 t/h are somewhat similar to the previous figures 3.3 and 3.4. Hence once again there was no of U-shaped trend.

Model for $V_p = 0.5V_a$:

$$\frac{\Delta P_s}{L} = \left[K \left(\frac{D\,(0.2V_a)^{0.5}\,\rho_a{}^{0.5}}{m_s{}^{0.5}} \right)^a \left(\frac{\rho_a{}^{1.5}(0.2V_a)^{2.5}}{m_s{}^{0.5}} \right) + \frac{\lambda_f V a^2 \rho_a L}{2D} \right] \tag{3.10}$$

For 69 mm ID-168 m L, P9-P10 (when $V_p = 0.5V_a$):

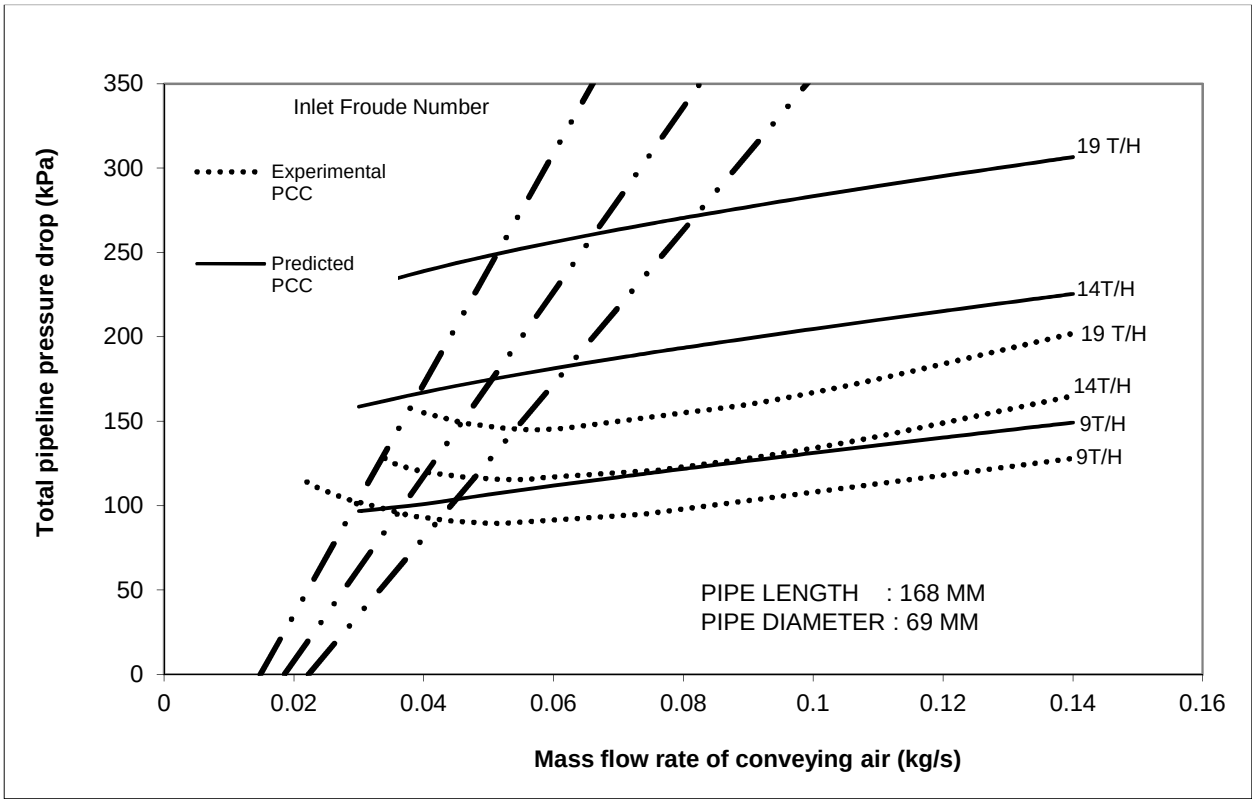

Figure 3.6: Comparison of Experimental and Predicted values of total pipeline pressure drop (fly ash: 69 mm I.D. - 168 m length, for P9-P10 model-I, where K≠ 1)

The predicted PCC for 9 t/h of mass flow rate of solid in the above figure 3.6 moved upward this showed that as the percentage of velocity of particle decreases the predicted line (9 t/h, 14 t/h, 19 t/h) moved accordingly. However there is no U-shaped trend obtained.

The PCC as shown in the figures 3.4, 3.5, 3.6 are looks similar to the PCC shown in the figure 3.3 but the lines of 9 t/h and 14 t/h are varying as the percentage of the velocity of air changes from 80% to first 90% then 70% and 50%. However the line of 9 t/h and 14 t/h are very close to experimental data line when the velocity of particle was 90% of the velocity of air. The model with the velocity of

particle equal to 90% of the velocity of air gives satisfactory results in plotting the PCC as all the graphs are resulting in straight line PCC which is quite considerable. Therefor the remaining PCC were plotted while taking the model with 90% criteria.

Now scaling-up the diameter from 69 mm ID to 105 mm ID and keeping the length constant the results are shown as under:

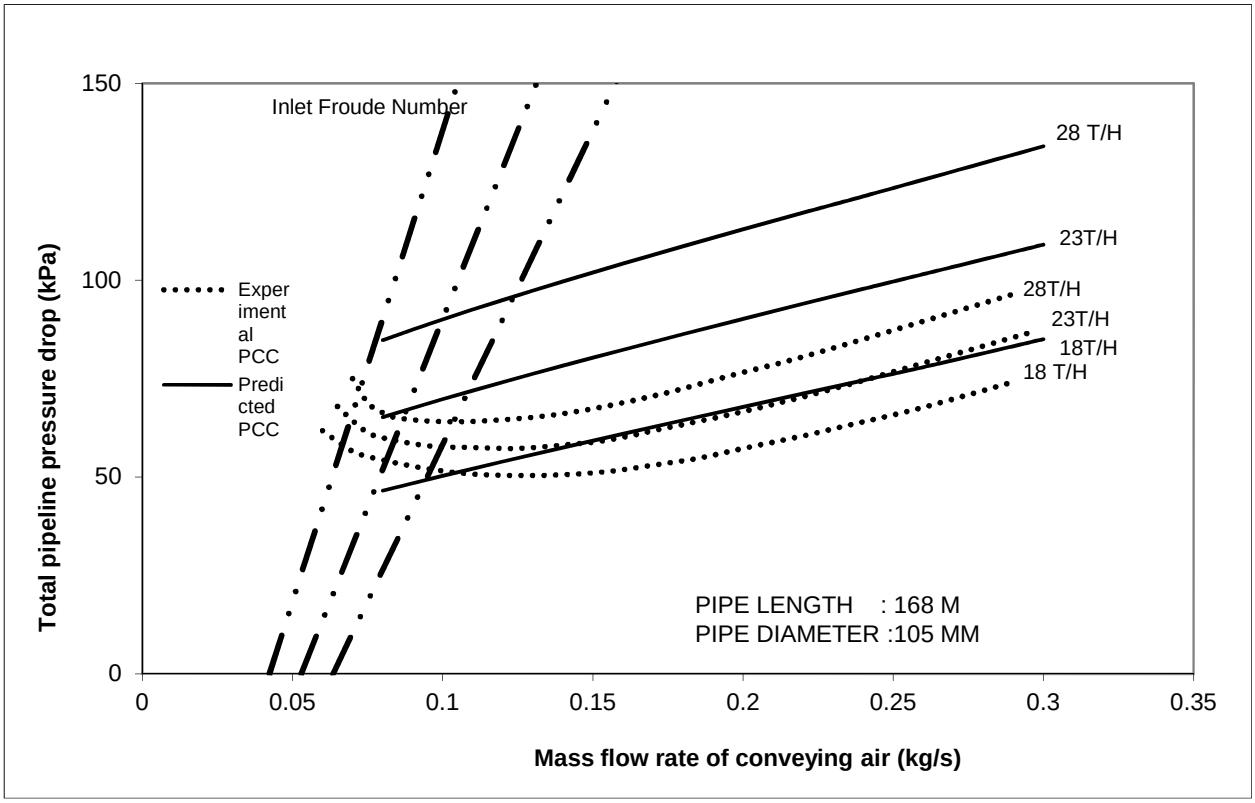

Figure 3.7: Comparison of Experimental and Predicted values of total pipeline pressure drop (fly ash: 105 mm I.D.-168 m length, for P9-P10 model-II, where K≠ 1).

The scaled-up diameter results in over predicted the experimental lines as it moved from dilute to dense phase region. The 18 t/h predicted line as compared to other two lines of 23 t/h and 28 t/h were less over predicted the experimental line. Hence, once again the U-shaped trend line was no formed.

Now scaling-up the length from 168 m L to 554 m L and keeping the diameter constant the results as shown below:

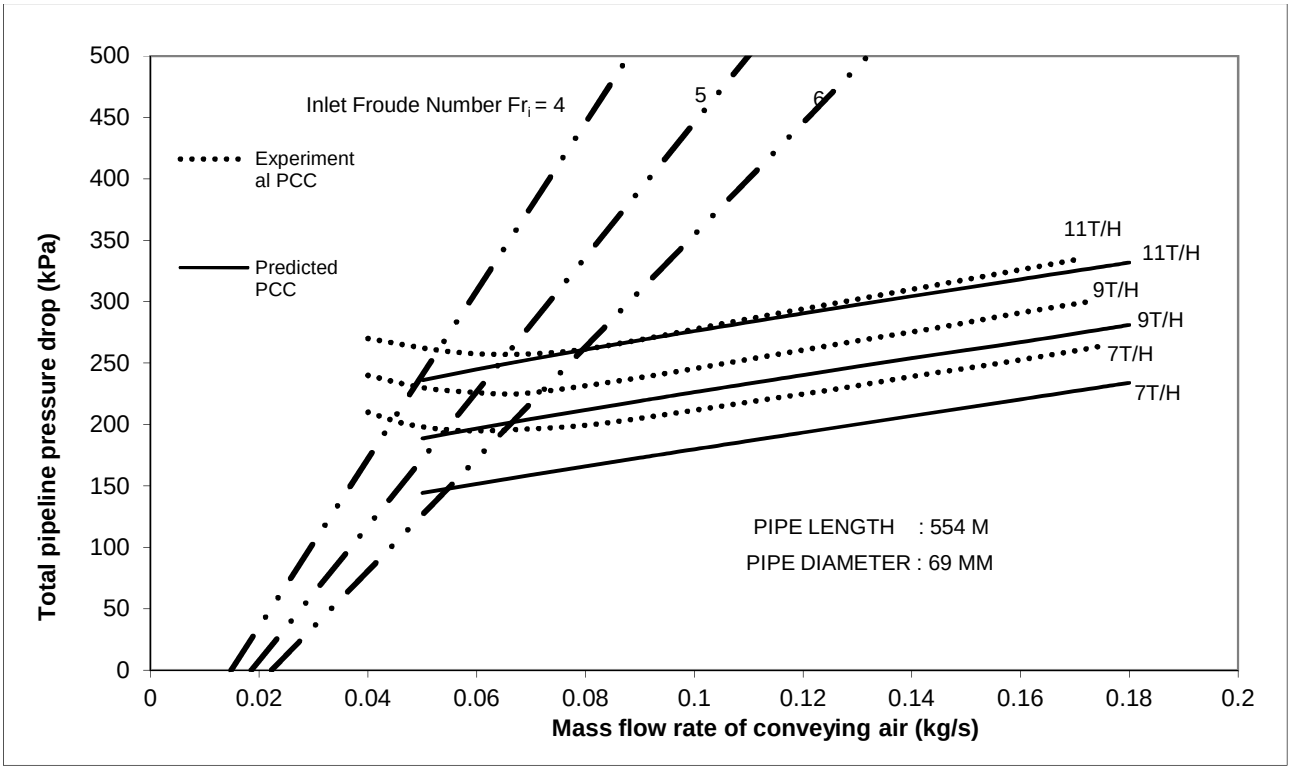

Figure 3.8: Comparison of Experimental and Predicted values of total pipeline pressure drop (fly ash: 69 mm I.D. - 554 m length, for P9-P10 model-III, where K≠ 1)

The scaled-up length of 554 m results in making the straight line PCC, which is under- predicted the experimental data. It seems that the 11 t/h of mass flow rate of solid the predicted line were somewhat closer to the experimental line. The developed model was further used for predicting the pressure drop for the tapping point P11-P12 and the results plotted in the PCC as below:

For 69 mm ID-168 m L, P11-P12:

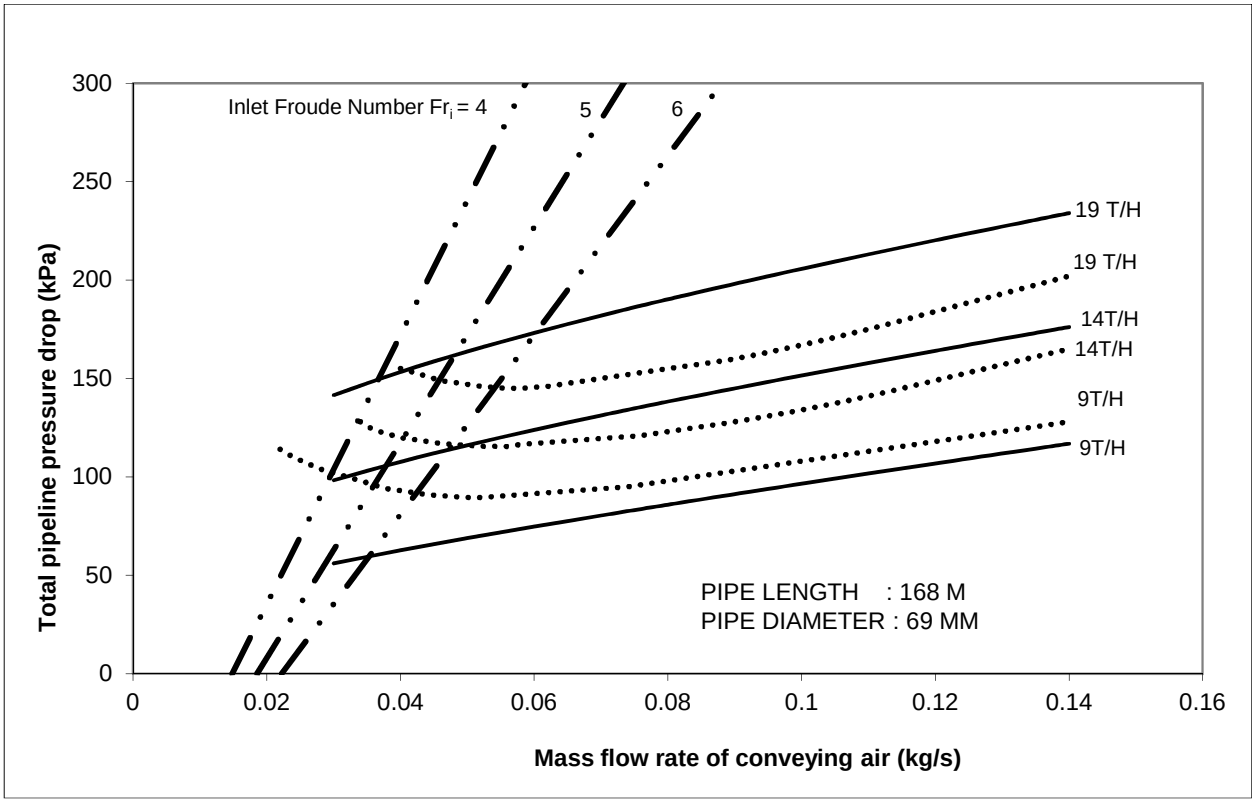

Figure 3.9: Comparison of Experimental and Predicted values of total pipeline pressure drop (fly ash: 69 mm I.D.-168 m length, for P11-P12 model-I, where K≠ 1).

From the figure 3.9 it showed that the low mass flow rate solid i.e. 9 t/h the line under predicts the experimental data line. As the mass flow rate of solid increases i.e. 14 t/h and 19 t/h the predicted line over predicts the experimental data line. Hence there is no U-shaped trend line obtained.

Now scaling-up the diameter from 69 mm to 105 mm:

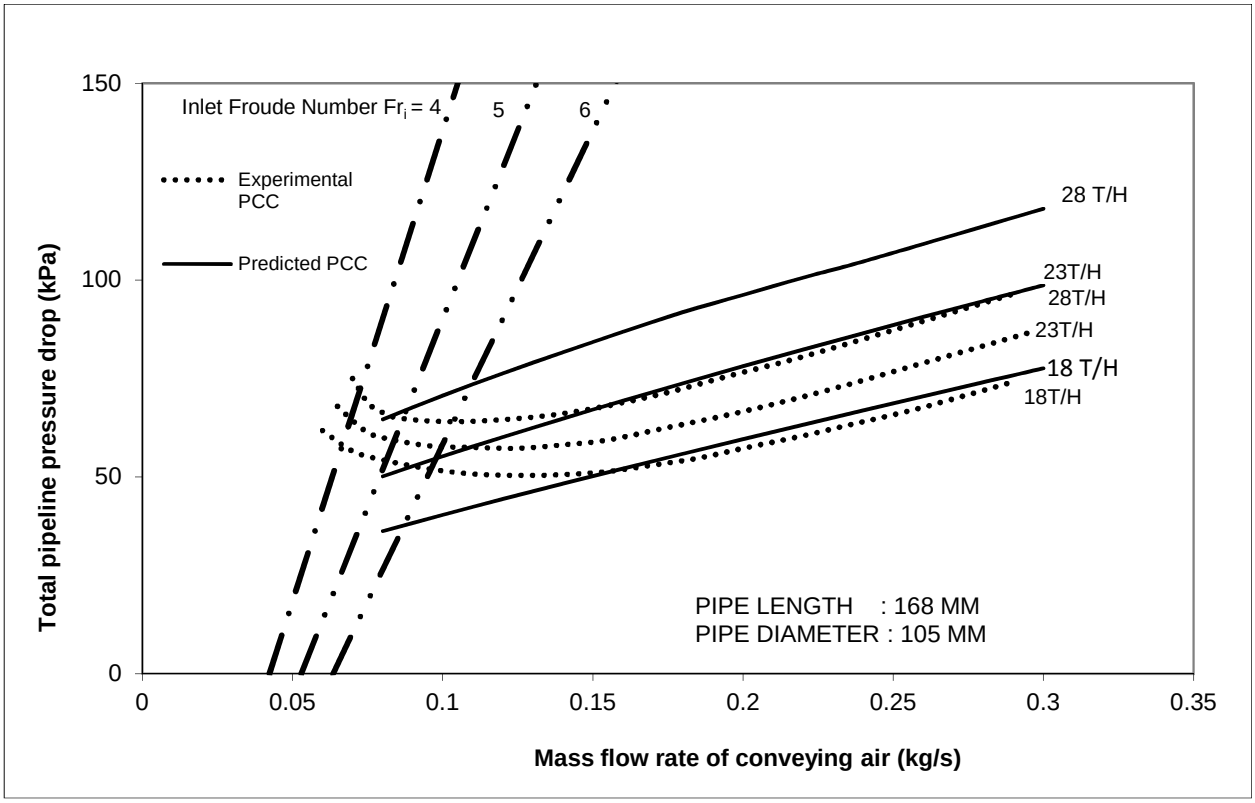

Figure 3.10: Comparison of Experimental and Predicted values of total pipeline pressure drop (fly ash: 105 mm I.D. - 168 m length, for P11-P12 model-II, where K≠ 1).

The results showed in figures 3.10 after scaling-up the diameter was over predicted the experimental data. The predicted PCC trend line in figure 10 is not indicating the U-shaped lines. The predicted PCC for diameter scale-up (105 mm I.D. × 168 m long pipe) provide over-prediction in dense-phase.

Now scaling-up the length from 168 m to 554 m L:

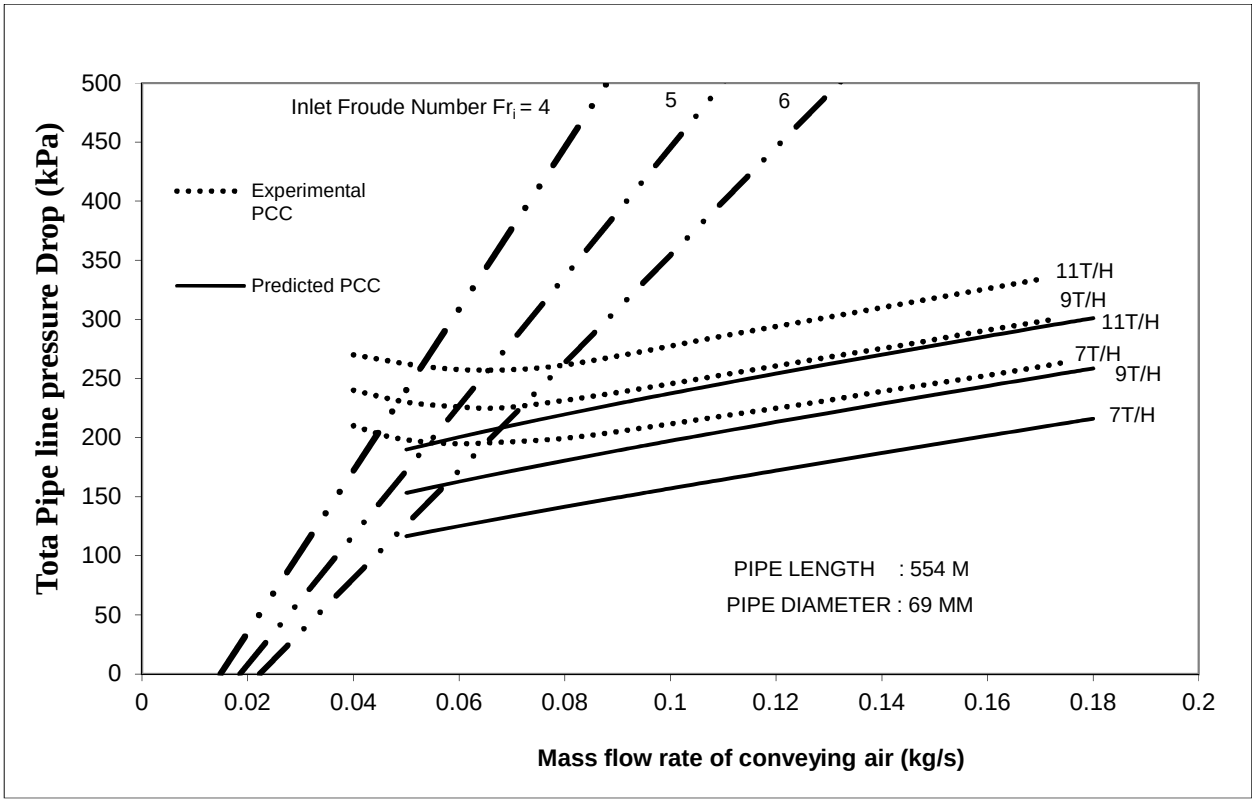

Figure 3.11: Comparison of Experimental and Predicted values of total pipeline pressure drop (fly ash: 69 mm I.D. - 554 m length, for P11-P12 model-III, where K≠ 1)

The scaled-up for length in figure 3.11 the predicted PCC provide under-prediction in dilute phase region. However, the shape of the predicted PCC did not appeared to indicate a “U”-shaped trend.

Super Imposing:

The purpose of plotting the predicted PCC over the experimental PCC was to check whether the developed model was appropriate or not. What is the percentage of error between the predicted lines and the experimental lines. That error analysis was done in the later part, but before that all the PCC been superimposed with the experimental data for individual mass flow rate of solid (in Tonnes per Hour).

The super impositions of the models are done so that it will be easier to see all the PCC which was drawn against the experimental PCC, so that it will easy to study. Now the next step was the super imposition which was done below for all the models:

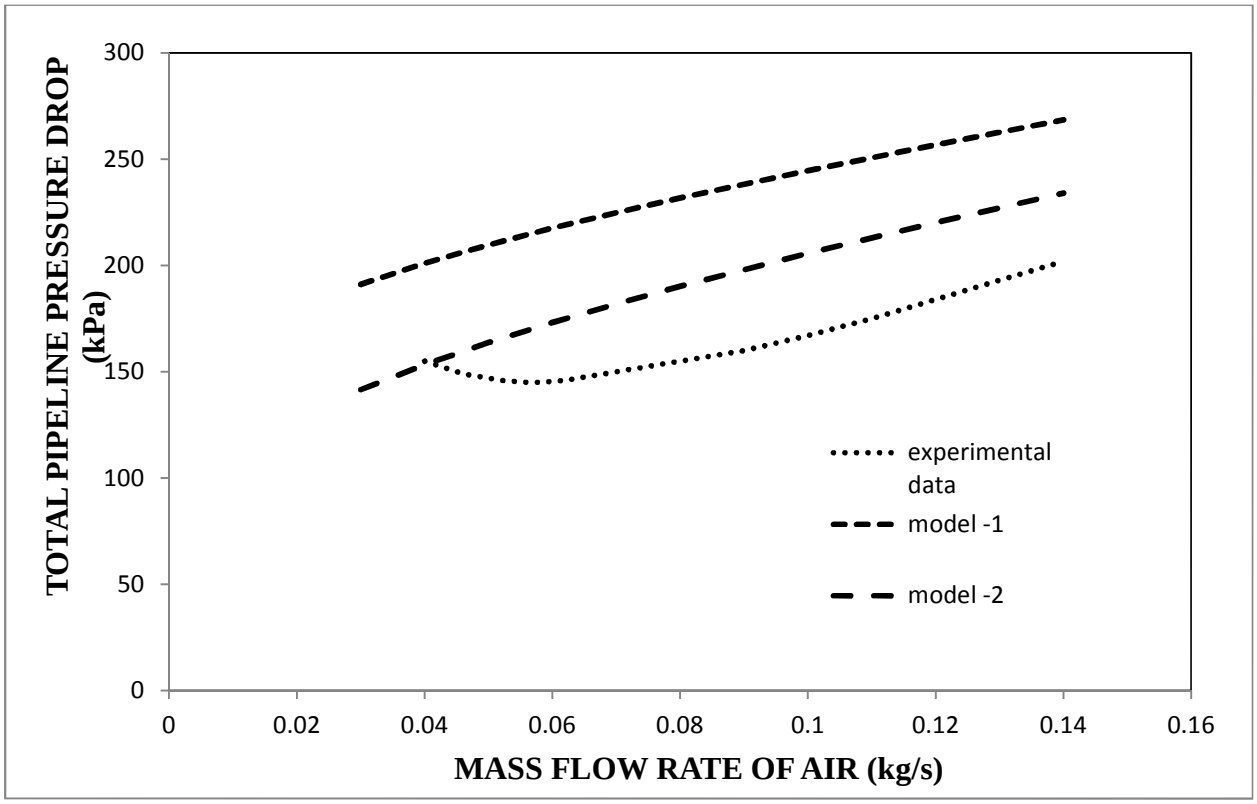

Figure 3.12: Comparison between experimental data versus model-1 and model-2 for 69 mm ID-168 m Long (19 t/h)

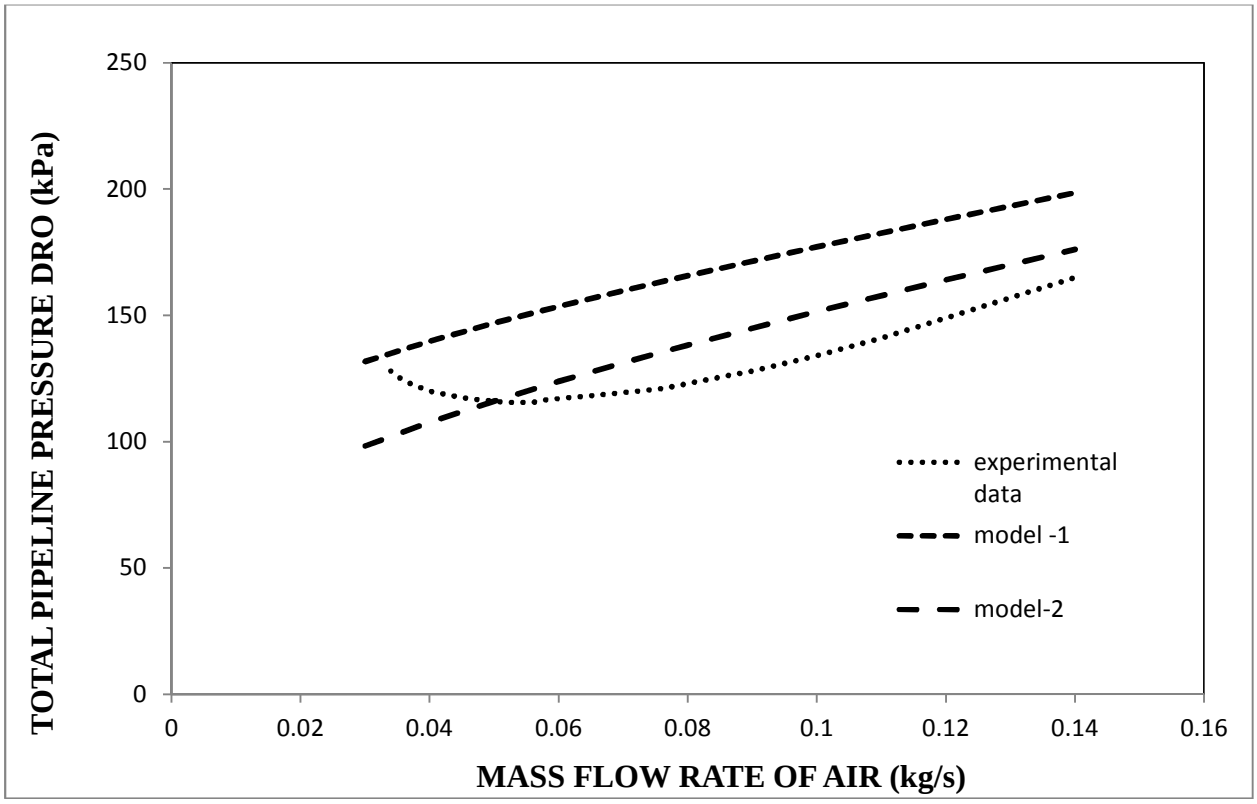

Figure 3.13: Comparison between experimental data versus model-1 and model-2 for 69 mm ID - 168 m Long (14 t/h).

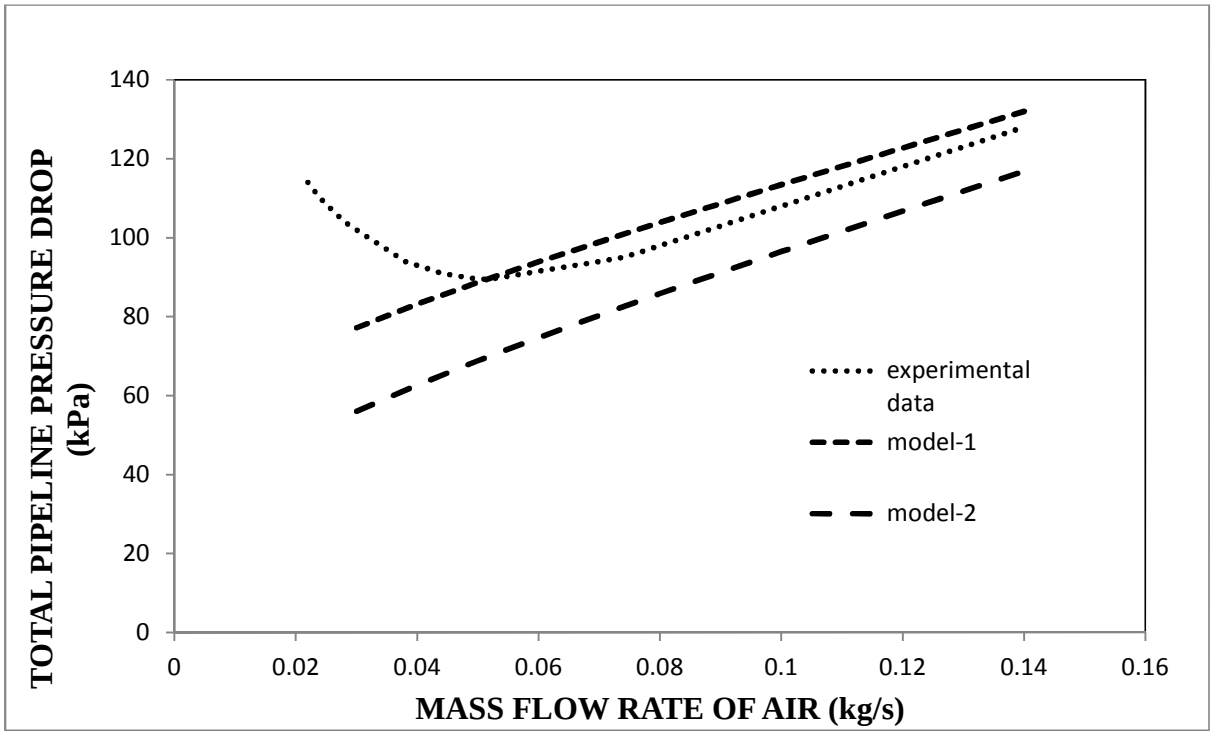

Figure 3.14: Comparison between experimental data versus model-1 and model-2 for 69 mm ID - 168 m Long (9 t/h).

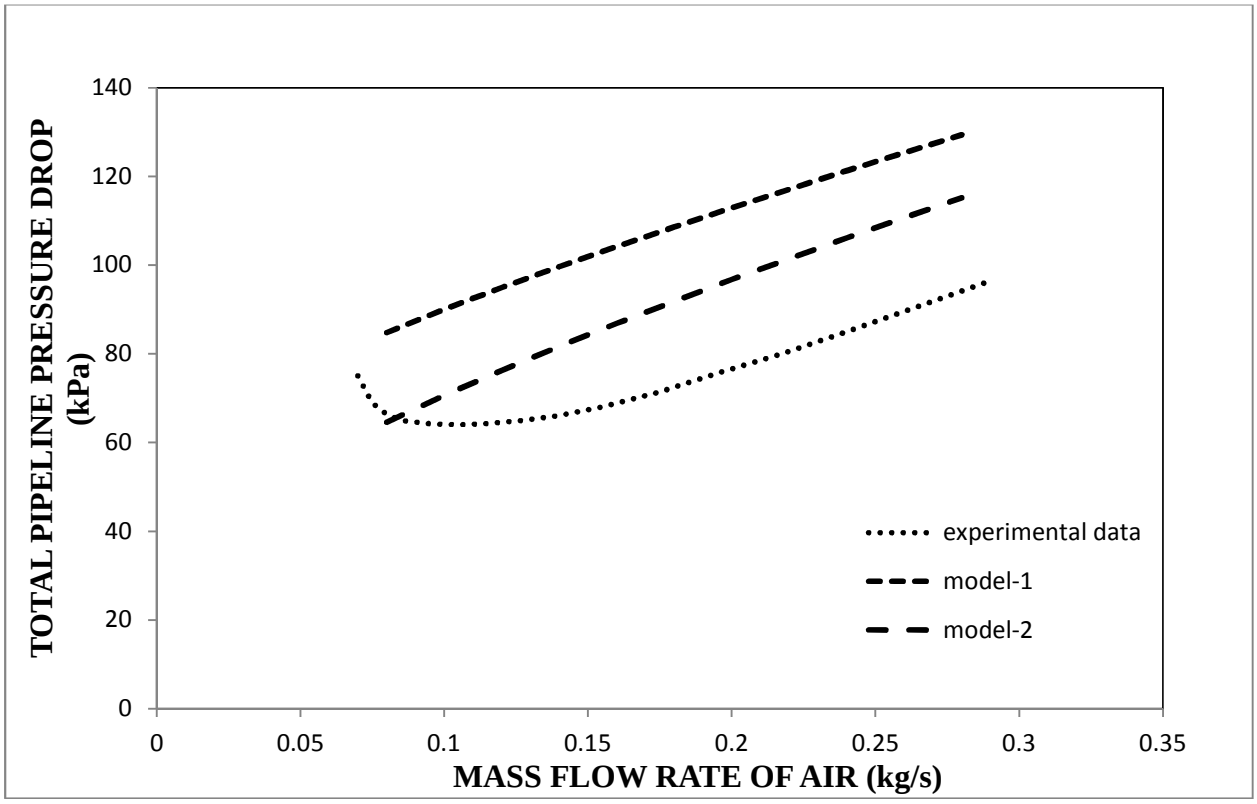

Figure 3.15: Comparison between experimental data versus model-1 and model-2 for 105 mm ID-168 m Long (28 t/h).

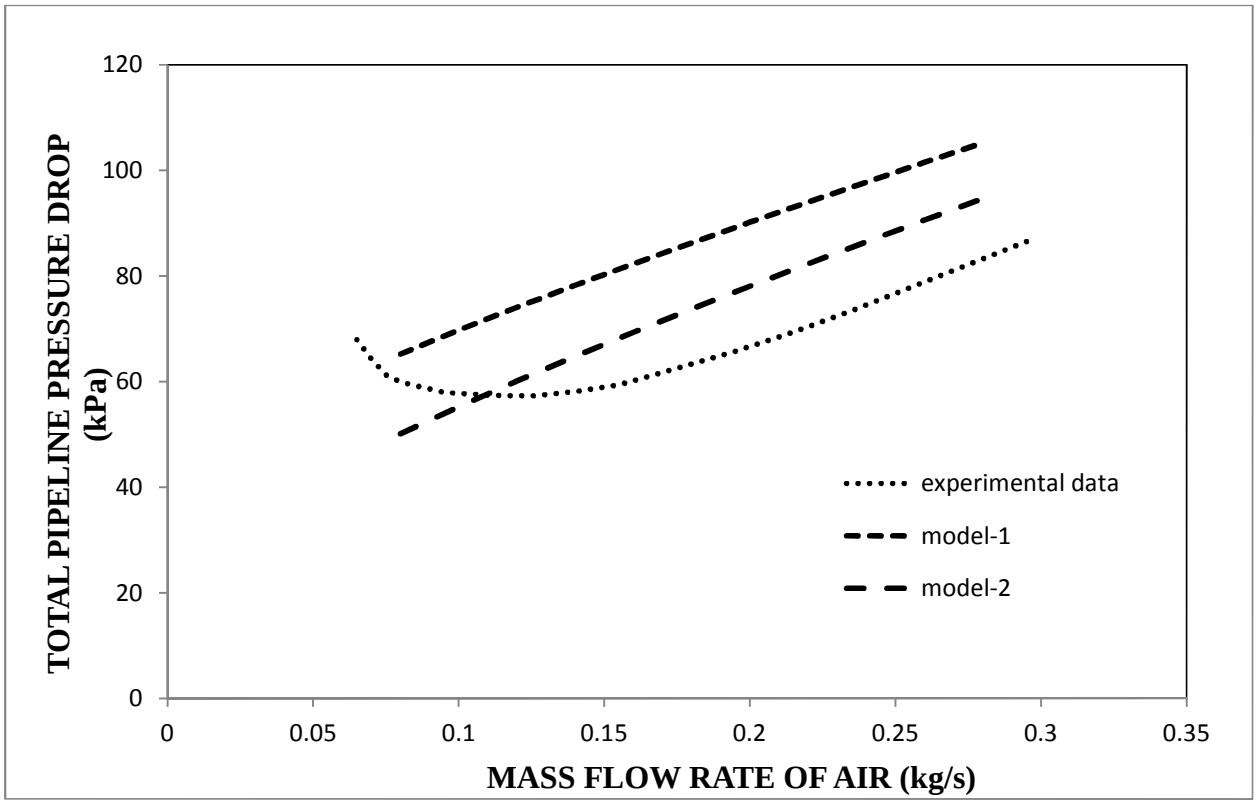

Figure 3.16: Comparison between experimental data versus model-1 and model-2 for 105 mm ID-168 m Long (23 t/h).

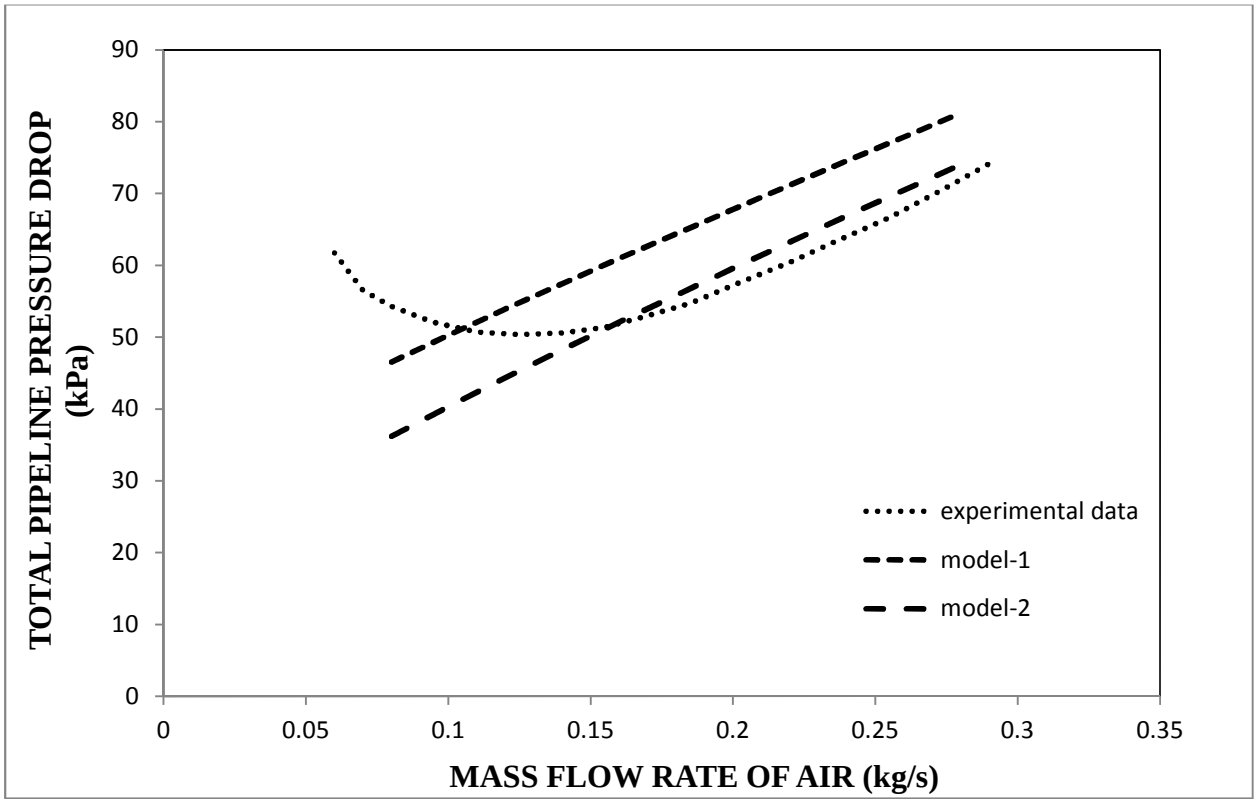

Figure 3.17: Comparison between experimental data versus model-1 and model-2 for 105 mm ID - 168 m Long (18 t/h).

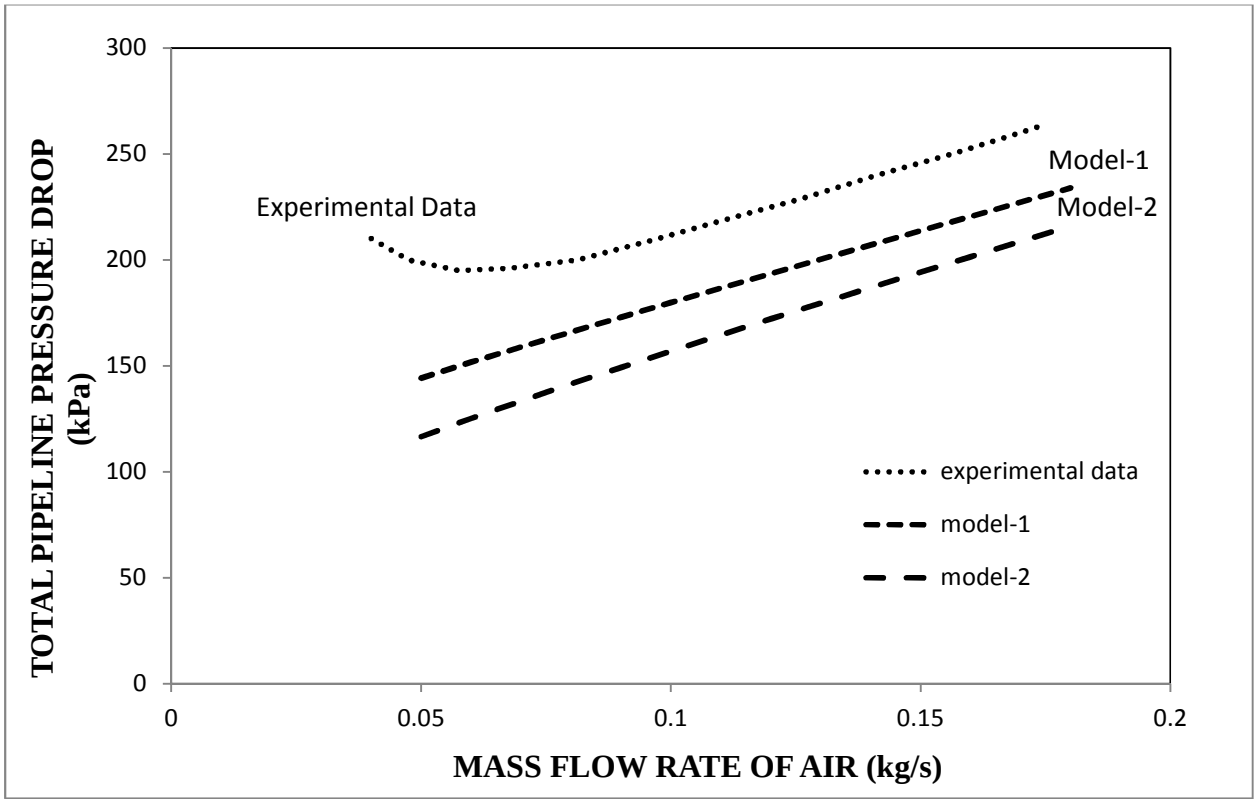

Figure 3.18: Comparison between experimental data versus model-1 and model-2 for 69 mm ID - 554 m Long (7 t/h).

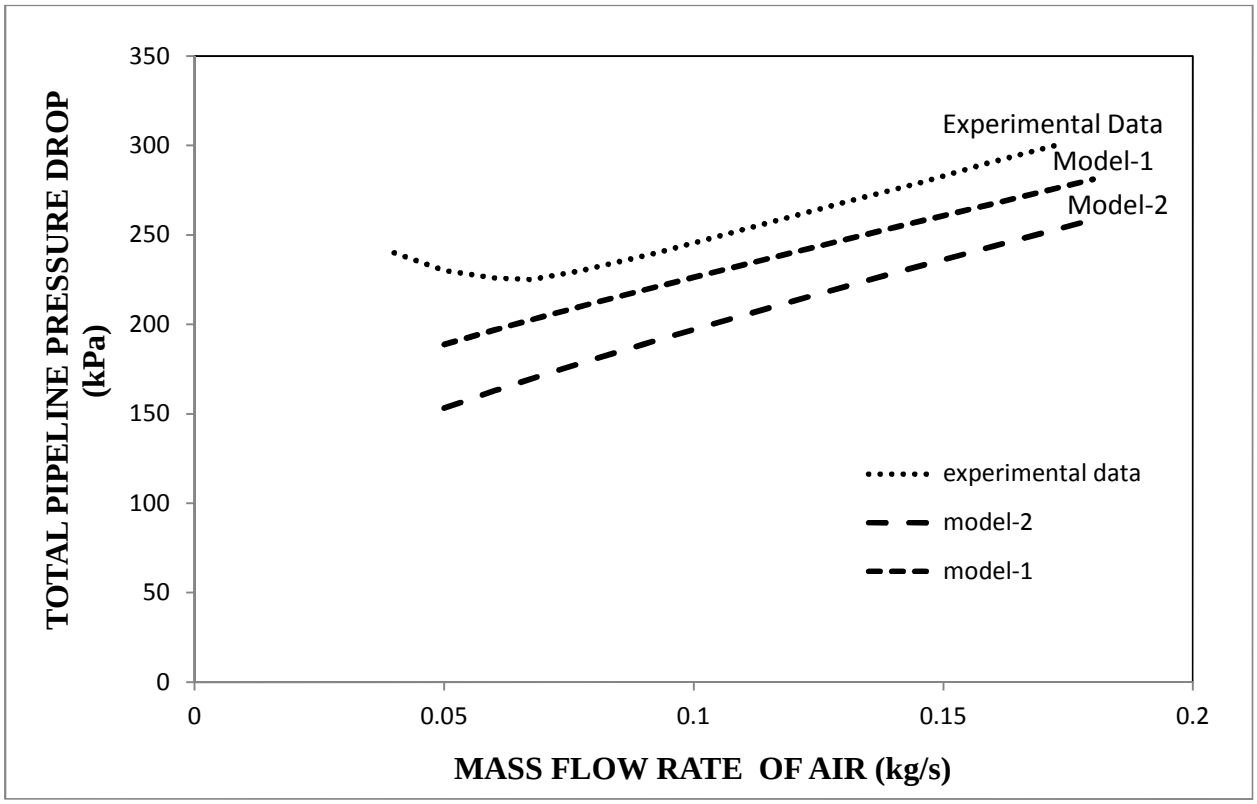

Figure 3.19: Comparison between experimental data versus model-1 and model-2 for 69 mm ID - 554 m Long (9 t/h).

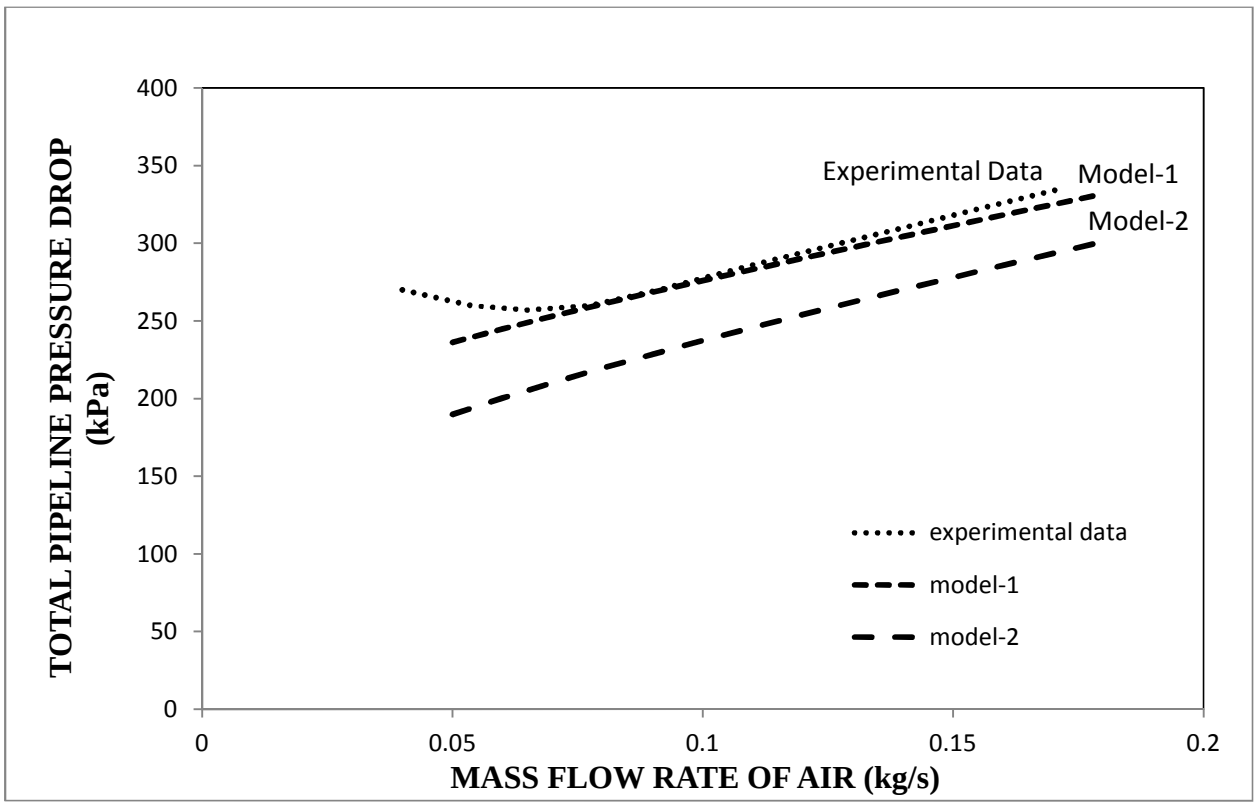

Figure 3.20: comparison between experimental data versus model-1 and model-2 for 69 mm ID - 554 m Long (11 t/h).

3.2.1.1 Error Analysis:

The purpose of this analysis was to determine the error in the data of the developed model over the experimental data. For that the data was gathered from both experimental as well as from predicted data and putted in the below mentioned formula:

$$\left|\frac{\text{predicted data}-\text{experimental data}}{\text{predicted data}}\right| \qquad (3.8)$$

By applying this formula the values of selected points occurred, after that the average of those points were taken and then it will be multiply by 100 to get it into the percentage form. The average of those points was then divided by the total number of values.

This analysis was done on the predicted data of fly ash which was obtained from the developed model and check whether that model satisfy the experimental data or not. The formula used for percentage error:

$$\text{Percentage error} = \Sigma \left| \frac{\text{predicted data} - \text{experimental data}}{\text{predicted data}} \right| \text{x } 100 \qquad (3.9)$$

By applying the above mentioned formula the percentage error values was obtained for the individual mass flow rate of solid in tonnes per hour and this was showed in the tabular form below:

Table 1: Shows the percentage of error at various mass flow rate of solid for fly ash .

Mass flow rate of solid (t/h)	Error (%)
For 69-168 (P9-P10) 19 t/h	29
14 t/h	21
9 t/h	5.63
For 105-168 28 t/h	30.36
23 t/h	22.58
18 t/h	10.17
For 69-554 11 t/h	1.75
9 t/h	10.13
7 t/h	18.74
For 69-168 (P11-P12)	

19 t/h	13.71
14 t/h	5.35
9 t/h	19.48
For 105-168 28 t/h	18.9
23 t/h	20.39
18 t/h	17.52
For 69-554 11 t/h	16.61
9 t/h	24.42
7 t/h	32.64

3.2.2 ESP DUST:

The total pipeline Pneumatic Conveying Characteristics was obtained for ESP dust with 69 mm ID-168 m Length, 105 mm ID-168 m Length, 69 mm ID-554 m Length are presented in figures by taking the velocity of the particle (V_p) will be 90% of the velocity of the air (V_a). The total pipeline pressure drop (ΔP) includes all the losses of the entire pipeline. The total pipeline PCC were obtained using steady state data from P9-P10 pressure tapping point data for a wide range of air and solids flow rates (Wypych et al., 2005). The total pipelines PCC are shown below:

Model for ESP dust:

$$\frac{\Delta P_s}{L} = \left[K \left(\frac{D\,(0.1V_a)^{0.5}\,\rho_a{}^{0.5}}{m_s{}^{0.5}} \right)^{a} \left(\frac{\rho_a{}^{1.5}(0.1V_a)^{2.5}}{m_s{}^{0.5}} \right) + \frac{\lambda_f V a^2 \rho_a L}{2D} \right] \tag{3.11}$$

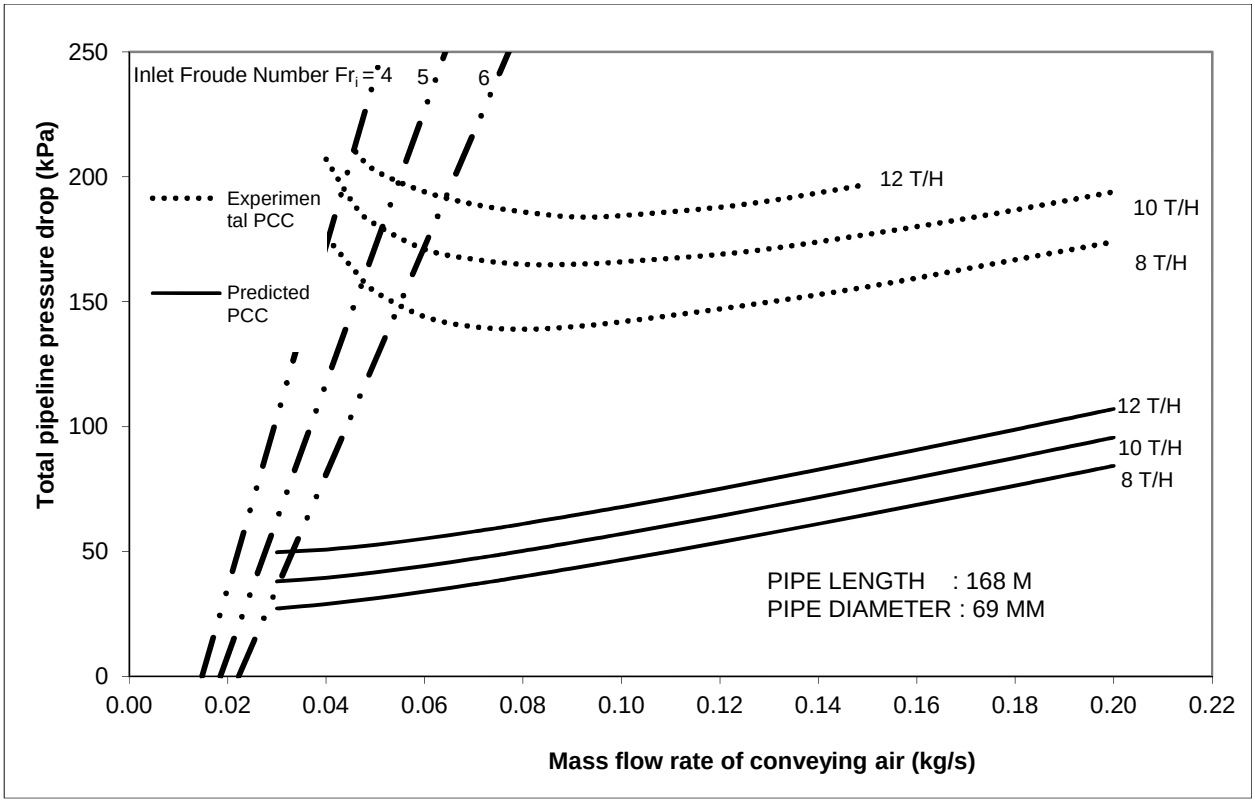

Figure 3.21: Comparison of Experimental and Predicted values of total pipeline pressure drop (ESP Dust: 69 mm I.D. - 168 m length, for P9-P10 model-I, where K≠ 1)

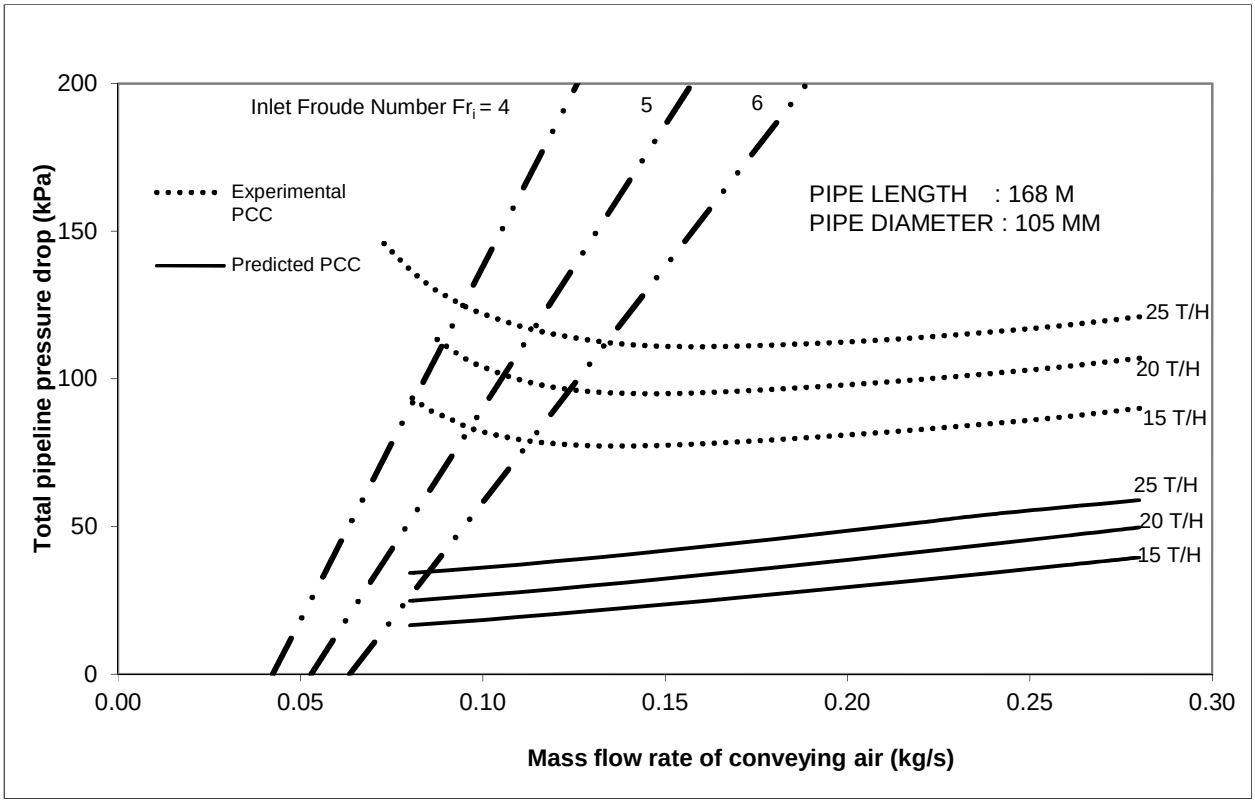

Figure 3.22: Comparison of Experimental and Predicted values of total pipeline pressure drop (ESP Dust: 105 mm I.D. - 168 m length, for P9-P10 model-II, where K≠ 1)

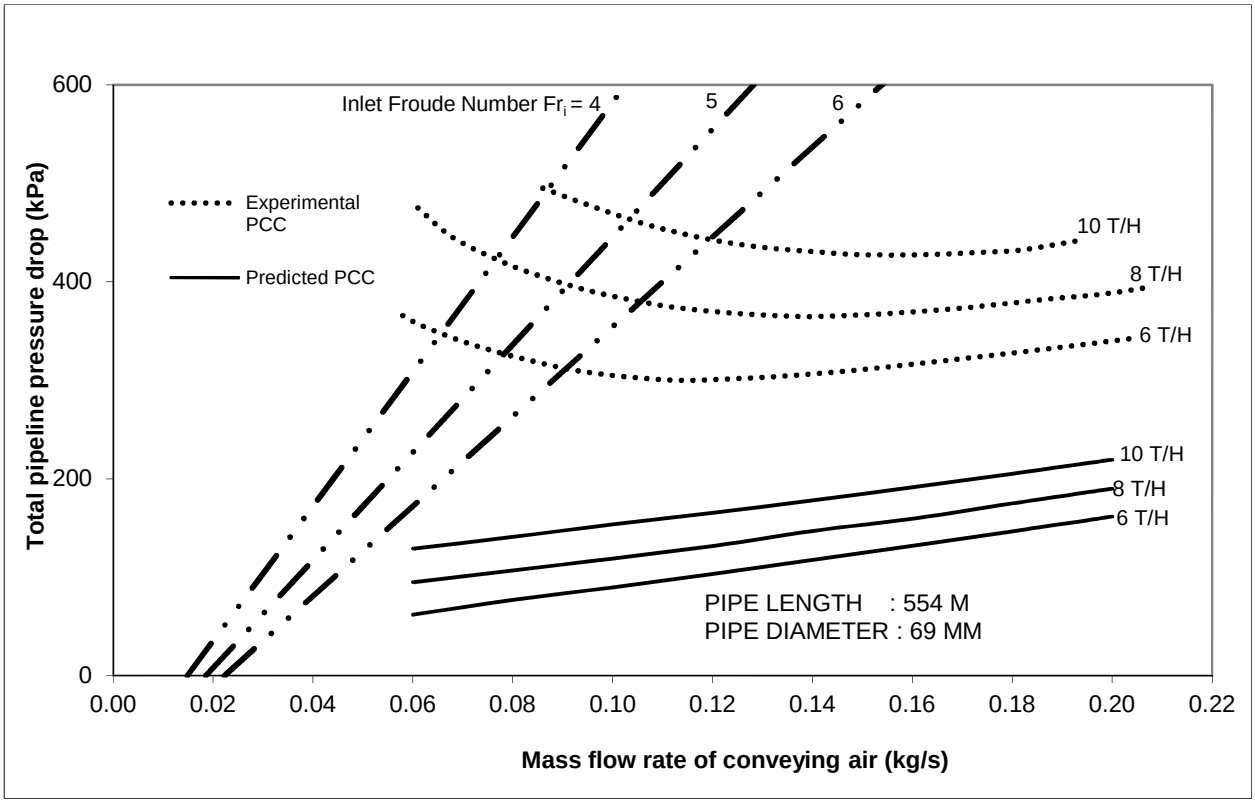

Figure 3.23: Comparison of Experimental and Predicted values of total pipeline pressure drop (ESP Dust: 69 mm I.D. - 554 m length, for P9-P10 model-III, where K≠ 1)

The figures 3.21, 3.22, 3.23 show that for all the pipes, the predicted pressure drop lines of a developed model were more under-predicted the experimental data lines for the static pressure tapping points P9-P10 because of the dense phase region. As all the predicted line in the above figures were looked quite similar. The lines were not making the U-shaped trend. Hence the predicted model was not appropriate for the ESP Dust data. The line come in the plotted PCC are straight lines.

Chapter 4: Four Layer Modelling

4.1 Introduction:

The concept of layer modelling in the pipeline was first developed by Wilson (1976) for liquid-solid flow, which has been adopted to model dense phase conveying of powders in pneumatic conveying system. In those years modelling the dense phase region was a difficult task and still it is difficult task for researchers. After few years Stegmaier (1978) came up with their model for predicting the pressure drop and also for finding scaling-up technique. As the time passed researchers (Levy and Mason (2000), Jones and Williams (2003), Wypych and Yi (2003), Mallick (2010)) studied/predicted or developed the two layer or three layer models.

Levy and Mason (2000) studied the two layer model for non-suspension gas-solid flow in pipes. The parametric study was conducted in their work to assess the influence of the boundary conditions on the overall behaviour of the model. Besides this they calculated the mass and momentum transfer between the two layers. Whereas Wypych and Yi (2003) suggested that optimum pneumatic conveying of the bulk materials could be achieved by controlling the air mass flow rate within certain range, and appropriate selection of pipe diameters. They presented a new theoretical model based on the observed unstable flow mechanism and stability criteria for the purpose of predicting transport boundaries. The pneumatic conveying of granular material through a horizontal pipe can exhibit three main flow modes: low-velocity slug flow, dilute-phase flow with suspended particles/strands and strand flow over a stationary layer (for low solid mass flow rates) or moving layer (for high solid mass flow rate). They said that modelling relied on the particle and bulk properties of material being conveyed and the pipe wall properties. However, Mallick (2010) developed the two layer model based on the actual flow condition in dense-phase (i.e. considering the presence of a non-suspension layer). He considered in his thesis that, as the interface between the non-suspension and suspension layers are not very distinct under real flow conditions and also the height of the non-suspension layer keeps on fluctuating due to the highly turbulent nature of flow.

After reviewing the literature, two layer and three layer models for pressure drop in the dense phase region came into light; beside this no work had done on developing the four layer model and predicting the pressure drop for dense phase region. So a study was conducted to develop the four layer model approach for dense phase region.

4.2 Assumption:

- Layers are separated by well-defined boundaries.
- The flow is caused by sharing action, upper layers are in shearing (i.e. in forward direction) the lower layer (i.e. backward direction).
- Within each layer, particle velocity is different from layer to layer.
- Bulk densities of particles were also different with in each layer.

4.3 Four Layer Model Approach:

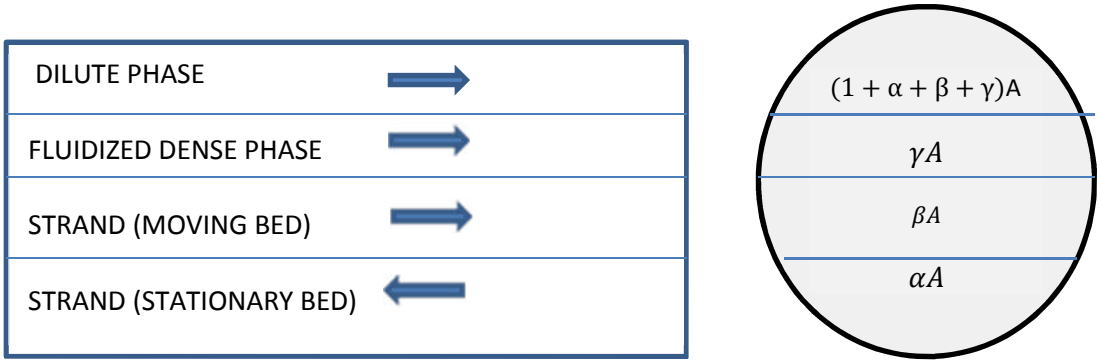

Figure 4.1: Shows a Four layer model.

Where:

α, β, γ, {1-(α+ β+ γ)} are the fraction of pipe cross-section in stationary, strand, fluidized dense phase and dilute phase.

Particle size distribution (PSD) of fly ash and ESP dust samples have been done by the graphs which are showed in appendix A. The graphs which were plotted between the particle diameter and volume were divided into 4 equal sections. Then average of each section was taken and noted, while doing this the values was obtained for fly ash and ESP dust. Then average was taken for each fly ash sample through this the particle size was obtained. The same method was applied to found the particle size for ESP dust. Density of particle was then found from the graph plotted between the diameter of particle and the density of particle (graph used from the Wypych, 2006). This is how the particle size was distributed to the layers of the above showed predicted model. After getting those points the Barth's equation (4.1) with Stegmaier model (4.2) was used for getting the pressure drop for various points with different tonnes per hour.

The Barth's (1958) equation:

$$\Delta P = (\lambda_f + m^* \lambda_s) \frac{\rho L V^2}{2D} \qquad (4.1)$$

The Stegmaier (1978) model:

$$\lambda_s = 2.1\ (m^*)^{-0.3}\ Fr^{-2}\ (Fr_{sd})^{0.5}\ \left(\frac{D}{ds}\right)^{0.1} \qquad (4.2)$$

The Stegmaier (1978) model was used because his work was a major advancement towards the use of power function type formats to represent solids friction factor. He investigated a number of fine and coarse particles, including fly ash, alumina, quartz powder, sand, catalyst for horizontal transport (with particle size and particle density ranging from 15 to 112 μm and 1500 to 4100 kg/m3, respectively) and established a correlation for solids friction factor.

Modifying the Stegmaier (1978) model:

The Stegmaier model (4.2) was divided into four parts according to the diameter of particle and the terminal velocity. After divided that model we get λ_{s1}, λ_{s2}, λ_{s3}, λ_{s4} which was then added to get λ_s^* . The procedure of dividing the λ_s was adopted because of the four layer pressure drop prediction.

Where:

$$\lambda_{s1} = 2.1\,(m^*)^{-0.3}\,Fr^{-2}\,(Fr_{sd1})^{0.5}\left(\frac{D}{ds_1}\right)^{0.1} \tag{4.3}$$

$$\lambda_{s2} = 2.1\,(m^*)^{-0.3}\,Fr^{-2}\,(Fr_{sd2})^{0.5}\left(\frac{D}{ds_2}\right)^{0.1} \tag{4.4}$$

$$\lambda_{s3} = 2.1\,(m^*)^{-0.3}\,Fr^{-2}\,(Fr_{sd3})^{0.5}\left(\frac{D}{ds_3}\right)^{0.1} \tag{4.5}$$

$$\lambda_{s4} = 2.1\,(m^*)^{-0.3}\,Fr^{-2}\,(Fr_{sd4})^{0.5}\left(\frac{D}{ds_4}\right)^{0.1} \tag{4.6}$$

$$\lambda_s = \Sigma\,(\lambda_{s1}, \lambda_{s2}, \lambda_{s3}, \lambda_{s4}) \tag{4.7}$$

And

$$\lambda_s' = m^*\lambda_s$$

The Barth equation was used for the predicting the pressure drop for total pipeline pressure drop. The equation was expressed as:

$$\Delta P = (\lambda_f + m^*\lambda_s)\,\frac{\rho L V^2}{2D} \tag{4.8}$$

Here some modification was done, the variables $(m^*\,\lambda_s)$ was taken as λ_s' so the equation becomes:

$$\Delta P = \left(\lambda_f + \lambda_s'\right)\,\frac{\rho L V^2}{2D} \tag{4.9}$$

Now the Stegmaier (1978) model was modified for predicting the pressure for four layer model and see how the PCC were plot. The modified Stegmaier model is expressed as:

$$\lambda_s = K\,(m^*)^a\,(Fr)^b\left(\frac{\rho_a}{\rho_s}\right)^c\left(\frac{d_s}{D}\right)^d \quad (4.10)$$

Here (Fr_{sd}) was replaced by $\left(\frac{\rho_a}{\rho_s}\right)$ and $\left(\frac{D}{d_s}\right)$ replaced by $\left(\frac{d_s}{D}\right)$

Where the above dimensionless numbers expressed as:

$$m^* = \frac{m_s}{m_f}$$

$$Fr = \frac{v}{\sqrt{gD}}$$

And λ_s were find out by the Barth's equation:

$$\lambda_s = \frac{\left(\frac{2D\Delta P}{L\rho V^2}\right)}{m^*} - \lambda_f \quad (4.11)$$

The above model was implemented for wide range of products data, the reason for this was to see weather this model works or not. After getting the data it was then solved and the regression method was done with the conditions K≠1 and K=1. The values of R^2 was obtained are 0.95 (for K≠1) and 0.97 (for K=1) with this the values of different variables was obtained. Then the model with R^2 = 0.97 was selected.

The pressure drop values were obtained by the above mentioned model and with the help of 'MACRO' (integrating software used in Excel 2003). The PCC plotted with the obtained values is shown as below for 69 mm I.D. – 168 m length for fly ash with modified Stegmaier (1978) :

For 69 mm I.D. - 168 m Long for fly ash with modified Stegmaier (1978) model:

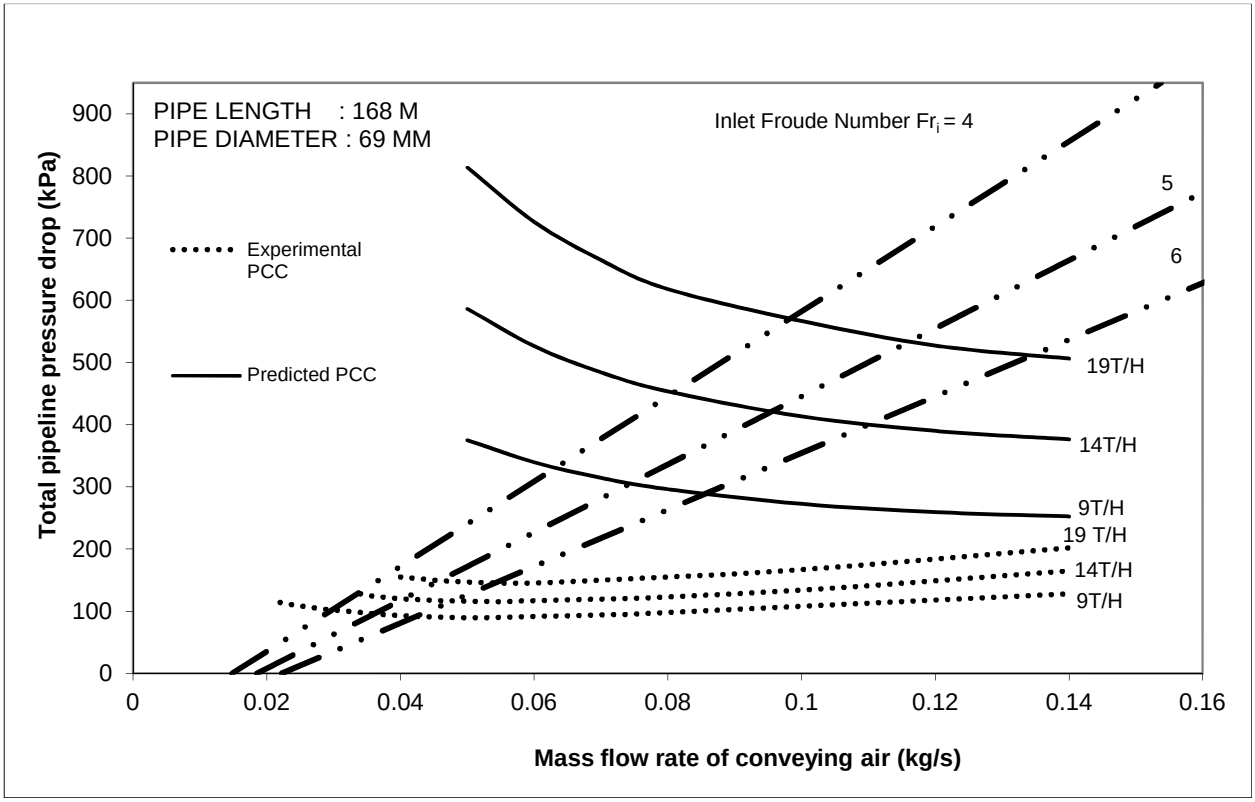

Figure 4.1: PCC for "Straight Pipe" Pressure Loss for ESP dust and 69 mm I.D. – 168 m long pipe.

The PCC obtained in the above graph with the modified Stegmaier (1978) model was too over predicted the experimental data which was not appropriate. After getting the above PCC the decision was taken to skip the Stegmaier (1978) model and instead of this weber (1981) model which used pipe diameter instead of particle diameter was taken. The Weber (1981) model was shown below:

$$\lambda_s = 2.1\,(m^*)^{-0.3}\,Fr^{-2}\,(Fr_{sD})^{0.5}\left(\frac{D}{ds}\right)^{0.1} \qquad (4.12)$$

Now the same procedure was done for changing the $\lambda_s$and making this to λ_s' and use the Barth equation to solve for the pressure drop. Here we saw that the Weber (1981) model gave good results

for predicting the pressure drop and for the λ_s' values it came satisfactory. The predicted PCC with Weber (1981) model was then super imposed with the PCC data taken from Mallick (2010). The PCC plotted with the weber (1981) model are shown below for various pipelines and diameters.

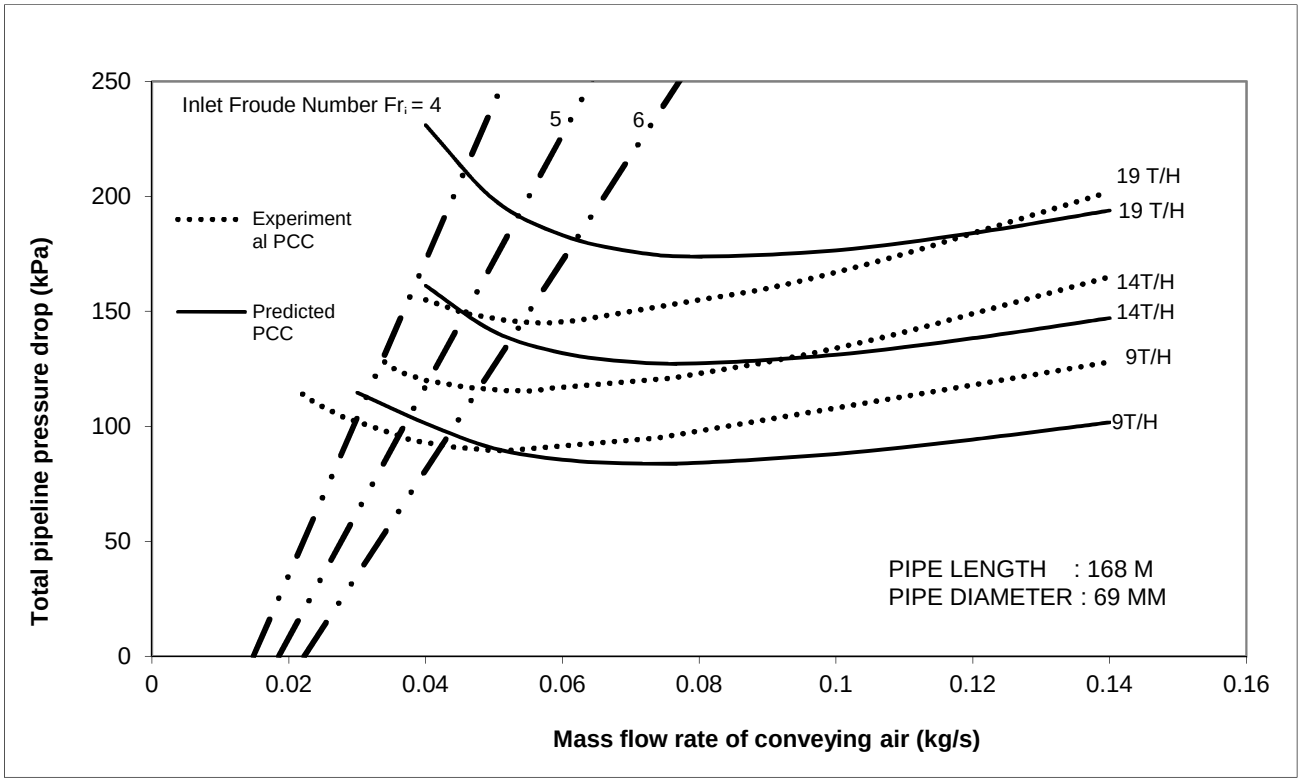

Figure 4.2: PCC for "Straight Pipe" Pressure Loss for Fly Ash and 69 mm I.D. – 168 m long pipe.

From the above PCC it showed that in the dilute phase region the predicted lines over predict the experimental lines and as the flow moves from dilute to dense phase the predicted line under predicts the experimental lines. As the mass flow rate of solid increases (i.e. from 9 t/h -19 t/h) the predicted line moves in upward direction. The predicted lines showed U-shaped trend.

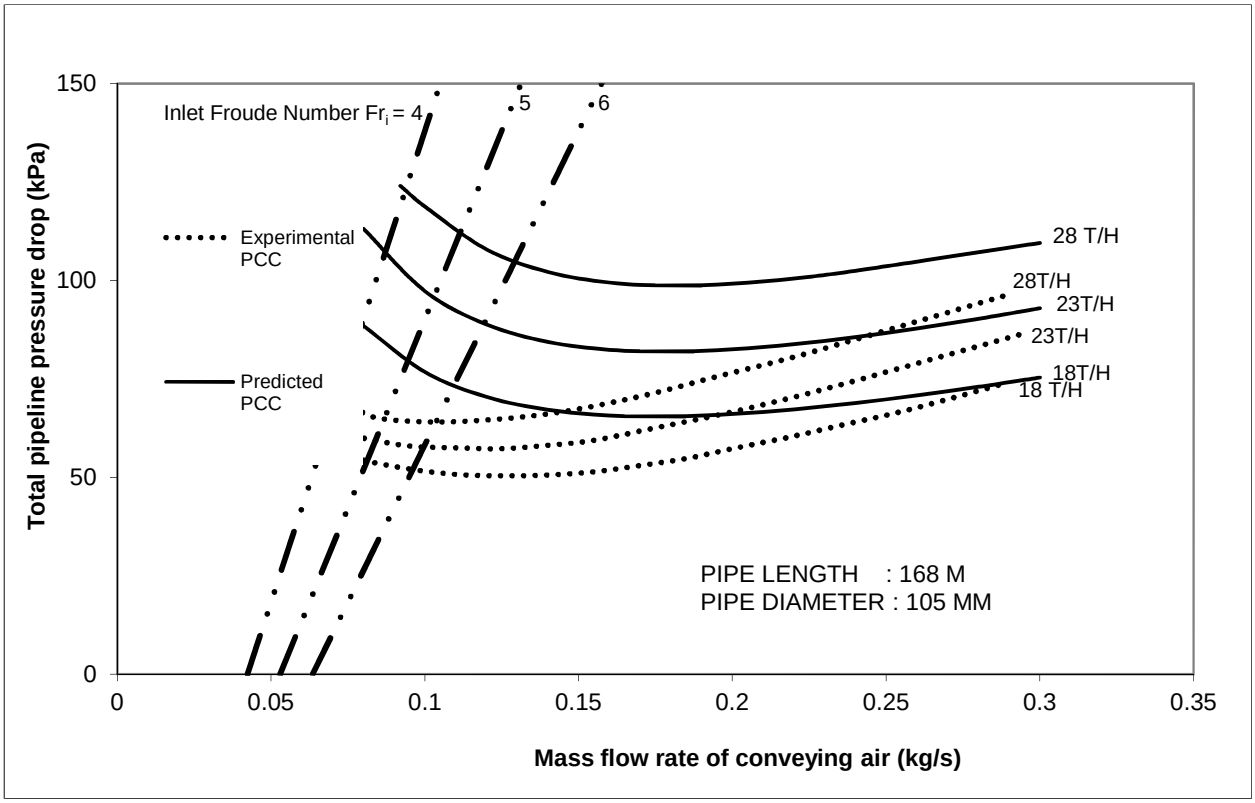

Figure 4.3: PCC for "Straight Pipe" Pressure Loss for Fly Ash and 105 mm I.D. – 168 m long pipe.

The plotted PCC in the above graph over predicts the experimental line as the mass flow rate of solid increases from 18 t/h to 28 t/h. as the flow moves from dilute to dense phase the predicted line keep on over predicting the experimental lines. The predicted lines showed U-shaped trend.

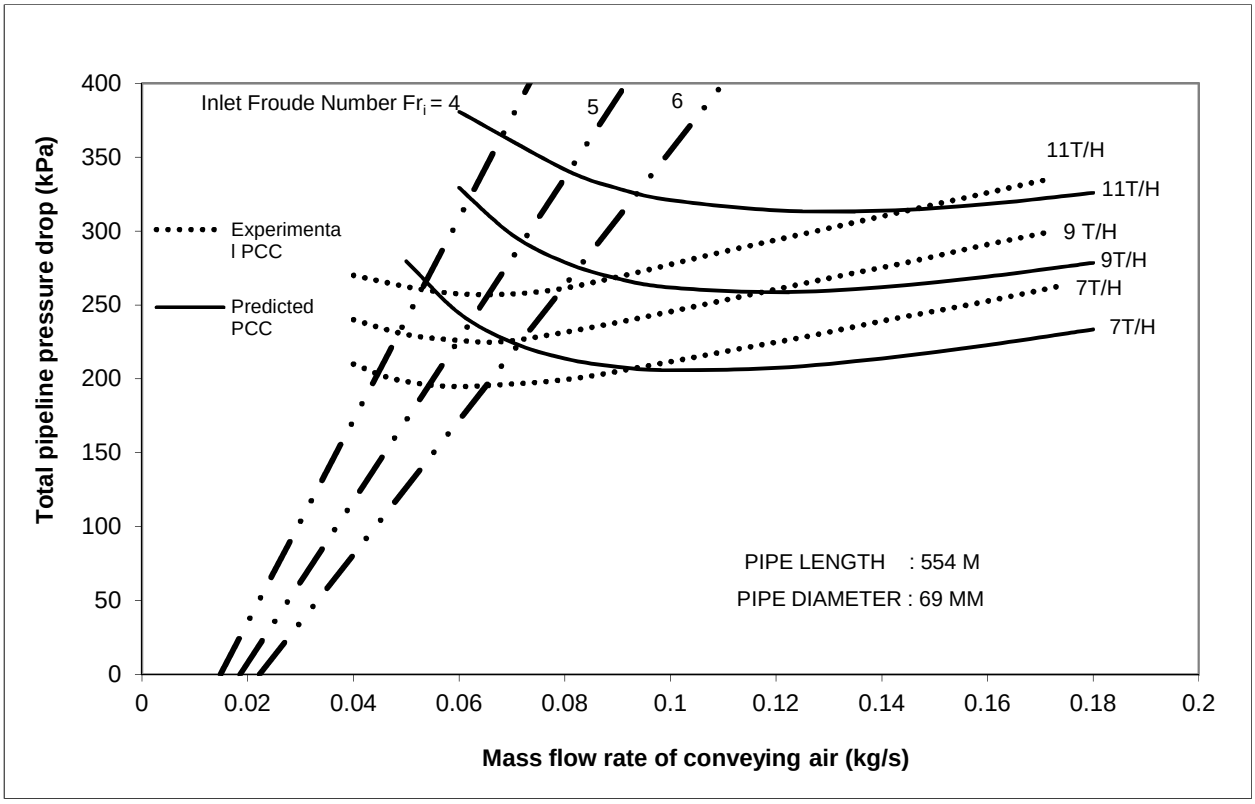

Figure 4.4: PCC for "Straight Pipe" Pressure Loss for Fly Ash and 69 mm I.D. – 554 m long pipe.

The PCC plotted in the above figure seem bit similar to the previous figure 24. As the lines plotted over the experimental lines first over predicts in dilute phase and then after moving towards the dense phase it under predicts the experimental line.

Super imposing:

Now the below plotted PCC are then super imposed with the PCC plotted from the experimental data taken from Mallick (2010) thesis and the predicted data and Weber (1981) model and the results are shown below:

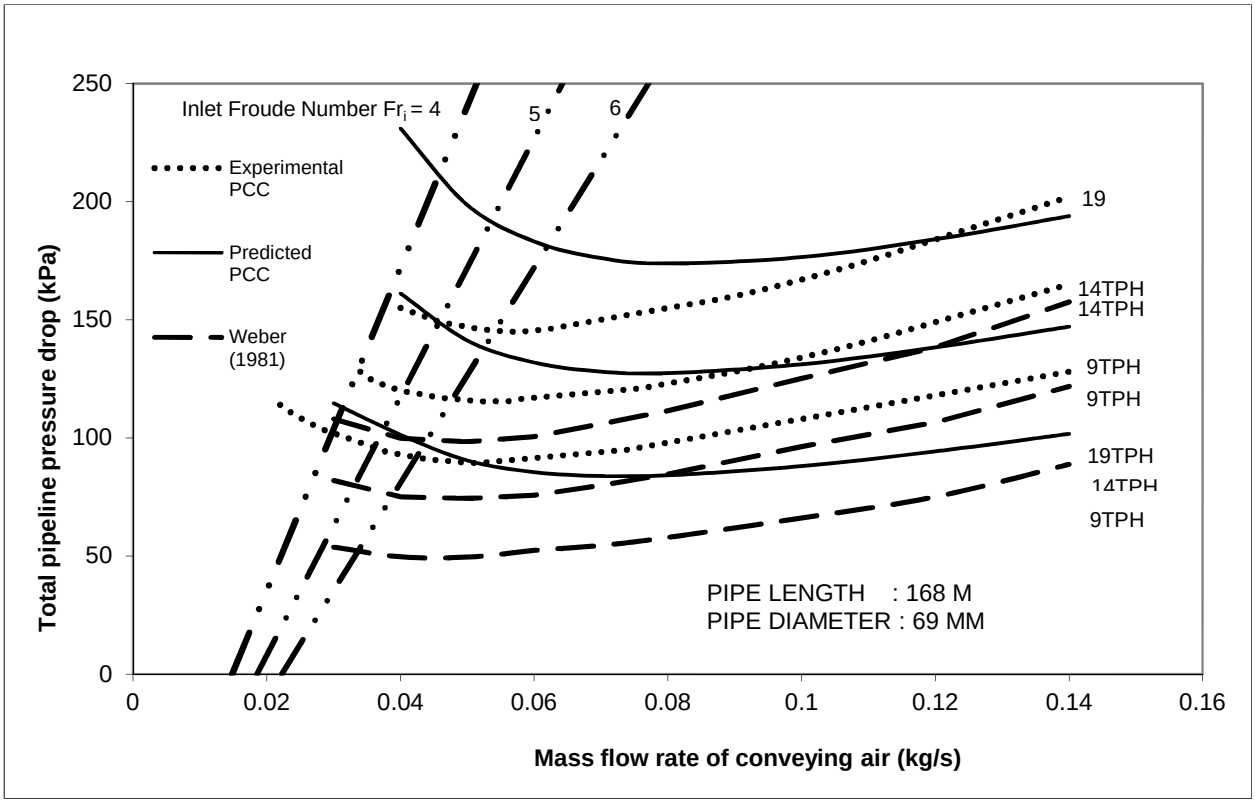

Figure 4.5: PCC for "Straight Pipe" Pressure Loss for Fly Ash and 69 mm I.D. – 168 m long pipe.

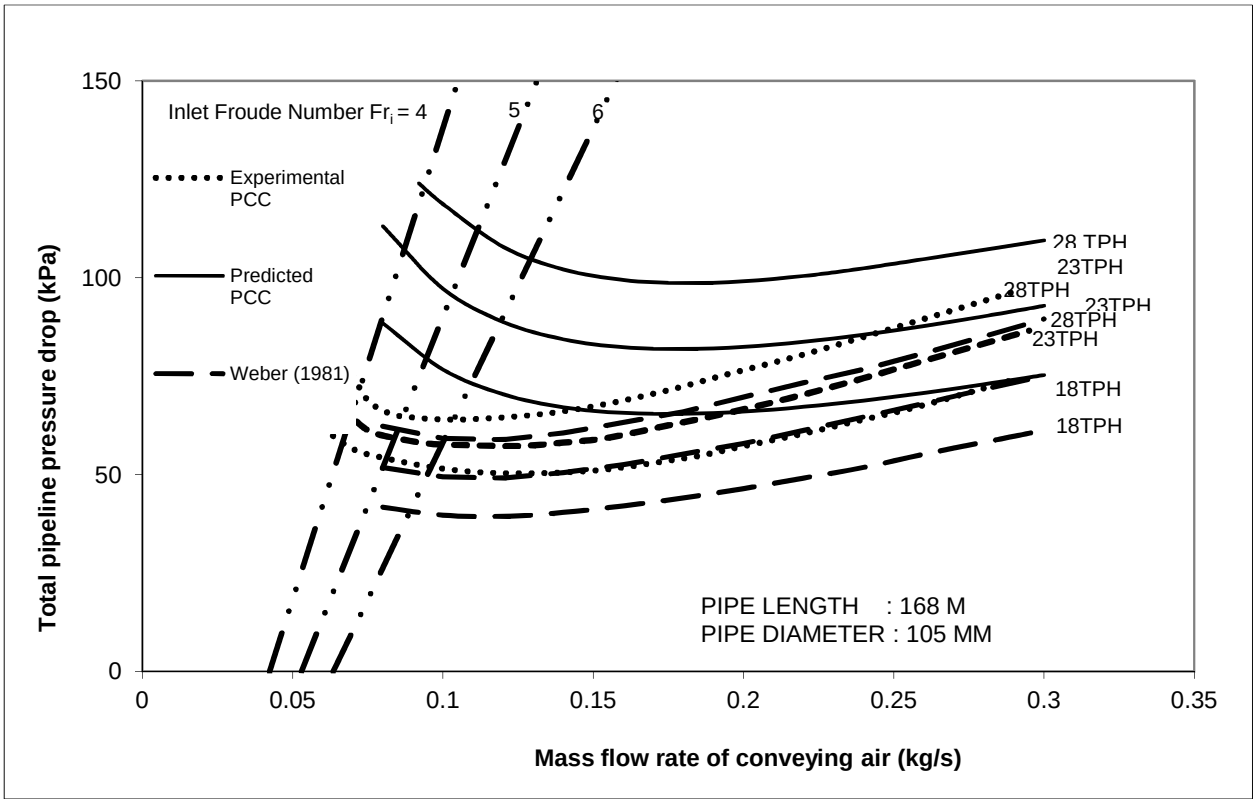

Figure 4.6: PCC for "Straight Pipe" Pressure Loss for Fly Ash and 105 mm I.D. – 168 m long pipe.

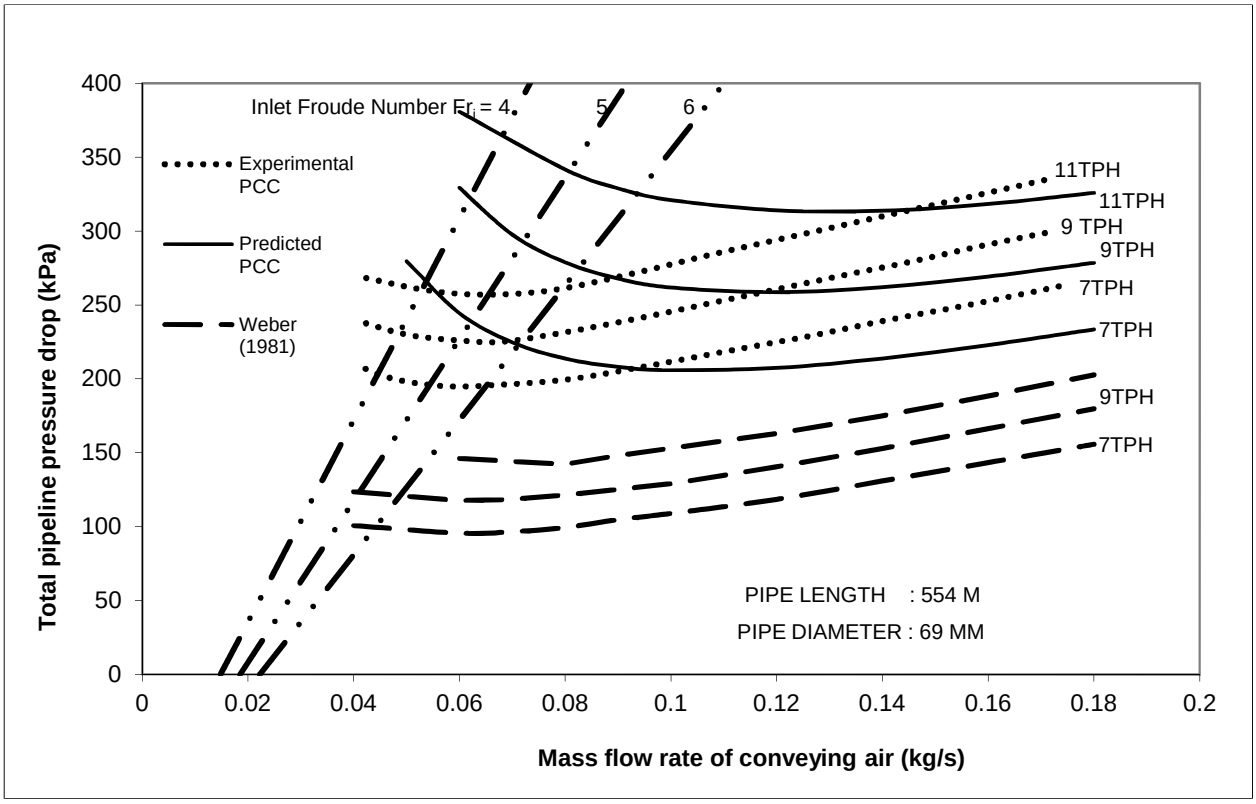

Figure 4.7: PCC for "Straight Pipe" Pressure Loss for Fly Ash and 69 mm I.D. – 554 m long pipe.

PCC plotted for ESP DUST:

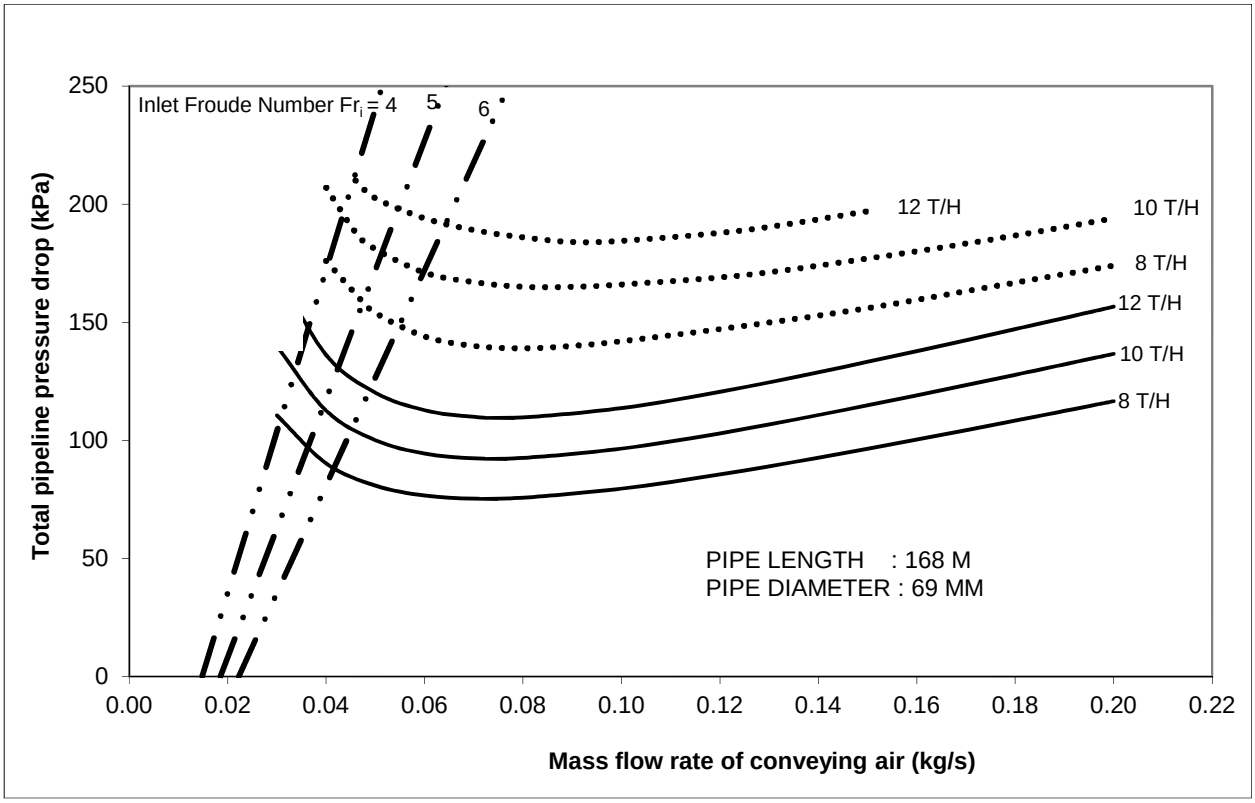

Figure 4.8: PCC for "Straight Pipe" Pressure Loss for ESP dust and 69 mm I.D. – 168 m long pipe.

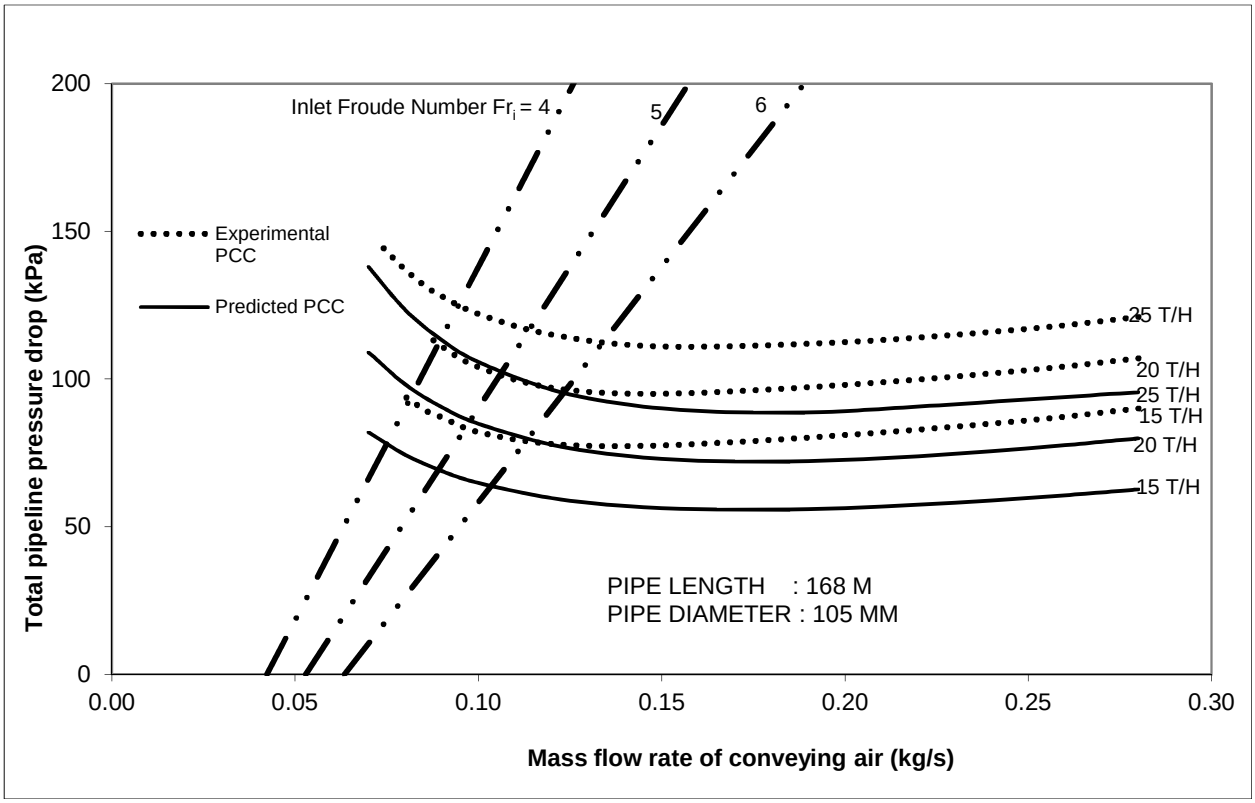

Figure 4.9: PCC for "Straight Pipe" Pressure Loss for ESP dust and 105 mm I.D. – 168 m long pipe.

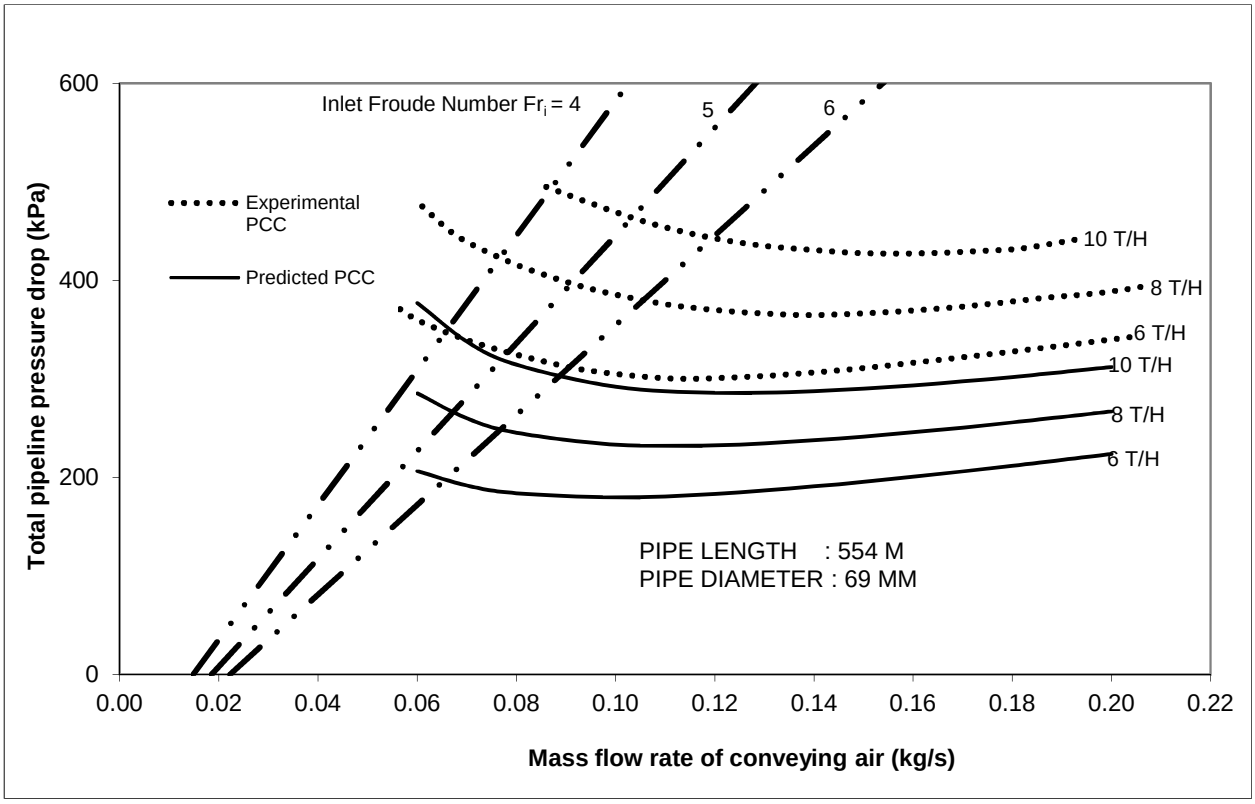

Figure 4.10: PCC for "Straight Pipe" Pressure Loss for ESP dust and 69 mm I.D. – 554 m long pipe.

The plotted PCC in the above figures 4.8, 4.9, 4.10 are under predicts the experimental data. The predicted lines were obtained by modified Weber (1981) model which showed satisfactory results. The predicted model is somewhat accurate for the ESP DUST.

4.4 Error Analysis:

The purpose of this analysis was to determine the error in the data of the developed model over the experimental data. For that the data was gathered from both experimental as well as from predicted data and put in the below mentioned formula:

$$\left|\frac{\text{predicted data} - \text{experimental data}}{\text{predicted data}}\right| \qquad (4.12)$$

This analysis was done on the predicted data of fly ash which was obtained from the developed model and checked whether that model satisfy the experimental data or not. The formula used for percentage error:

$$\text{Percentage error} = \Sigma \left| \frac{\text{predicted data} - \text{experimental data}}{\text{predicted data}} \right| \text{x } 100 \qquad (4.13)$$

By applying the above mentioned formula the percentage error values were obtained for the individual mass flow rate of solid in tonnes per hour and this is shown in the tabular form below:

Table 2: shows the percentage of error at various mass flow rate of solid.

Mass Flow Rate Of Solid (t/h)	Error (%)
For 69-168 (P9-P10)	
19 t/h	12.28
14 t/h	10.39
9 t/h	17.03
For 105-168	
28 t/h	27.67
23 t/h	21.67
18 t/h	15.34
For 69-554	
11 t/h	14.68
9 t/h	11.45
7 t/h	10.77

Chapter 5: Conclusion and Future Work

5.1 Conclusion:

As mentioned in the chapter 1, the main aim of this thesis was to develop the four layer model approach and to predict the pressure drop for dense phase region in pneumatic conveying system. The literature survey carried out with the aim of exploring the pressure drop predicting techniques which are simple and reliable in their application of both dilute and dense phase conveying. The studies conducted by various researchers were believed to be an important contribution to the knowledge in pneumatic conveying system.

The PCC plotted from the data obtained from the modified Stegmaier (1978) model for four layer modelling approach for fly ash was too over predicted, the reason for that was the Stegmaier model worked which with ESP dust quite effectively rather than fly ash. For this reason the Weber (1981) model was taken and modified for predicting the pressure drop for dense phase region and plotted the PCC with the experimental data. The modified Weber (1981) model results in over prediction for diameter and length scaled-up conditions for fly ash, however these over prediction generally occurred due to diameter and length scale-up. There seems to be a substantial relative improvement in the accuracy of pressure drop predictions.

5.2 Future work:

The following areas of investigation require further attention:

- The “modified Weber (1981)” modelling procedure conducted in this thesis for fly ash and lengths/diameters of pipes, it is preferable that the method be further evaluated for different powders and for various pipe segments.

- Wide range of dense-phase conveying data are to be used for evaluating the accuracy of the "4-layer" modelling method.

- Further work must be done to predict a pressure drop modelling which will work effectively well for both dense- and dilute-phase, empirical approach will be used for the modelling. The flow of multi solid particles in various regions/layers is to be studied empirically

List of symbols

ΔP : Pressure drop [$\mathrm{kg/ms^2}$]

ρ_s : Solid density [$\mathrm{kg/m^3}$]

ρ_f : Fluid density [$\mathrm{kg/m^3}$]

ε : Strand porosity

g : Gravitational acceleration [$\mathrm{m/s^2}$]

f_r : Friction factor

ΔL : Pipe length [m]

Fri : Friction factor

ΔP_z : Pressure drop necessary for the transport of solid materials [$\mathrm{kg/ms^2}$]

w_f : Single particle, fall velocity

Fr_p : Particle Froude number

$F_{s.fl.}$: Combination of non-dimensional groups for suspended particles

V_{rel} : Average relative velocity between fluid and particle [m/s]

A_1, A_2 : Area of the cross section occupied by the dense and dilute layers

S_1, S_2 : Wetted perimeter of the dense and the dilute layers

S_{mg}, S_{ms} : Gas phase mass transfer and solid phase mass transfer between the layers

ρ_g, ρ_s : Density of gas particles and density of solid particles [$\mathrm{kg/m^3}$]

μ_w : Dynamic wall-friction factor

C_w : Particle wall cohesion [Pa]

ρ_p : Particle density [$\mathrm{kg/m^3}$]

K_w : Fr constant in Tsuji's equation

$\emptyset_w$: Angle of wall friction [°]

f_P : Particle-particle friction factor

ε_{st} : Voidage strand section

ΔP : pressure drop in pipeline [kPa]

L : Length of the pipe [m]

D : Diameter of pipe [mm]

$\rho_{f,ave}$: Average fluid density [$\mathrm{kg/m^3}$]

v_{ave} : Average fluid velocity [$\mathrm{m/s}$]

m^* : Non-dimensional relationship between the mass flow of the particles and the mass flow of the fluid $\left(\frac{M_s}{M_f}\right)$.

G_s: Solids flow rate [$\mathrm{m/s}$]

Q_a : Air flow rate [$\mathrm{m/s}$]

E : Power consumption coefficient,

L : The total length of conveying pipeline.

$\frac{\Delta \mathrm{P}}{\mathrm{L}}$: Pressure drop per unit length [$\mathrm{N/m^3}$]

λ_{1g} , λ_{2g} : Darcy friction factor of gas phase.

ρ_s : Solid density [kg/m^3]

ρ_g : Gas density [kg/m^3]

f_{1s} : Solid friction factor.

D_1 : Inner diameter of pipe [m]

C_1, C_2 : Particle distribution coefficient.

ϵ : Voidage.

U_{1ga}^2, U_{2ga}^2 : Actual gas velocity [m/s]

U_{1s}^2 : Solid velocity [m/s]

g : Gravitational acceleration constant [m/s]

f_w : Wall friction coefficient.

k1,k2 : Constants.

A : area [m^2]

References

Cai L., Xaioping C., Pan X., Changsui X., 2011, Effect of moisture content on conveying characteristics of pulverized coal for pressurized entrained flow gasification, Experimental Thermal and Fluid Science, 35(6) : 1143-1150.

Chattopadyay A., Madhusudana Rao M., Parameswaran M.A., 1989, Dense phase pneumatic conveying system for fine materials, Powder Handling and Processing, 1(1): 11-17.

Gupta S.K., Agarwal V.K., Singh S.N., Seshadri V., Mills D., Singh J., Prakash C., 2009, Prediction of minimum fluidization velocity for tailings materials, Powder Technology, 196 : 263-271.

Hong J., Shen Y., Tomita Y., Phase diagrams in dense phase pneumatic transport, Powder Technology, 1995, 84 : 213-219.

Huber N., Sommerfeld M., 1998, Modelling and numerical calculation of dilute-phase pneumatic conveying in pipe systems, Powder Technology, 99, : 90-101.

Hyder L.M., Bradley M.S.A., Reed A.R., Hettiaratchi K., 2000, An investigation into the effect of particle size on straight-pipe pressure gradients in lean phase conveying, Powder Technology, 112 : 235-243.

Hirota M., Sogo Y., Marutami T., Suzuki M., 2002, Effects of mechanical properties of powder on pneumatic conveying in inclined pipe, Powder Technology, 122(2,3), : 150-155.

Hettiaratchi K., Wooodhead S.R., Reed A.R., 1998, Comparison between pressure drop in horizontal and vertical pneumatic conveying pipelines, Powder Technology, 95 : 67-73.

Hong Jiang, Shen Yi-Shen, Lui Shu-Lin, 1993, A model for gas-solid stratified flow in horizontal dense-phase pneumatic conveying, Powder Technology, 77: 107-114.

Jones M.G., Williams K.C., 2003, Solid friction factors for fluidized dense-phase conveying, Particulate Science and Technology, 21(1), : 45-56.

Jones M.G., William K.C., 2008, Predicting the mode of flow in pneumatic conveying system-A review, Particuology, 6: 289-300.

Junfu Lu., Wai Wang, Quigliang Guan, Yuxin Wu, Hairui Yang, Jiansheng Zhang, 2011, Experimental study on the solid velocity in horizontal dilute phase pneumatic conveying of fine powders, Powder Technology, 212: 403-409.

Kumar U., Mishra R., Singh S.N., Seshadri V., 2003, Effect of particle gradation on flow characteristics of ash disposal pipeline, Powder Technology, 132, : 39-51.

Laour S., Molodtsof Y., 1998, Experimental characterization of the pressure drop in dense phase pneumatic transport at very low velocity, Powder Technology, 95, : 165-173.

Levy A. and Mason D.J., 2000, Two layer model for non-suspension gas-solids flow in pipes, Powder Technology, 112(3), : 263-262.

Littman H., Morgan III M.H., Jovanovic S.Dj., Paccione J.D., Grbavcic Z.B., Vukovic D.V., 1995, Effect of particle diameter, particle density and loading ratio on the effective drag coefficient in steady turbulent gas-solids transport, Powder Technology, 84, : 49-56.

Molerus O. and Wirth K.E., 1981, Prediction of pressure in horizontal segregated pneumatic conveying with particle strands sliding along bottom of the pipe, Journal Chemical Engineering., 4 : 278-284.

Molerus O., 1981, Prediction of pressure drop with steady state pneumatic conveying of solids in horizontal pipes, Chemical Engineering Science, 36(12) : 1977-1984.

Molerus O. and Wirth K.E., 1983, Prediction of pressure drop with pneumatic conveying of solids in horizontal pipes, Journal of Powder and Bulk Solids Technology, 7(2) : 17-20.

Molerus O., 1996, Overview pneumatic transport of solids, Powder Technology, 88 : 309-321.

Molerus O. and Heucke U., 1999, Pneumatic transport of coarse grained particles in horizontal pipes, Powder Technology, 102 : 135-150.

Molerus O., Burschka A., 1995, Pneumatic transport of coarse-grained materials, Chemical Engineering and Processing, 34: 173-184.

Mason D.J., Marjanovic P., Levy A., A simulation system for pneumatic conveying system, Powder Technology, 95 : 7-14.

Michaelides Efgtathios E., 1984, Model for the flow of solid particles in gases, Multiphase Flow, 10(1): 61-77.

Pan R., 1999, Material properties and flow modes in pneumatic conveying, Powder Technology, 104: 157-163.

Rinoshika A. and Suzuki M., 2010, As experimental study of energy-saving pneumatic conveying system in a horizontal pipeline with dune flow, Powder Technology, 198(1), : 49-55.

Rinoshika A. and Yan F., 2010,Aapplication of high-speed PIV and image processing to measuring particle velocity and concentration in a horizontal pneumatic conveying with dune model, Powder Technology, 208(1), : 158-165.

Rizk F.A., 2006, Pneumatic conveyance of solids scale-up/ large scale systems, Bulk Solids Handling, 137-149.

Sanchez L., Vasquez N.A., Klinzing G.E., Dhodapkar S., 2005, Evaluation of models and correlations for pressure drop estimation in dense phase pneumatic conveying and an experimental analysis, Powder Technology, 153(3), 142-147.

Vasquez N.A., Sanchez L., Klinzing G.E., Dhodapkar S., 2003, Friction measurement in dense phase plug flow analysis, Powder Technology, 137 : 167-183.

Wypych P.W. and Yi J., 2003, Minimum transport boundary for horizontal dense-phase pneumatic conveying of granular materials, Powder Technology, 129(1-3) : 111-121.

Wang W., Quingliang G., Yuxin W., Hairui Y., Jiansheng Z., Junfu L., 2011, Experimental study on the solid velocity in horizontal dilute phase pneu,atic conveying of fine powders, powder technology, 212 : 403-409.

Weber M., 1991, Friction of the air and the air/solid mixture in pneumatic conveying, Bulk Solids Handling, 11(1): 99-102.

Wypych P.W. and Pan R., 1991, Determination of air-only pressure drop in pneumatic conveying systems, Powder Handling and Processing, 3(4): 303-309.

Wypych P.W. and Hastie D.B., 2006, Modelling solids friction factor for dense-phase pneumatic conveying of powders, Particle Technology, 1-6.

Williams K.C. and Jones M.G., 2003, Classification diagrams for dense phase pneumatic conveying, Powder Handling and Processing, 15(6): 368-373.

Appendix A

Programme for calculating the total pipeline pressure drop for 69 mm I.D. – 168 m Length by using "MACRO" (Mallick, 2010).

Horizontal straight section L1: 1st section from exit		
Pipe cross sectional area	m2	0.0037
solid loading ratio (m*)		17.857
Exit Condition		
density of air at exit	kg/m3	1.204
superficial air velocity at exit	m/s	31.088
Froude number at exit		37.786
Assumed Pressure loss	**kPa**	**7.380**
Entry Condition		
density of air at inlet	kg/m3	1.292
superficial air velocity at inlet	m/s	28.978
Froude number at inlet		35.221
Average Condition		
Average air density	kg/m3	1.248
Air velocity at average condition	m/s	29.996
Air viscosity at average condition	Pa.S	0.000018
Reylonds Number for average condition		142231.815
Froude Number for average condition		36.459
Solid friction factor (λs) for average condition		0.0000
Air only friction factor (λf) for average condition		0.017
Pressure drop for average condition	**kPa**	**11.185**
Pressure difference	kPa	**3.805**
Pressure at entry to the	kPa (g)	***11.185***

section		
Pressure at entry to the section	kPa (a)	112.510
Bend B1		
Air density at bend outlet	kg/m3	1.292
Air velocity at bend outlet	m/s	28.978
RB/r = Radius of curvature of bend/ pipe radius		28.986
Reynolds number (Re)		142231.815
Re. {r/RB}^2		169.291
Air only friction factor through bend (λfb)		0.478
Solid friction factor at bend outlet		1.319
Pressure drop due to solid + air through bend	kPa	13.034
Total pressure drop due to bend	**kPa**	**13.034**
Pressure at the entry of bend	kPa (g)	***24.219***
Pressure at the entry of bend	kPa (a)	125.544
Vertical lift loss due to elevation H		
Pipe cross sectional area	m2	0.0037
solid loading ratio (m*)		17.857
Exit Condition		
density of air at exit	kg/m3	1.492
superficial air velocity at exit	m/s	25.091
Froude number at exit		30.497
Assumed Pressure loss	**kPa**	**9.635**
Entry Condition		
density of air at inlet	kg/m3	1.607
superficial air velocity at inlet	m/s	23.302
Froude number at inlet		28.323
Average Condition		
Average air	kg/m3	1.549

density		
Air velocity at average condition	m/s	24.164
Air viscosity at average condition	Pa.S	0.000018
Reylonds Number for average condition		142231.815
Froude Number for average condition		29.370
Solid friction factor (λs) for average condition		0.0000
Air only friction factor (λf) for average condition		0.017
Pressure drop due to friction for average condition through lift of 'h'	**kPa**	**5.294**
Pressure drop due to Elevation of materials through evelation of 'H'	**kPa**	**6.482**
Total pressure loss through the elevation	**kPa**	**11.775**
Pressure difference	kPa	**2.140**
Pressure at entry to the section	kPa (g)	***35.995***
Pressure at entry to the section	kPa (a)	137.320
Bend B2		
Air density at bend outlet	kg/m3	1.607
Air velocity at bend outlet	m/s	23.302
RB/r = Radius of curvature of bend/ pipe radius		28.986
Reynolds number (Re)		142231.815
Re. {r/RB}^2		169.291
Air only friction factor through bend (λfb)		0.478
Solid friction factor at bend outlet		0.933
Pressure drop due to solid + air through bend	kPa	7.476
Total pressure drop due to bend	**kPa**	**7.476**
Pressure at the entry of bend	kPa (g)	***43.470***
Pressure at the entry of bend	kPa (a)	144.795
Horizontal straight section L2		
Pipe cross sectional area	m2	0.0037
solid loading ratio (m*)		17.857
Exit Condition		

density of air at exit	kg/m3	1.721
superficial air velocity at exit	m/s	21.755
Froude number at exit		26.442
Assumed Pressure loss	**kPa**	**0.228**
Entry Condition		
density of air at inlet	kg/m3	1.724
superficial air velocity at inlet	m/s	21.721
Froude number at inlet		26.401
Average Condition		
Average air density	kg/m3	1.722
Air velocity at average condition	m/s	21.738
Air viscosity at average condition	Pa.S	0.000018
Reylonds Number for average condition		142231.815
Froude Number for average condition		26.421
Solid friction factor (λs) for average condition		0.0000
Air only friction factor (λf) for average condition		0.017
Pressure drop for average condition	**kPa**	**20.556**
Pressure difference	kPa	**20.328**
Pressure at entry to the section	kPa (g)	***64.026***
Pressure at entry to the section	kPa (a)	165.351
Horizontal straight section L3		
Pipe cross sectional area	m2	0.0037
solid loading ratio (m*)		17.857
Exit Condition		
density of air at exit	kg/m3	1.724
superficial air velocity at exit	m/s	21.721
Froude number at exit		26.401

Assumed Pressure loss	**kPa**	**0.227**
Entry Condition		
density of air at inlet	kg/m3	1.968
superficial air velocity at inlet	m/s	19.024
Froude number at inlet		23.123
Average Condition		
Average air density	kg/m3	1.846
Air velocity at average condition	m/s	20.283
Air viscosity at average condition	Pa.S	0.000018
Reylonds Number for average condition		142231.815
Froude Number for average condition		24.654
Solid friction factor (λs) for average condition		0.0000
Air only friction factor (λf) for average condition		0.017
Pressure drop for average condition	**kPa**	**19.180**
Pressure difference	kPa	**18.953**
Pressure at entry to the section	kPa (g)	***83.206***
Pressure at entry to the section	kPa (a)	184.531
Bend B3		
Air density at bend outlet	kg/m3	1.968
Air velocity at bend outlet	m/s	19.024
RB/r = Radius of curvature of bend/ pipe radius		28.986
Reynolds number (Re)		142231.815
Re. {r/RB}^2		169.291
Air only friction factor through bend (λfb)		0.478
Solid friction factor at bend outlet		0.676
Pressure drop due to solid + air through bend	kPa	4.470
Total pressure drop due to bend	**kPa**	**4.470**
Pressure at the entry of bend	kPa (g)	***87.676***
Pressure at the entry of	kPa (a)	189.001

bend		
Horizontal straight section L4		
Pipe cross sectional area	m2	0.0037
solid loading ratio (m*)		17.857
Exit Condition		
density of air at exit	kg/m3	2.246
superficial air velocity at exit	m/s	16.667
Froude number at exit		20.258
Assumed Pressure loss	**kPa**	**0.035**
Entry Condition		
density of air at inlet	kg/m3	2.247
superficial air velocity at inlet	m/s	16.664
Froude number at inlet		20.254
Average Condition		
Average air density	kg/m3	2.247
Air velocity at average condition	m/s	16.665
Air viscosity at average condition	Pa.S	0.000018
Reylonds Number for average condition		142231.815
Froude Number for average condition		20.256
Solid friction factor (λs) for average condition		0.0000
Air only friction factor (λf) for average condition		0.017
Pressure drop for average condition	**kPa**	**2.466**
Pressure difference	kPa	**2.431**
Pressure at entry to the section	kPa (g)	***90.142***
Pressure at entry to the section	kPa (a)	191.467
Bend B4		

Air density at bend outlet	kg/m3	2.247
Air velocity at bend outlet	m/s	16.664
RB/r = Radius of curvature of bend/ pipe radius		28.986
Reynolds number (Re)		142231.815
Re. {r/RB}^2		169.291
Air only friction factor through bend (λfb)		0.478
Solid friction factor at bend outlet		0.548
Pressure drop due to solid + air through bend	kPa	3.200
Total pressure drop due to bend	**kPa**	**3.200**
Pressure at the entry of bend	kPa (g)	***93.343***
Pressure at the entry of bend	kPa (a)	194.668
Horizontal straight section L5		
Pipe cross sectional area	m2	0.0037
solid loading ratio (m*)		17.857
Exit Condition		
density of air at exit	kg/m3	2.314
superficial air velocity at exit	m/s	16.181
Froude number at exit		19.668
Assumed Pressure loss	**kPa**	**0.267**
Entry Condition		
density of air at inlet	kg/m3	2.317
superficial air velocity at inlet	m/s	16.159
Froude number at inlet		19.641
Average Condition		
Average air density	kg/m3	2.315
Air velocity at average condition	m/s	16.170
Air viscosity at average condition	Pa.S	0.000018
Reylonds Number for average condition		142231.815
Froude Number for average condition		19.654

Solid friction factor (λs) for average condition		0.0000
Air only friction factor (λf) for average condition		0.017
Pressure drop for average condition	**kPa**	**18.327**
Pressure difference	kPa	**18.060**
Pressure at entry to the section	kPa (g)	***111.670***
Pressure at entry to the section	kPa (a)	212.995
Horizontal straight section L6		
Pipe cross sectional area	m2	0.0037
solid loading ratio (m*)		17.857
Exit Condition		
density of air at exit	kg/m3	2.317
superficial air velocity at exit	m/s	16.159
Froude number at exit		19.641
Assumed Pressure loss	**kPa**	**0.266**
Entry Condition		
density of air at inlet	kg/m3	2.535
superficial air velocity at inlet	m/s	14.771
Froude number at inlet		17.953
Average Condition		
Average air density	kg/m3	2.426
Air velocity at average condition	m/s	15.434
Air viscosity at average condition	Pa.S	0.000018
Reylonds Number for average condition		142231.815
Froude Number for average condition		18.759
Solid friction factor (λs) for average condition		0.0000
Air only friction factor (λf) for average condition		0.017
Pressure drop for average condition	**kPa**	**17.493**

Pressure difference	kPa	**17.226**
Pressure at entry to the section	kPa (g)	***129.163***
Pressure at entry to the section	kPa (a)	230.488
Bend B5		
Air density at bend outlet	kg/m3	2.535
Air velocity at bend outlet	m/s	14.771
RB/r = Radius of curvature of bend/ pipe radius		28.986
Reynolds number (Re)		142231.815
Re. {r/RB}^2		169.291
Air only friction factor through bend (λfb)		0.478
Solid friction factor at bend outlet		0.452
Pressure drop due to solid + air through bend	kPa	2.366
Total pressure drop due to bend	**kPa**	**2.366**
Pressure at the entry of bend	kPa (g)	***131.529***
Pressure at the entry of bend	kPa (a)	232.854
Horizontal straight section L7		
Pipe cross sectional area	m2	0.0037
solid loading ratio (m*)		17.857
Exit Condition		
density of air at exit	kg/m3	2.768
superficial air velocity at exit	m/s	13.528
Froude number at exit		16.443
Assumed Pressure loss	**kPa**	**0.047**
Entry Condition		
density of air at inlet	kg/m3	2.768
superficial air velocity at inlet	m/s	13.525
Froude number at inlet		16.439

Average Condition		
Average air density	kg/m3	2.768
Air velocity at average condition	m/s	13.526
Air viscosity at average condition	Pa.S	0.000018
Reylonds Number for average condition		142231.815
Froude Number for average condition		16.441
Solid friction factor (λs) for average condition		0.0000
Air only friction factor (λf) for average condition		0.017
Pressure drop for average condition	**kPa**	**2.758**
Pressure difference	kPa	**2.711**
Pressure at entry to the section	kPa (g)	***134.287***
Pressure at entry to the section	kPa (a)	235.612
Acceleartion Pressure Loss at Feed Point		
Pipe cross sectional area	m2	0.0037
density of air at feed point	kg/m3	2.768
superficial air velocity at exit	m/s	13.525
solid loading ratio (m*)		17.857
Accelation pressure loss	**kPa**	**9.043**
Pressure at Feed point	kPa (g)	***143.329***
Pressure at Feed point	kPa (a)	244.654
Pressure drop contributed by Horizontal straight pipes	**kPa**	**91.966**
Pressure drop contributed by Vertical pipes + Bends + Entry losses	**kPa**	**51.363**
Total Pressure drop for the entire pipe	**kPa**	**143.329**

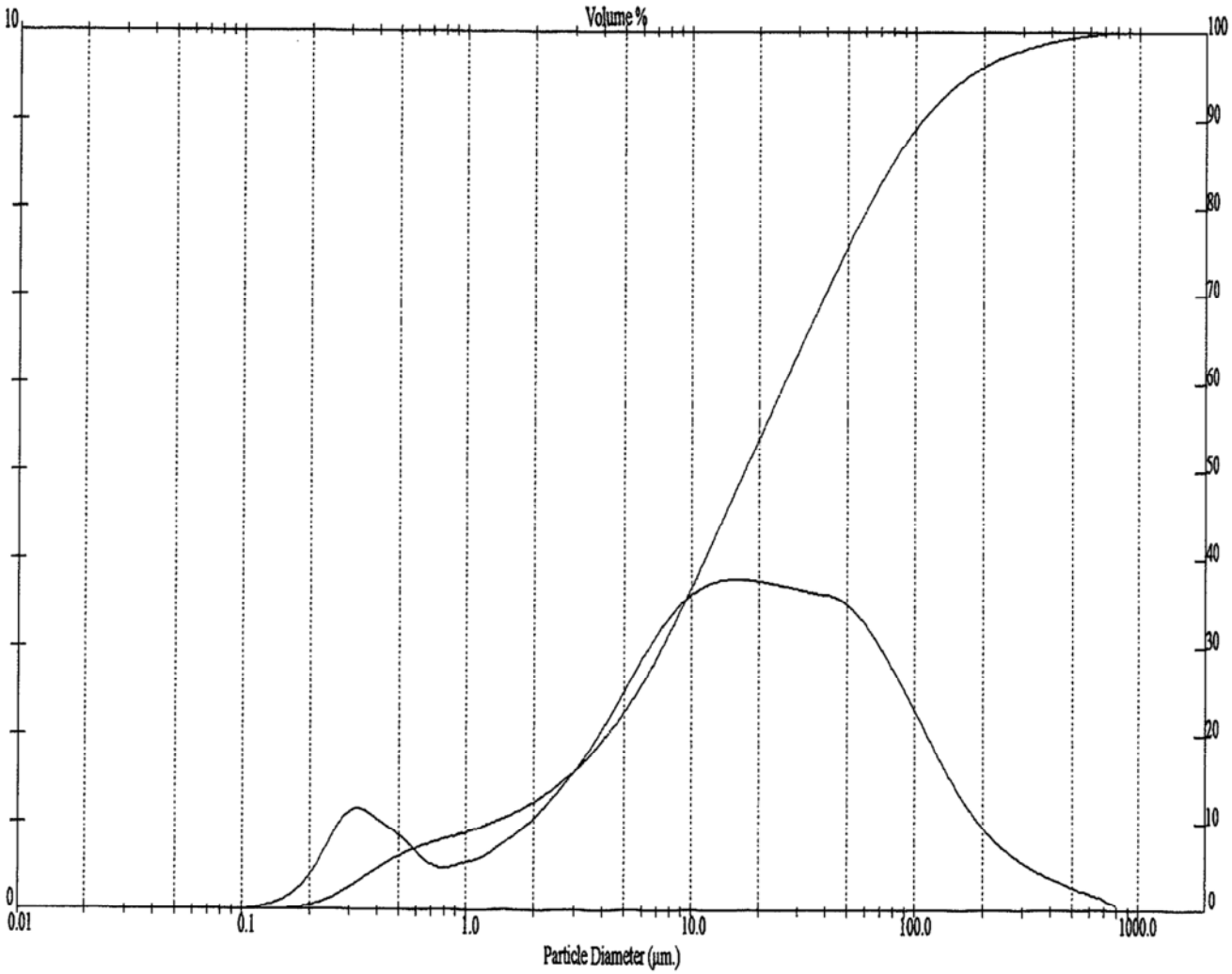

Figure A-1 Graph of fly ash used for particle size distribution (sample-1) (Mallick, 2010)

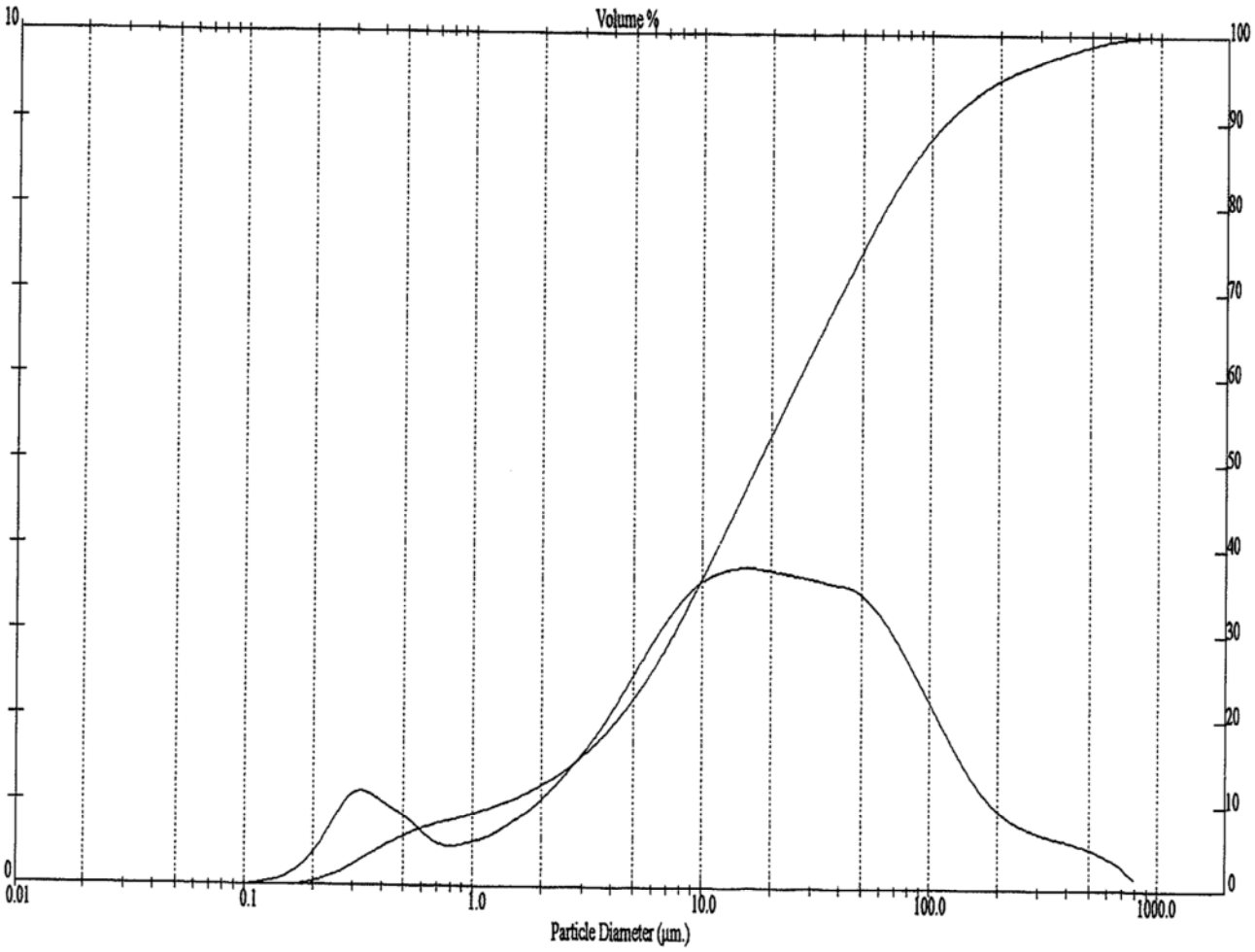

Figure A-2 Graph of fly ash used for particle size distribution (sample-2) (Mallick, 2010)

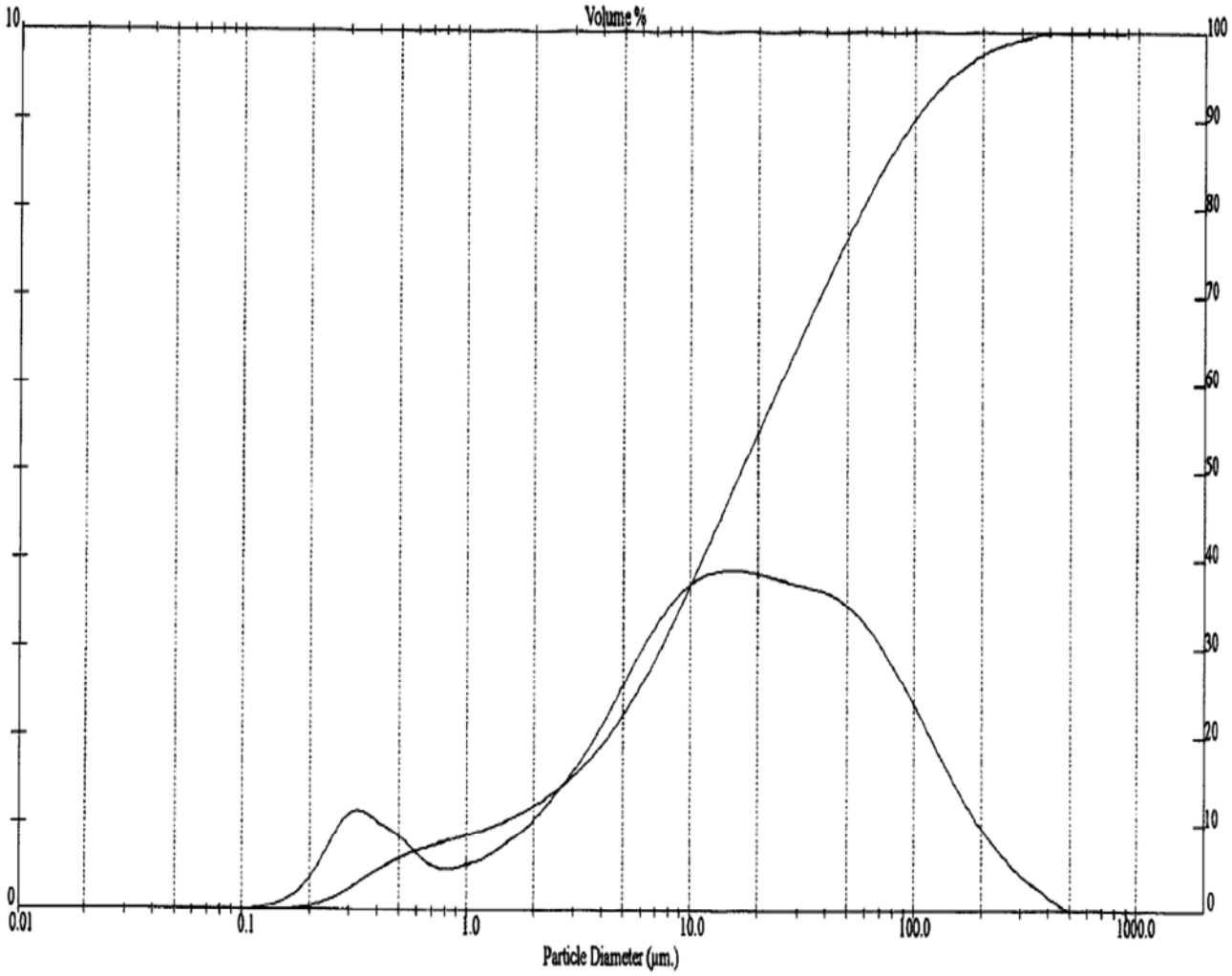

Figure A-3 Graph for fly ash used for particle size distribution (sample-3) (Mallick, 2010)

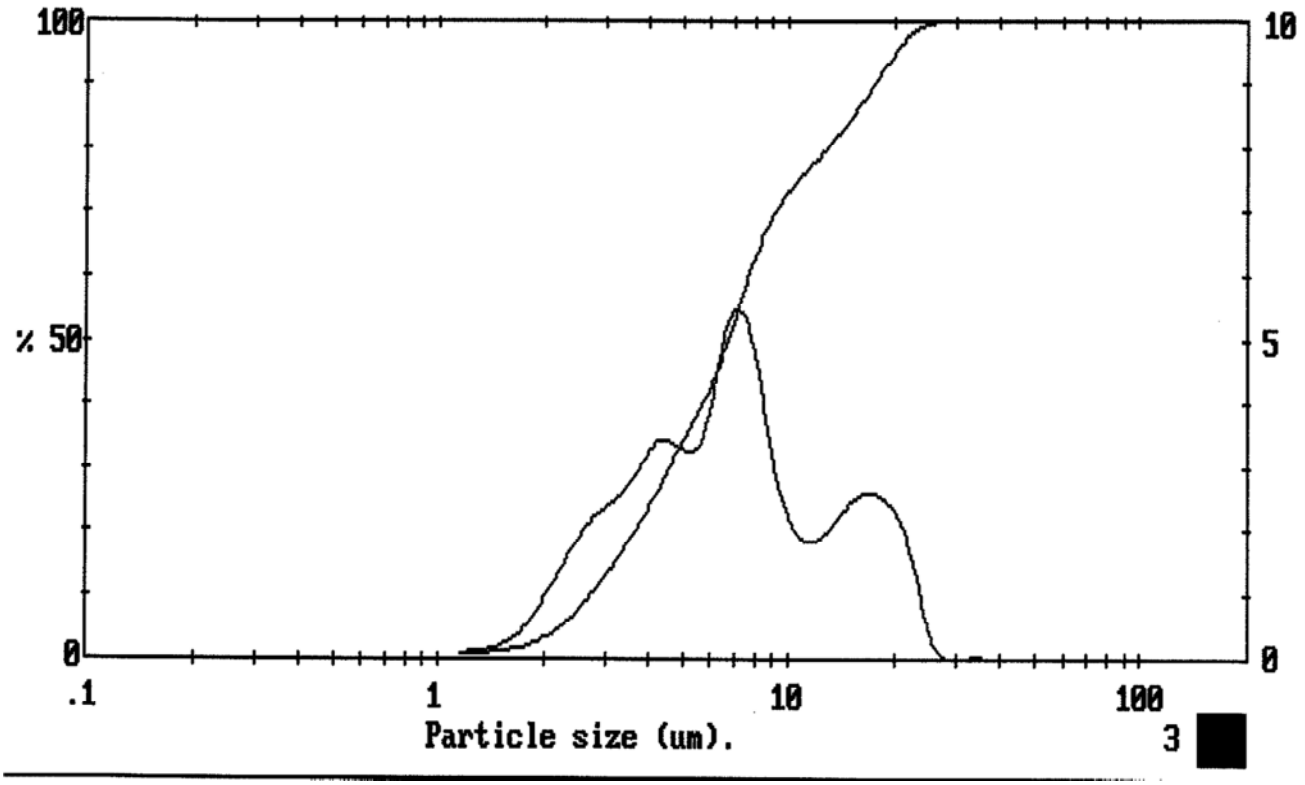

Figure A-4 Graph for ESP dust used for particle size distribution (sample-1) (Mallick, 2010)

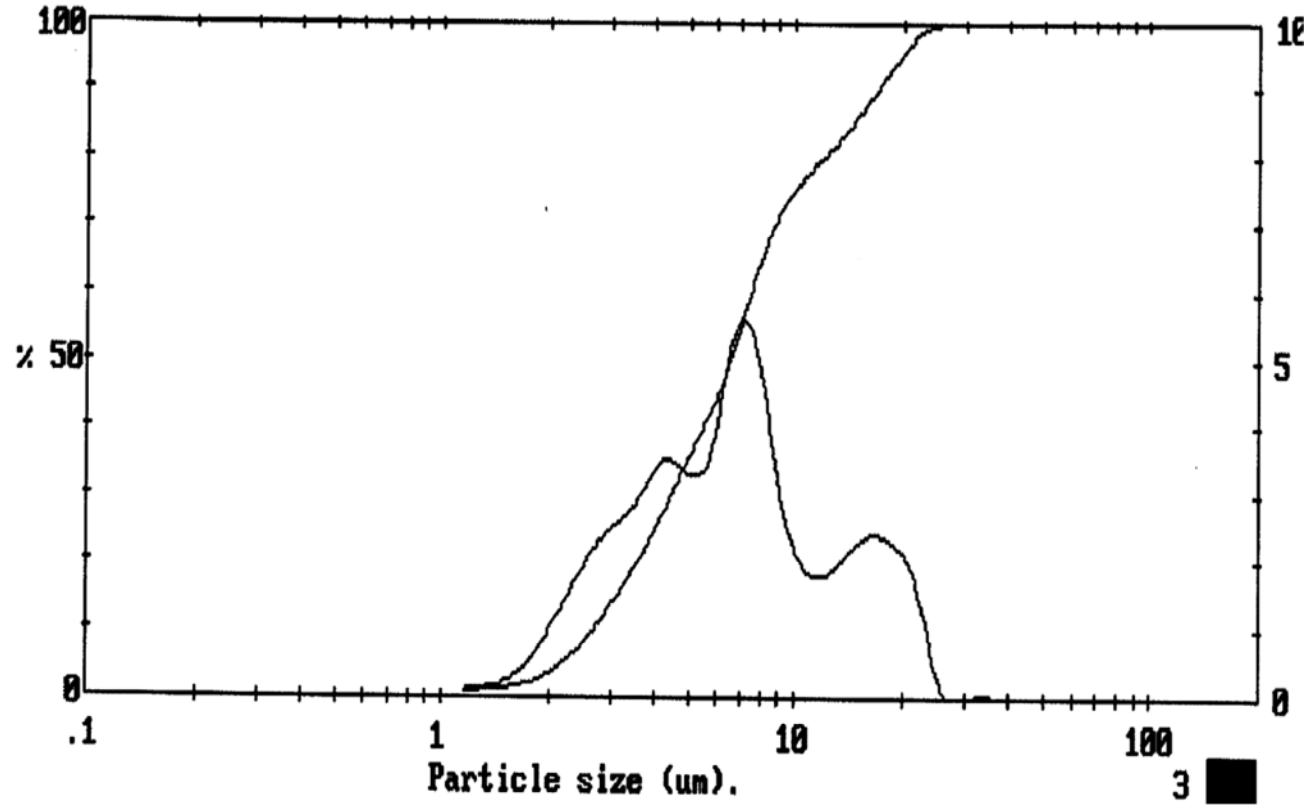

Figure A-5 Graph for ESP dust used for particle size distribution (sample-2) (Mallick, 2010)